A review of the role of the Atlantic meridional overturning circulation in Atlantic multidecadal variability and associated climate impacts

Reviews of Geophysics

REVIEW ARTICLE
10.1029/2019RG000644

Special Section:
Atlantic Meridional Overturning Circulation: Reviews of Observational and Modeling Advances

A Review of the Role of the Atlantic Meridional Overturning Circulation in Atlantic Multidecadal Variability and Associated Climate Impacts

Rong Zhang[1], Rowan Sutton[2], Gokhan Danabasoglu[3], Young-Oh Kwon[4], Robert Marsh[5], Stephen G. Yeager[3], Daniel E. Amrhein[6], and Christopher M. Little[7]

[1]Geophysical Fluid Dynamics Laboratory, National Oceanic and Atmospheric Administration, Princeton, NJ, USA, [2]National Centre for Atmospheric Science, Department of Meteorology, University of Reading, Reading, UK, [3]Climate and Global Dynamics Laboratory, National Center for Atmospheric Research, Boulder, CO, USA, [4]Physical Oceanography Department, Woods Hole Oceanographic Institution, Woods Hole, MA, USA, [5]School of Ocean and Earth Science, National Oceanography Centre, University of Southampton, Southampton, UK, [6]School of Oceanography and Department of Atmospheric Sciences, University of Washington, Seattle, WA, USA, [7]Atmospheric and Environmental Research, Inc., Lexington, MA, USA

Key Points:
- There is strong evidence that multidecadal variability of the AMOC is a key driver of AMV and associated climate impacts
- The AMOC-AMV linkage is consistent with observed key elements of AMV, and it is important to use multivariate metrics to understand AMV
- AMOC-induced Atlantic meridional heat transport and net surface heat flux anomalies are crucial for many AMV-related climate impacts

Correspondence to:
R. Zhang,
Rong.Zhang@noaa.gov

Citation:
Zhang, R., Sutton, R., Danabasoglu, G., Kwon, Y.-O., Marsh, R., Yeager, S. G., et al. (2019). A review of the role of the Atlantic Meridional Overturning Circulation in Atlantic Multidecadal Variability and associated climate impacts. *Reviews of Geophysics*, *57*. https://doi.org/10.1029/2019RG000644

Received 19 JUN 2018
Accepted 18 APR 2019
Accepted article online 29 APR 2019
Corrected 27 JUN 2019

This article was corrected on 27 JUN 2019. See the end of the full text for details.

Abstract By synthesizing recent studies employing a wide range of approaches (modern observations, paleo reconstructions, and climate model simulations), this paper provides a comprehensive review of the linkage between multidecadal Atlantic Meridional Overturning Circulation (AMOC) variability and Atlantic Multidecadal Variability (AMV) and associated climate impacts. There is strong observational and modeling evidence that multidecadal AMOC variability is a crucial driver of the observed AMV and associated climate impacts and an important source of enhanced decadal predictability and prediction skill. The AMOC-AMV linkage is consistent with observed key elements of AMV. Furthermore, this synthesis also points to a leading role of the AMOC in a range of AMV-related climate phenomena having enormous societal and economic implications, for example, Intertropical Convergence Zone shifts; Sahel and Indian monsoons; Atlantic hurricanes; El Niño–Southern Oscillation; Pacific Decadal Variability; North Atlantic Oscillation; climate over Europe, North America, and Asia; Arctic sea ice and surface air temperature; and hemispheric-scale surface temperature. Paleoclimate evidence indicates that a similar linkage between multidecadal AMOC variability and AMV and many associated climate impacts may also have existed in the preindustrial era, that AMV has enhanced multidecadal power significantly above a red noise background, and that AMV is not primarily driven by external forcing. The role of the AMOC in AMV and associated climate impacts has been underestimated in most state-of-the-art climate models, posing significant challenges but also great opportunities for substantial future improvements in understanding and predicting AMV and associated climate impacts.

1. Introduction

The Atlantic Ocean is unique due to the existence of North Atlantic Deep Water (NADW) formation in the northern North Atlantic, a vital component of the Atlantic Meridional Overturning Circulation (AMOC; e.g., Broecker et al., 1976; Buckley & Marshall, 2016; Defant, 1941; Gordon, 1986; Killworth, 1983; Kuhlbrodt et al., 2007; Marshall & Schott, 1999; Schmitz, 1995; Stommel, 1957, 1958; Talley et al., 2003; Warren, 1981; Wüst, 1935). The AMOC, which includes the northward flow of warm salty water in the upper Atlantic and the southward flow of the transformed cold fresh NADW in the deep Atlantic, is a major source for the substantial northward Atlantic heat transport across the equator (e.g., Bryan, 1962; Ganachaud & Wunsch, 2000; Hastenrath, 1980, 1982; Sverdrup, 1957; Talley, 2003; Trenberth & Caron, 2001; Trenberth & Fasullo, 2008; Trenberth & Solomon, 1994). The AMOC is suggested to have played a critical role in abrupt climate change events centered in the Atlantic seen in many paleoclimate records (e.g., Alley, 2007; Broecker et al., 1985; Cheng et al., 2009; Clark et al., 2002; McManus et al., 2004; Rahmstorf, 2002).

Although the profound role of AMOC in the climate system has been recognized for decades, it remains a challenge for most climate models to simulate a realistic AMOC structure and associated Atlantic

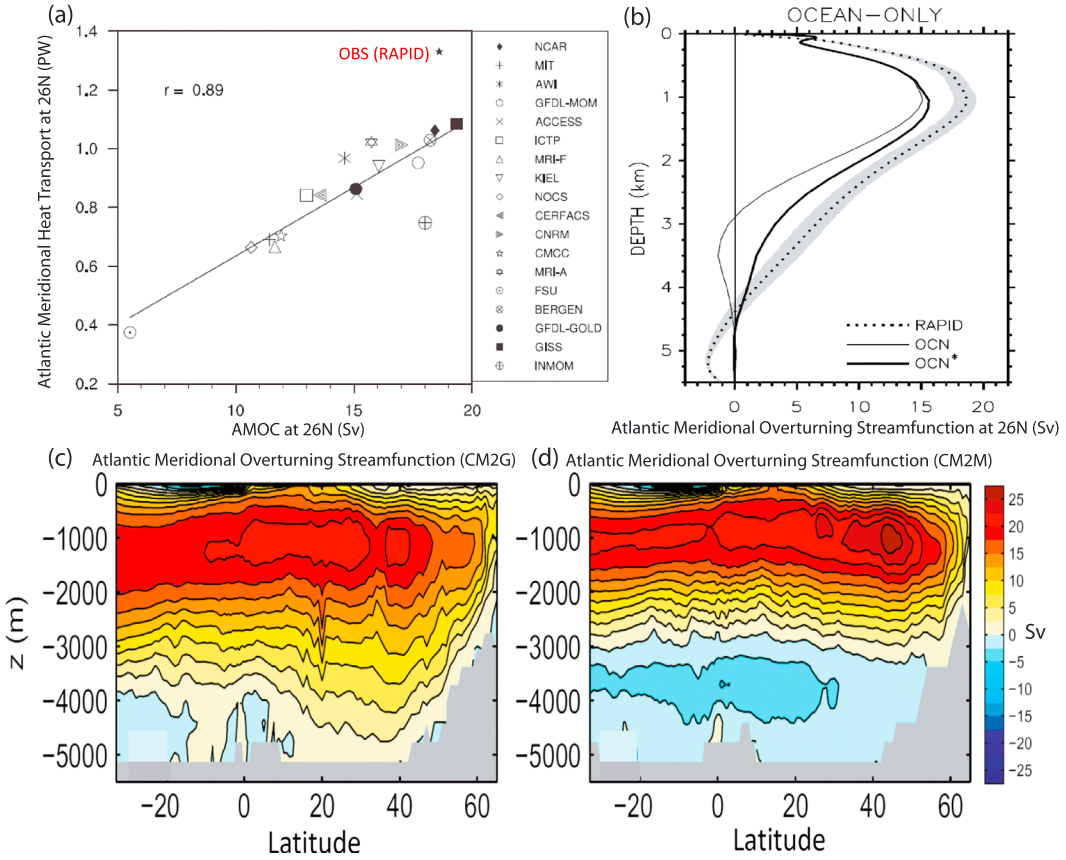

Figure 1. Comparison of simulated climatological mean Atlantic meridional heat transport (PW) and AMOC (Sv) with the observations (RAPID data). (a) Simulated climatological mean Atlantic meridional heat transport versus climatological mean AMOC strength (the maximum of Atlantic meridional overturning streamfunction) at 26°N from multiple OGCMs forced with atmospheric reanalysis data, compared with the RAPID data (black star), adapted from Danabasoglu et al. (2014). Reprinted from Ocean Modelling, 73, Danabasoglu et al., North Atlantic simulations in Coordinated Ocean-ice Reference Experiments phase II (CORE-II). Part I: Mean states, pp. 76–107, Copyright 2014, with permission from Elsevier. (b) Simulated climatological mean Atlantic meridional overturning streamfunction as a function of depth at 26°N in the National Center for Atmospheric Research (NCAR) OGCM forced with atmospheric reanalysis data with (black line) and without (gray line) the Nordic Seas overflow parameterization, compared with the RAPID data (dotted line), adapted from Danabasoglu et al. (2010), © Copyright 2010 AMS. (c, d) Simulated climatological mean Atlantic meridional overturning streamfunction in two Geophysical Fluid Dynamics Laboratory (GFDL) CGCMs coupled with an isopycnal-coordinate ocean component (c, CM2G) and a *z*-coordinate ocean component (d, CM2M) respectively, adapted from H. Wang, Legg, and Hallberg (2015). Reprinted from Ocean Modelling, 86, H. Wang, Legg, and Hallberg, Representations of the Nordic Seas overflows and their large-scale climate impact in coupled models, pp. 76–92, Copyright 2015, with permission from Elsevier.

meridional heat transport. For example, the simulated Atlantic meridional heat transport in most coupled or ocean-only general circulation models (CGCMs/OGCMs) is often substantially smaller than that observed (Figure 1a; Danabasoglu et al., 2014), which is closely related to the simulated shallower AMOC lower limb than that observed by the U.K.-U.S. Rapid Climate Change (RAPID) program (Figure 1b; e.g., Danabasoglu et al., 2014; Msadek et al., 2013; Roberts et al., 2013; Wang & Zhang, 2013; Wang et al., 2014). Climate models with parameterized or improved Nordic Seas overflows (a significant component of the deep AMOC) can simulate a deeper AMOC similar to that observed (Figure 1b) and thus enhanced Atlantic meridional heat transport (Danabasoglu et al., 2010; R. Zhang, Delworth, et al., 2011). CGCMs with a level-(*z*-)coordinate ocean component often simulate a much shallower AMOC due to excessive numerical diapycnal mixing (Figure 1d), whereas CGCMs with an isopycnal-coordinate ocean component often simulate a much deeper AMOC more comparable to observations (Figure 1c) due to more realistic diapycnal mixing and thus presumably a better representation of entrainment associated with the Nordic Seas overflow waters (H. Wang, Legg, & Hallberg, 2015).

The existence of the NADW formation and its connection to AMOC also make the Atlantic a formidably difficult region to model. The deficiency in modeling the mean state AMOC structure leads to a pronounced cold sea surface temperature (SST) bias in the midlatitude North Atlantic in many CGCMs (Wang et al., 2014). Stronger and more realistic Nordic Seas overflows can lead to a more realistic pathway of the North Atlantic Current through its interaction with the bathymetry and thus reduce the cold SST bias in the mid-latitude North Atlantic (e.g., R. Zhang, Delworth, et al., 2011; Talandier et al., 2014; H. Wang, Legg, & Hallberg, 2015). The simulated AMOC mean state bias is also tightly coupled to the substantial North Atlantic sea surface salinity (SSS) bias (especially over the NADW formation sites) in CGCMs (Drews et al., 2015; Park et al., 2016; Talandier et al., 2014). In addition to the biases in the mean state, the low-frequency AMOC variability at multidecadal timescales is also substantially underestimated in many CGCMs (Kim, Yeager, Chang, & Danabasoglu, 2018; Xu et al., 2018; Yan et al., 2018). This is likely linked to the mean state biases in the AMOC structure and the North Atlantic SST/SSS (Park et al., 2016) and the biases in the amplitudes of the anomalous surface heat and/or freshwater buoyancy forcing affecting the low-frequency AMOC variability (Kim, Yeager, Chang, & Danabasoglu, 2018; Xu et al., 2018). The above model deficiencies pose a serious challenge when using current CGCMs to understand and predict the role of AMOC in climate.

During the twentieth century, basin-scale multidecadal fluctuations have been observed in the Atlantic SST. Based on the pioneering analyses of the observed data over the North Atlantic region, Bjerknes (1964) hypothesized that the low-frequency AMOC variability associated with changes in NADW formation plays an active role in the observed basin-scale multidecadal variations in North Atlantic SST and associated sea level pressure (SLP) through related changes in Atlantic meridional heat transport and air-sea coupling. Bjerknes emphasized that the mechanisms at work at multidecadal timescales are quite different from those operating at interannual timescales. Many subsequent observational and climate modeling studies have lent support to Bjerknes' hypothesis (e.g., Delworth et al., 1993; Delworth & Mann, 2000; Deser & Blackmon, 1993; Enfield & Mestas-Nuñez, 1999; Folland et al., 1986; Kushnir, 1994; Latif et al., 2004; Schlesinger & Ramankutty, 1994). For example, at multidecadal timescales, the anomalous Atlantic SST pattern induced by AMOC variability in an unforced control simulation (i.e., with fixed external radiative forcing) of a CGCM is remarkably similar to that reconstructed from paleo records (Delworth & Mann, 2000). The large-scale multidecadal variability observed in the Atlantic has been referred to as the "Atlantic Multidecadal Oscillation (AMO)" to emphasize the "multidecadal" character of this oceanic phenomenon (Kerr, 2000) and particularly to distinguish it from interannual ocean variability forced by the leading mode of atmospheric circulation variability over the North Atlantic, the North Atlantic Oscillation (NAO; Enfield et al., 2001). Recent studies suggest that the term "Atlantic Multidecadal Variability (AMV)" is more appropriate than the term AMO, because the observed multidecadal fluctuations in the Atlantic may not be an oscillation at a single frequency but consist of a broader band of low-frequency signals (e.g., Sutton et al., 2018; Zhang, 2017). The transition between positive and negative AMV phases could have occurred through abrupt decadal shifts, involving various oceanic processes (e.g., Nigam et al., 2018; Thompson et al., 2010).

The traditional AMV index is often defined as a 10-year running mean (or low-pass filtering) of linearly detrended SST anomalies averaged over the entire North Atlantic, as first proposed by Enfield et al. (2001). This linear detrending does not cleanly separate the multidecadal variability from the nonlinear global-scale signal (Trenberth & Shea, 2006). A variety of alternative methods has been proposed to remove the nonlinear global-scale signal from the North Atlantic mean SST (e.g., Frajka-Williams et al., 2017; Frankignoul et al., 2017; Knight, 2009; Sutton et al., 2018; Terray, 2012; Ting et al., 2009; Trenberth & Shea, 2006; Yan et al., 2019). Many previous studies have consistently attributed observed AMV primarily to internal variability associated with the AMOC (e.g., DelSole et al., 2011; Knight, 2009; Ting et al., 2009; Trenberth & Shea, 2006; Z. Wu, Huang, et al., 2011; Zanchettin et al., 2014). On the other hand, some recent studies have proposed the hypotheses that AMV is primarily a direct response of the North Atlantic SST to either changes in external radiative forcing (e.g., Bellomo et al., 2018; Bellucci et al., 2017; Booth et al., 2012; Murphy et al., 2017) or stochastic atmospheric forcing (e.g., Cane et al., 2017; Clement et al., 2015, 2016), although these views have been questioned (e.g., Drews & Greatbatch, 2016, 2017; Kim, Yeager, & Danabasoglu, 2018; O'Reilly et al., 2016; Sun et al., 2018; Yan et al., 2017, 2018, 2019; Zhang, 2017; Zhang et al., 2013, 2016). The traditional AMV index, which is based on the North Atlantic SST anomalies as first proposed by Enfield et al. (2001), is convenient to use due to the availability of SST records over the instrumental period and the close linkage of SST with climate impacts. However, the above contrasting views on

the mechanisms of AMV underscore the need for a more holistic perspective that takes into account more than just North Atlantic SST anomalies. The debate over AMV mechanisms is related to the serious model deficiencies in current CGCMs. For example, the underestimated low-frequency AMOC variability in CGCMs may amplify the relative role of external radiative forcing or stochastic atmospheric forcing in AMV (Kim, Yeager, Chang, & Danabasoglu, 2018).

Many recent studies have identified a rich set of key elements of observed AMV, in addition to multidecadal North Atlantic SST variability. AMV is associated with a dipole SST pattern over the entire Atlantic (e.g., Hodson et al., 2010, 2014; Latif et al., 2006; Roberts et al., 2013; D. Zhang, Msadek, et al., 2011; Zhang et al., 2013) and with coherent multivariate low-frequency variability seen in, for example, subpolar North Atlantic ocean-driven surface turbulent heat fluxes, SST, sea surface salinity (SSS), upper ocean heat/salt content, and tropical North Atlantic subsurface temperature (e.g., Ba et al., 2013, 2014; Chen & Tung, 2014, 2018; Gulev et al., 2013; Robson, Sutton, Lohmann, et al., 2012; Robson et al., 2016; Wang et al., 2010; Wang & Zhang, 2013; Zhang, 2007, 2017; Zhang et al., 2013, 2016). The observed AMV index has also been defined alternatively as the difference between the standardized low-pass filtered subpolar North Atlantic mean SST anomalies and the anticorrelated standardized low-pass filtered SLP anomalies averaged over low-mid latitude North Atlantic (Klotzbach & Gray, 2008); the standardized low-pass filtered detrended subpolar North Atlantic mean SSS anomalies (Zhang, 2017); or the normalized leading principal component of combined detrended North Atlantic SST, SSS, and upper ocean heat/salt content anomalies using a multivariate analysis (Yan et al., 2019). The coherent multivariate low-frequency variability observed in the Atlantic provides important additional information that may help to resolve the controversies regarding the mechanisms of AMV that arise when SST is considered in isolation.

Numerous studies focusing on AMV and multidecadal AMOC variability have been strongly motivated by their significant impacts on many important climate phenomena, such as those on Intertropical Convergence Zone (ITCZ) shifts, Sahel/Indian summer monsoon rainfall, Atlantic hurricanes, and summer climate over Europe and North America (e.g., Folland et al., 1986; Goldenberg et al., 2001; Sutton & Hodson, 2005; Knight et al., 2006; Zhang & Delworth, 2006). In this synthesis paper, we review recent progress in understanding the role of AMOC in AMV and associated climate impacts, especially over the course of the U.K.-U.S. RAPID and U.S. AMOC programs. The central theme of this paper is related to, but has a different emphasis from, a recent review paper on AMOC by Buckley and Marshall (2016). In particular, the present review synthesizes the observed key elements of AMV, recent observational and modeling evidence for a leading order role for the AMOC and its associated Atlantic meridional heat transport in AMV, and many recent studies on AMOC/AMV-related impacts on various climate phenomena with important societal and economic implications. AMV and associated climate impacts are potentially predictable at the decadal timescale (e.g., Hermanson et al., 2014; Matei et al., 2012; Msadek et al., 2014; Robson, Sutton, & Smith, 2012, 2014; Yan et al., 2018; Yang et al., 2013; Yeager et al., 2012, 2015, 2018; Yeager & Robson, 2017; Zhang, 2017; Zhang & Zhang, 2015), and a better understanding of their linkage with the AMOC will be crucial for understanding the sources of decadal predictability and for improving future prediction skill of AMV and associated climate impacts. Understanding of these linkages is severely limited by the brevity of available instrumental data and biases in current climate model simulations. In this review, paleoclimate proxy records are thus also considered in tandem with modern observations and climate simulations to provide a comprehensive picture of the current scientific landscape with respect to AMOC-AMV-climate connections and the outstanding challenges that must be addressed to make further progress.

The structure of this review paper is as follows. We discuss the observed key elements of AMV in section 2, the observational and modeling evidence for the AMOC-AMV linkage in section 3, and the observed and simulated climate impacts of multidecadal AMOC variability and AMV in section 4. Related decadal predictability and prediction studies are discussed also in sections 3 and 4. Section 5 is devoted to the paleo evidence on AMV, multidecadal AMOC variability, and associated climate linkages. Conclusions and challenging issues are presented in section 6.

2. Observed Key Elements of AMV

This section reviews recent studies on the observed key elements of AMV, including the SST pattern associated with AMV and its time evolution, AMV-related coherent multivariate variability, and the relative

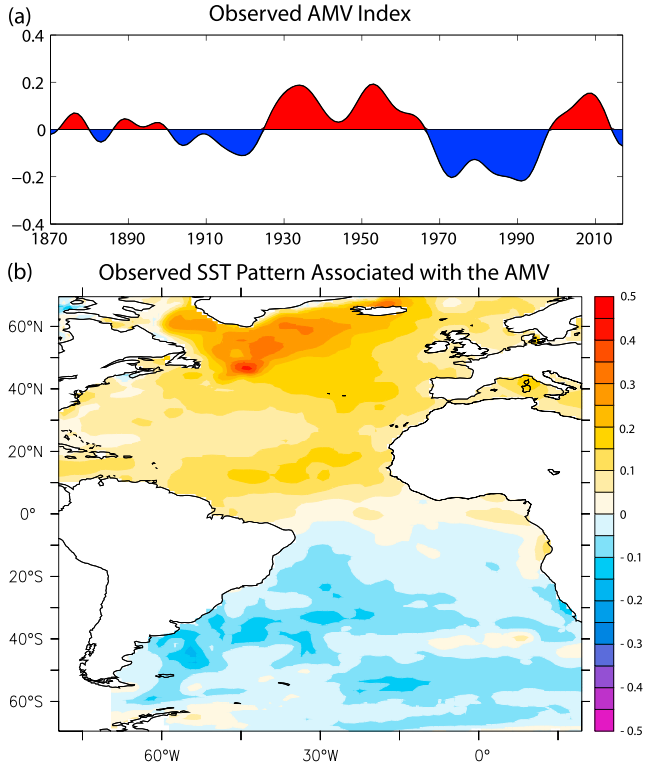

Figure 2. Observed AMV index and SST pattern associated with AMV derived from Hadley Centre Sea Ice and Sea Surface Temperature data set (HADISST) data set (Rayner et al., 2003). (a) Observed AMV index, defined as the 10-year low-pass-filtered area-weighted average of residual SST anomalies over the North Atlantic (80°W to 0°E, 0–65°N). The residual SST anomaly at each grid point is computed by removing the local component regressed on the global mean SST anomaly. This nonlinear detrending method for AMV has also been used in Gulev et al. (2013) and Frankignoul et al. (2017) to remove the nonuniform global scale signal, but it neglects the contribution of AMV to the global scale signal. (b) Observed SST pattern associated with AMV, that is, regression of residual SST anomalies on the observed AMV index shown in (a).

importance of Atlantic variability at the low frequency band (multidecadal timescales) compared with that at the high frequency band (interannual timescales). The observed AMV refers to the large-scale variability in the Atlantic at multidecadal timescales that might be caused by internal variability, changes in external forcing, or a combination of both. The observed key elements represent a crucial benchmark for understanding the mechanisms of AMV.

2.1. Observed SST Pattern Associated With AMV

The observed AMV index (with the component regressed on the global-scale climate change signal removed) exhibits pronounced multidecadal variations: Positive phases occurred during the middle of the twentieth century and since around 1995, and negative phases occurred during the early twentieth century and during the 1964–1995 period (Figure 2a). The SST pattern associated with AMV is often derived by regressing detrended SST anomalies on the AMV index (Knight et al., 2005; Ruiz-Barradas et al., 2013; Sutton & Hodson, 2005). The positive AMV phase is characterized in observations by a horseshoe pattern of anomalous warming over the North Atlantic (with stronger amplitudes in the subpolar region) and a much weaker anomalous cooling over the South Atlantic (Figure 2b). This SST dipole over the entire Atlantic resembles the interhemispheric asymmetric SST response to an abrupt AMOC weakening simulated in many CGCMs with a flipped sign (e.g., Dahl et al., 2005; Dong & Sutton, 2002, 2007; LeGrande et al., 2006; Stouffer et al., 2006; Timmermann et al., 2007; Vellinga & Wood, 2002; Zhang & Delworth, 2005), suggesting that multidecadal variations of the AMOC and associated Atlantic meridional heat transport are important for the observed AMV (Hodson et al., 2010, 2014; Latif et al., 2006; Roberts et al., 2013; Zhang et al., 2013; D. Zhang, Msadek, et al., 2011). Furthermore, the dipole SST pattern over the entire Atlantic is an observed key element of AMV and is linked to the observed bipolar seesaw pattern over the twentieth century, that is, anticorrelated multidecadal variations between the Arctic and Antarctic surface air temperature (Chylek et al., 2010), which will be discussed in section 4.6.

Over the North Atlantic, the observed monopolar SST pattern associated with AMV can be distinguished from the tripolar SST pattern (opposite sign in the subtropical region from that in the subpolar and tropical areas) induced by the NAO at interannual timescales (Cayan, 1992; Delworth et al., 2017; Deser et al., 2010; Kushnir, 1994; Marshall et al., 2001; Visbeck et al., 2003). The high spatial coherence of the observed AMV SST pattern over the entire North Atlantic is another key observed feature of AMV that can be reproduced in CGCMs showing a relatively strong linkage/correlation between the AMOC and AMV (e.g., Danabasoglu et al., 2012; Sun et al., 2018). The time evolution of the observed North Atlantic SST pattern associated with AMV reveals that the SST signal in the middle- to high-latitude North Atlantic lasts longer (i.e., appears earlier and decays later) than the SST signal in other regions and that it propagates into the tropical North Atlantic along a horseshoe pathway (Drews & Greatbatch, 2017; Kavvada et al., 2013; Ruiz-Barradas et al., 2013). Similarly, during the negative shift of AMV in the 1960s and 1970s, the stronger surface cooling in the subpolar North Atlantic led the weaker surface cooling in the tropical North Atlantic by 2 years and persisted longer, suggesting that the weaker tropical AMV signal may have responded to the stronger extratropical AMV signal (Hodson et al., 2014).

2.2. Observed Coherent Multivariate Variability Associated With AMV

Observational evidence suggests that AMV is associated with coherent multidecadal variability in surface turbulent heat fluxes over the midlatitude North Atlantic, a region characterized by large climatological surface turbulent heat fluxes (Figure 3a), with more (less) heat released into the atmosphere during a positive

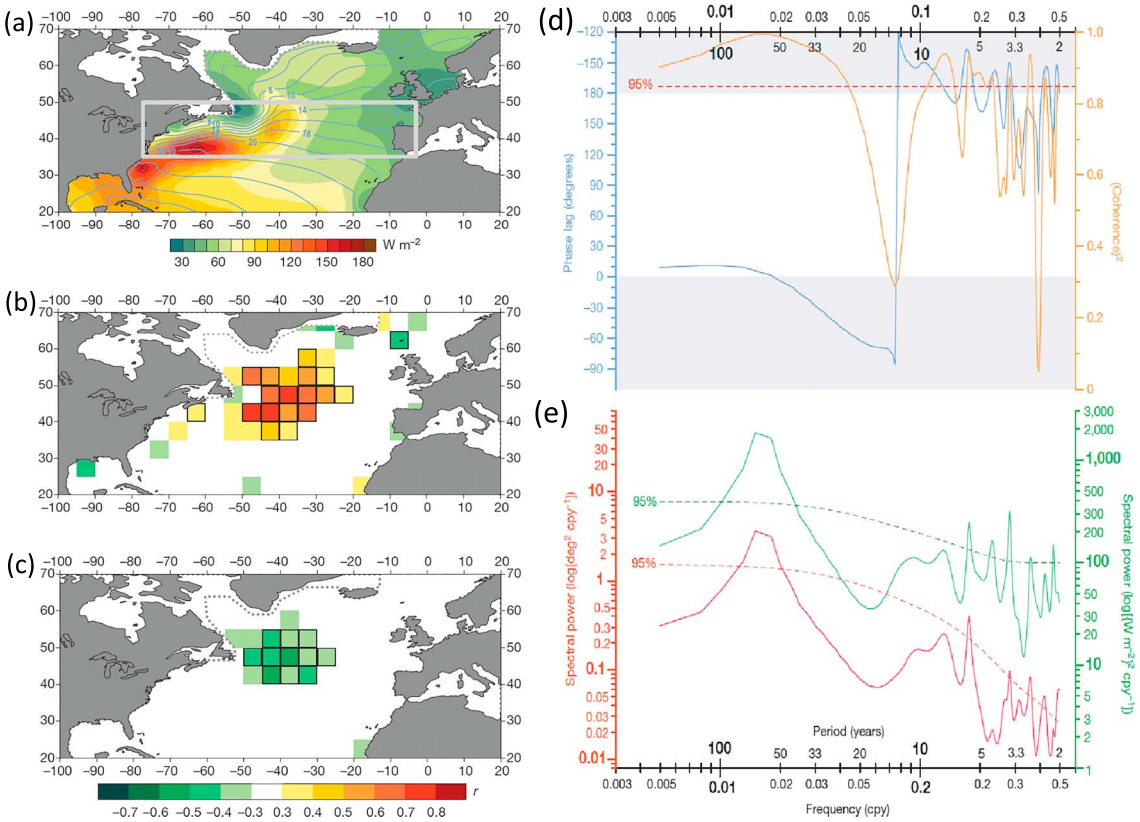

Figure 3. Observed North Atlantic SST and surface turbulent heat fluxes and the correlations/cross spectra between their detrended anomalies. Positive heat fluxes indicate the heat being transferred from ocean to atmosphere. (a) Spatial maps of observed climatological SST (contour lines) and surface turbulent heat fluxes (color shading). (b, c) Correlations between the observed detrended North Atlantic SST index averaged over the midlatitudes (35–50°N) and the observed local detrended anomalous surface turbulent heat fluxes (sensible plus latent heat fluxes) for the multidecadal long-term component (b) and the interannual short-term component (c), separated based on an 11-year running mean. Black boxes in (b, c) indicate the 95% significance level. (d) Squared coherence (orange) and phase lag (blue) between observed detrended midlatitude North Atlantic SST index and surface turbulent heat fluxes over central midlatitude North Atlantic. A phase lag close to 0 (180°) indicates that SST and surface fluxes are in-phase (antiphase). Gray shading shows the range of negative phase lags. (e) Power spectra of the above SST index (red) and surface turbulent heat fluxes (green). There is a significant peak around 60-year period in both spectra. Thin dashed lines in (d, e) indicate 95% significance levels. Frequencies on the *x* axis are in cycles per year (cpy) and corresponding periods in years are indicated. Adapted from Gulev et al. (2013). Reprinted by permission from Springer Customer Service Centre GmbH: Springer Nature, Nature, North Atlantic Ocean control on surface heat flux on multidecadal timescales, Gulev et al., Copyright 2013.

(negative) AMV phase (Figure 3b; Gulev et al., 2013). Hence, the surface turbulent heat fluxes provide a negative feedback to SST anomalies on multidecadal timescales. This relationship is reversed at interannual timescales (i.e., stronger surface turbulent heat loss is associated with reduced SST and vice versa, Figure 3c), supporting the hypothesis first proposed by Bjerknes (1964) that at multidecadal timescales ocean dynamics play an active role in the observed AMV, while at interannual timescales the North Atlantic Ocean is passively forced by the atmosphere. The cross-spectral analysis between observed SST and surface turbulent heat flux anomalies averaged over the region consistently reveals their in-phase relationship at multidecadal timescales and out-of-phase relationship at interannual timescales, with a sharp transition in between (Figure 3d; Gulev et al., 2013). Similar results have been found in recent modeling studies, that is, there is a positive correlation (or regression) between the net upward surface heat flux and SST anomalies associated with AMV in the subpolar North Atlantic in CGCMs (Drews & Greatbatch, 2016, 2017; O'Reilly et al., 2016; Yan et al., 2018; Zhang, 2017; Zhang et al., 2016). At low frequencies, the correlation and regression between the net upward surface heat flux and SST anomalies are key indicators of the relative roles of oceanic versus atmospheric forcing in driving SST anomalies, with a larger positive regression coefficient indicating a stronger role for oceanic forcing (Zhang, 2017).

Many recent studies have indicated that observed AMV is associated with coherent multidecadal variations in subpolar North Atlantic SST, SSS, and upper ocean heat/salt content. For example, observational analyses

demonstrate that multidecadal subpolar North Atlantic SSS variations are coherent and in-phase with the subpolar AMV SST signal (e.g., Friedman et al., 2017; Zhang, 2017; Zhang et al., 2013) and lead the tropical AMV SST signal by about 2 years (Zhang, 2007). The observed AMV signal is also evident in coherent multidecadal variations of the subpolar North Atlantic upper ocean heat and salt content (e.g., Chen & Tung, 2014, 2018; Frajka-Williams et al., 2017; Häkkinen et al., 2013; Kavvada et al., 2013; Polyakov et al., 2010; Robson et al., 2016; Robson, Sutton, Lohmann, et al., 2012; Seidov et al., 2017; Wang et al., 2010; Yeager & Danabasoglu, 2014; Zhang, 2008, 2017). Significantly high coherence between observed detrended subpolar North Atlantic SST (upper ocean heat content) and SSS (upper ocean salt content) anomalies only exists at low frequencies (multidecadal timescales) and not at high frequencies (interannual timescales), as also found in a CGCM (Zhang, 2017). The contribution of oceanic advective processes to the time tendency of SST and SSS becomes more important at longer timescales, and at decadal and longer timescales, the subpolar North Atlantic SST and SSS anomalies are mainly forced by the oceanic advective processes and not by atmospheric heat/freshwater fluxes or Ekman transport (Mignot & Frankignoul, 2003), consistent with Bjerknes' hypothesis. The ratio of contributions from oceanic advective processes to atmospheric fluxes/Ekman transport is even higher for SSS than for SST (Mignot & Frankignoul, 2003). Cross-spectral analysis suggests that at multidecadal timescales, both the observed subpolar North Atlantic SST (upper ocean heat content) and SSS (upper ocean salt content) variations are dominated by ocean dynamics, whereas at interannual timescales, they are mainly forced by stochastic flux exchange with the atmosphere (Zhang, 2017). The observed AMV and upper subpolar North Atlantic temperature are also anticorrelated with multidecadal variations of deep subpolar North Atlantic temperature, which are closely linked to changes in NADW (Kim, Yeager, & Danabasoglu, 2018; Polyakov et al., 2010). Over the tropical North Atlantic, the observed multidecadal SST variations associated with AMV are significantly anticorrelated with the observed multidecadal variations in the subsurface temperature (e.g., Polyakov et al., 2010; Wang et al., 2010; Wang & Zhang, 2013; Zhang, 2007). This depth dependence of tropical ocean temperature anomalies associated with AMV is also seen in CGCMs subject to abrupt AMOC change (Chiang et al., 2008; Zhang, 2007).

2.3. Frequency Domain Characteristics of the Observed AMV

The null hypothesis for extratropical SST variability has been in general a “red noise” response to atmospheric “white noise” forcing and thus is characterized by a red noise power spectrum and an exponentially decaying autocorrelation with a short persistence timescale of a few months (e.g., Frankignoul, 1985; Frankignoul & Hasselmann, 1977; Hasselmann, 1976; Reynolds, 1978). A key question is whether SST anomalies associated with observed AMV are just the multidecadal component of a red noise process or whether they exhibit enhanced multidecadal power above that expected from a red noise process. If the observed Atlantic SST anomalies were a red noise response, their autocorrelation would be dominated by a rapid exponential decay with a short decorrelation timescale and would not be predictable at the decadal timescale. In regions with deep winter mixed layers, the SST anomalies for only winter months would have a longer (interannual) persistence timescale; however, when all months of the year are considered, the autocorrelation of SST anomalies would have a shorter persistence timescale than that obtained by considering only winter SST anomalies (Deser et al., 2003).

The success of many recent initialized decadal prediction experiments in reproducing the observed subpolar AMV signal at decadal lead times (e.g., Hermanson et al., 2014; Matei et al., 2012; Msadek et al., 2014; Robson, Sutton, & Smith, 2012, 2014; Yang et al., 2013; Yeager et al., 2012, 2015, 2018; Yeager & Robson, 2017) contrasts sharply with low predictability expected from the red noise hypothesis. Moreover, spectra of observed SST and surface turbulent heat flux anomalies over the midlatitude North Atlantic both exhibit a significant peak at multidecadal timescales, inconsistent with a red noise process (Figure 3e; Gulev et al., 2013). The autocorrelations of the observed monthly subpolar North Atlantic SST and SSS variations (with all months of the year considered) do not have the form of a simple exponential decay; they exhibit a kink separating two different persistent timescales (Zhang, 2017). For shorter time lags (high-frequency component), the autocorrelations can be explained by the red noise process with a short exponential decay timescale; for longer time lags (low-frequency component), the autocorrelations diverge from the red noise fit and exhibit decadal persistence. The percentages of the total variance (power) explained by the multidecadal component in their corresponding power spectra are also much higher than that expected from a red noise

process, consistent with their much higher autocorrelations at longer time lags. This observed key element of AMV is also simulated in a CGCM control simulation where it can be linked to multidecadal AMOC variability (Zhang, 2017).

Most instrumental records are too short to adequately resolve multidecadal characteristics of the observed AMV. The world's longest instrumental temperature record is the 353-year extended data of Central England Temperature; this record varies in phase at multidecadal timescales with the observed AMV index over the industrial era, suggesting that it is a reasonable AMV proxy; a wavelet analysis of this record exhibits significant multidecadal variability above a red noise background (Tung & Zhou, 2013). Other, longer, proxies for AMV also show significant multidecadal variability above the background red noise level (section 5).

2.4. Summary

In this section, we have reviewed the following observed key elements of AMV:

1. SST anomalies associated with observed AMV exhibit a dipole pattern over the entire Atlantic and a monopolar pattern over the North Atlantic with high spatial coherence.
2. The AMV SST signal is characterized by propagation from the extratropical North Atlantic into the tropical North Atlantic along a horseshoe pathway.
3. The observed AMV is correlated with multidecadal variations in the ocean-driven surface turbulent heat fluxes, with more heat released from the midlatitude North Atlantic Ocean into the atmosphere during a positive AMV phase.
4. There is high coherence between observed subpolar North Atlantic SST, SSS, and upper ocean heat and salt content variations but only for low frequencies (i.e., multidecadal timescales). The variations in the upper and deep subpolar North Atlantic temperature associated with AMV are anticorrelated.
5. The observed tropical North Atlantic surface and subsurface temperature variations associated with AMV are also significantly anticorrelated.
6. The autocorrelations of the observed subpolar North Atlantic SST and SSS clearly deviate from that expected from a red noise process in that they exhibit decadal persistence, corresponding to multidecadal peaks in spectral power.

The above-observed key elements of AMV should be considered together in order to develop a complete understanding of the driving mechanisms of AMV.

3. AMOC-AMV Linkage

This section reviews a few hypotheses for AMV mechanisms without an essential role for AMOC, the most recent studies on observational and modeling evidence for the linkage between multidecadal AMOC variability and AMV, the relationship of this linkage with Atlantic decadal predictability and prediction, and the origins of observed key elements of AMV.

3.1. Hypotheses for AMV Mechanisms Without an Essential Role for AMOC

Several hypotheses for AMV mechanisms without an essential role for AMOC have been proposed recently. For example, the observed AMV is explained mainly as a direct response of the North Atlantic SST to changes in external radiative forcings (Bellomo et al., 2018; Bellucci et al., 2017; Booth et al., 2012; Dunstone et al., 2013; Mann & Emanuel, 2006; Murphy et al., 2017). In particular, anthropogenic aerosols are implicated as a prime driver of the observed AMV, because the observed AMV index (based on linearly detrended basin-averaged low-pass-filtered North Atlantic SST anomalies) is well reproduced in the twentieth-century externally forced CGCM historical simulations if aerosol indirect effects are included (Figure 4a; Booth et al., 2012). That is, an increase in the linearly detrended AMV SST index is forced by the increased downward shortwave radiative heat flux induced by the decreased anthropogenic aerosols through their interaction with clouds (Booth et al., 2012). However, the simulations examined by Booth et al. (2012) substantially underestimated the observed warming trend in the North Atlantic upper ocean heat content, suggesting that the aerosol indirect effects are strongly overestimated in the model (Zhang et al., 2013). Furthermore, the observed decline in the subpolar AMV SST signal over the most recent decade is inconsistent with the recently observed change (a slight decrease) in anthropogenic aerosols over the North Atlantic region but consistent with the directly observed AMOC decline over this period (e.g.,

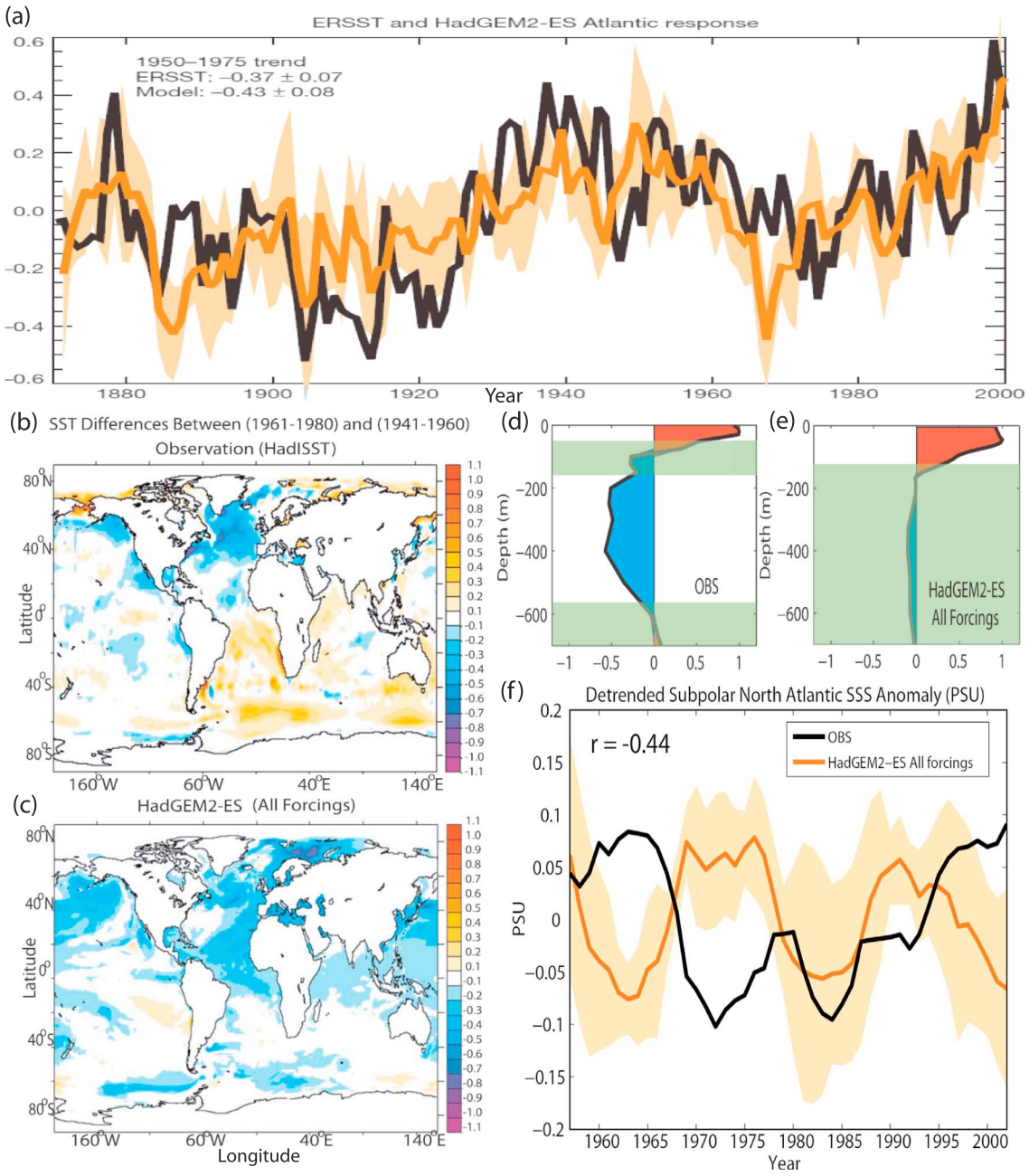

Figure 4. Comparison of observations (OBS) with results from the ensemble mean externally forced historical simulation of the CGCM with aerosol indirect effects (HadGEM2-ES) used in Booth et al. (2012). (a) Area-averaged North Atlantic SST anomalies from HadGEM2-ES (orange line: ensemble mean; shading: spread) and from the U.S. National Oceanic and Atmospheric Administration's Extended Reconstructed SST, that is, ERSST (black line), adapted from Booth et al. (2012). Reprinted by permission from Springer Customer Service Centre GmbH: Springer Nature, Nature, Aerosols implicated as a prime driver of twentieth-century North Atlantic climate variability, Booth et al., Copyright 2012. (b, c) SST difference pattern (K) between negative (1961–1980) and positive (1941–1960) AMV epochs. (d, e) Regression of averaged tropical North Atlantic Ocean temperature anomaly at different depths on the standardized tropical North Atlantic SST anomaly, normalized by the maximum absolute value of each regression, respectively (green shading: not statistically significant at the 90% level). (f) Detrended subpolar North Atlantic SSS anomalies (PSU) from HadGEM2-ES (orange line: ensemble mean; shading: spread) and from observations (black line), both are pentadally averaged and there is an anticorrelation between them ($r = -0.44$). Panels (b–f) are adapted from Zhang et al. (2013), © Copyright 2013 AMS.

Robson et al., 2016; Smeed et al., 2018; Yan et al., 2017). In a recent study, the high correlation between the observed AMV index (based on linearly detrended basin-averaged low-pass-filtered North Atlantic SST anomalies) and the simulated ensemble mean AMV index from a large ensemble of twentieth-century

historical simulations has been shown to arise by coincidence from concurrent warming (via different mechanisms) after the 1990s (Kim, Yeager, & Danabasoglu, 2018).

The variances of the linearly detrended AMV SST index in CGCM historical simulations are significantly affected by the externally forced component and are larger than those in unforced simulations, leading to the conclusion that external radiative forcings are essential in driving the observed AMV (Murphy et al., 2017; Bellomo et al., 2017). However, the amplitudes of the unforced component of AMV and multidecadal AMOC variability in most CGCMs are substantially underestimated due to model deficiencies (e.g., Kim, Yeager, Chang, & Danabasoglu, 2018; Park et al., 2016; Yan et al., 2018), and this underestimation amplifies the relative role of external radiative forcings in AMV (Kim, Yeager, Chang, & Danabasoglu, 2018). In contrast to the proposed essential role of external radiative forcings in driving the observed AMV (e.g., Bellomo et al., 2017; Bellucci et al., 2017; Booth et al., 2012; Dunstone et al., 2013; Mann & Emanuel, 2006; Murphy et al., 2017), hindcasts with prescribed changes in external radiative forcings but no initialization in ocean states are not able to predict the observed AMV (Hermanson et al., 2014; Kim, Yeager, & Danabasoglu, 2018; Matei et al., 2012; Msadek et al., 2014; Robson, Sutton, & Smith, 2012, 2014; Yeager et al., 2012, 2018; Yeager et al., 2018).

The aerosol-forcing mechanism for the observed AMV is supported by the close match in the linearly detrended North Atlantic SST time series between observations and the externally forced response simulated in some climate models (e.g., Booth et al., 2012) but is not supported by many of the observed key elements of AMV reviewed in section 2. For example, the simulated response to anthropogenic aerosols (Booth et al., 2012) does not explain the observed Atlantic dipole SST pattern (Figures 4b and 4c) and the observed anticorrelation between multidecadal tropical North Atlantic surface and subsurface temperature variations (Figures 4d and 4e). The simulated detrended subpolar North Atlantic SSS anomalies in Booth et al. (2012) are anticorrelated with the observed detrended subpolar North Atlantic SSS anomalies (Figure 4f), which have been shown to vary coherently with the observed subpolar AMV SST signal at low frequencies (Zhang et al., 2013). The aerosol-forcing mechanism also fails to explain the observed AMV-related anticorrelated multidecadal variations between upper and deep subpolar North Atlantic temperature (Kim, Yeager, & Danabasoglu, 2018) and the observed propagation of the extratropical AMV SST signal into the tropics. In summary, many observed key elements of AMV reviewed in section 2 are incompatible with the hypothesis that the observed AMV is primarily driven by changes in external radiative forcing. Additionally, the resemblance in the linearly detrended basin-averaged SST-based AMV index between the observation and the externally forced response simulated in some climate models could be an artifact of linear detrending; the resemblance breaks down using the nonlinear detrending method with the signal associated with the global mean SST removed (Yan et al., 2019).

Volcanic aerosols have also been proposed as an important pacemaker for AMV through their direct radiative impact on tropical North Atlantic SSTs and indirect impact on the winter NAO and associated multidecadal AMOC changes (Otterå et al., 2010). Ensemble simulations of the last millennium using various combinations of external forcings suggest that, in general, volcanic aerosols act to amplify AMV by inducing positive AMOC anomalies that persist for decades (Otto-Bliesner et al., 2016). Other modeling studies suggest that the influence of volcanic aerosols on AMOC variability is mainly at the bidecadal (~20-year) timescale through the interaction with freshwater flux entering the North Atlantic (e.g., Swingedouw et al., 2015), and the sign of the AMOC response could be opposite depending on the size of the volcanic eruptions (e.g., Mignot et al., 2011; Swingedouw et al., 2015). As will be discussed in section 5.1, the comparison of long paleo reconstructed AMV index with various solar and volcanic forcing reconstructions suggest that changes in solar and volcanic forcing have affected AMV, but their combined contribution explains less than one third of AMV variance over the past 12 centuries (J. Wang, Yang, et al., 2017).

More recently, AMV has been proposed to be a direct red noise response of the North Atlantic SST to stochastic atmospheric-induced surface heat flux forcing, without a role for ocean heat transport/circulation changes, because the North Atlantic SST patterns associated with AMV (Figures 5a and 5b) and the North Atlantic SST spectra are similar in CGCMs with ocean dynamics and in slab ocean models (i.e., models with their atmospheric component coupled to a slab ocean) without ocean dynamics (Clement et al., 2015). However, the fundamental equations and mechanisms for AMV are very different between CGCMs and slab ocean models (Zhang et al., 2016). In contrast to slab ocean models, multidecadal net downward surface heat

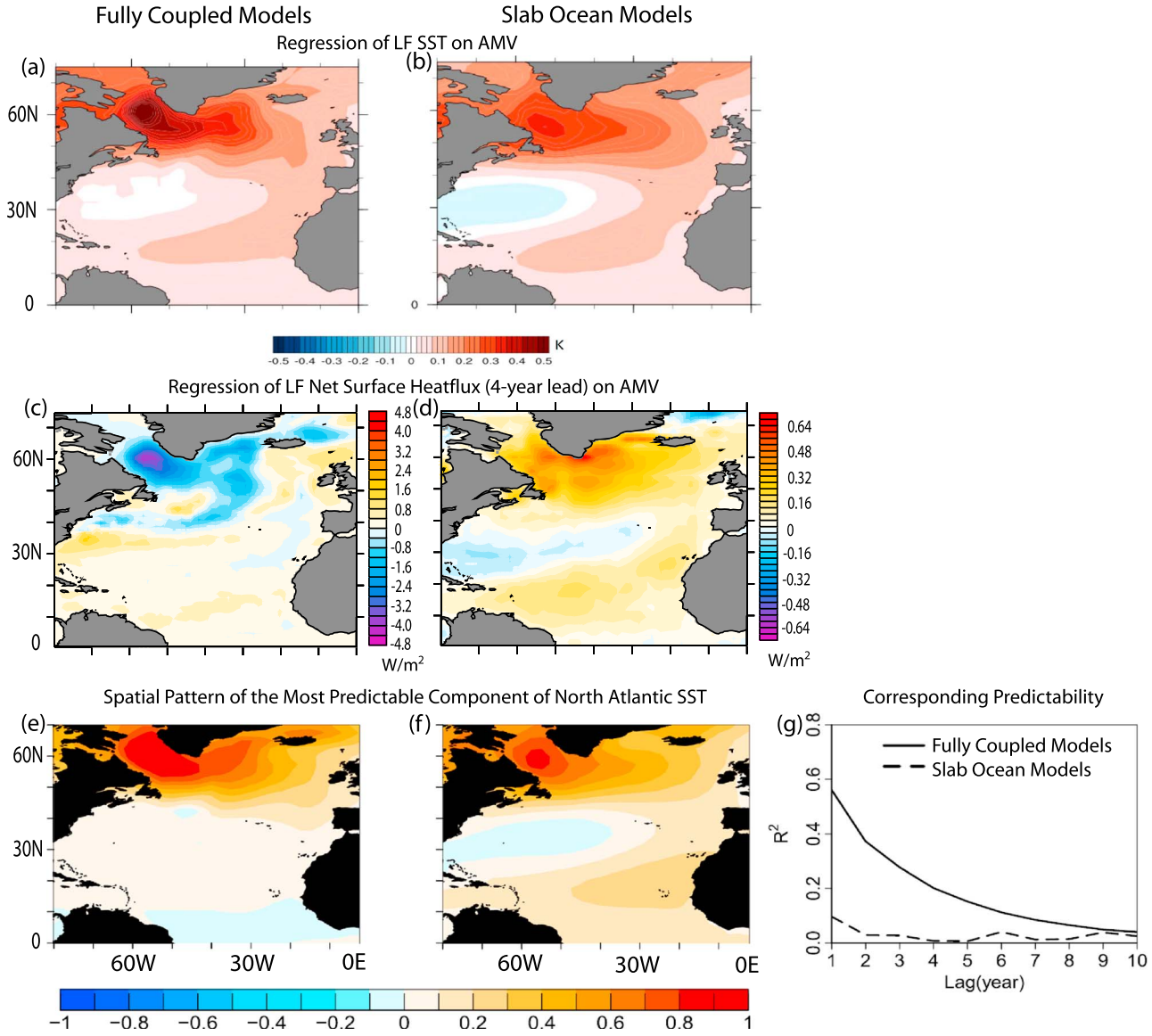

Figure 5. Comparison of results in control simulations from a subset of Coupled Model Intercomparison Project Phase 3 (CMIP3) CGCMs and slab ocean models (i.e., models with their atmospheric component coupled to a slab ocean). (a, b) Multimodel mean regression of the 10-year low-pass-filtered (LF) North Atlantic SST anomalies on the standardized AMV index in CGCMs (a) and slab ocean models (b) from Clement et al. (2015). Reprinted with permission from AAAS. (c, d) Multimodel mean regression of LF North Atlantic net downward surface heat flux anomalies on the standardized AMV index with the AMV index lagged by 4 years in CGCMs (c) and slab ocean models (d) from Zhang et al. (2016). Reprinted with permission from AAAS. (e–g) Multimodel mean spatial patterns of the most predictable component in the North Atlantic SST in CGCMs (e) and slab ocean models (f) and the corresponding predictability (g) from Yan et al. (2018). Each spatial pattern in (e, f) has no unit, and the multiplication of the spatial pattern and its corresponding time series (which carries the unit K) gives the temperature variations.

flux anomalies in CGCMs do not serve as a forcing for AMV but have a negative correlation/regression with AMV over the subpolar North Atlantic to damp the effect of the anomalous ocean heat transport convergence (Figures 5c and 5d). This negative correlation is consistent with observations (Gulev et al., 2013) and many other recent analyses using CGCMs (Drews & Greatbatch, 2016, 2017; O'Reilly et al., 2016). Note here the net surface heat flux is positive downward (Figures 5c and 5d), whereas the surface turbulent heat fluxes shown in Figure 3 are positive upward. In a red noise model, without the realistic damping of SST from subsurface ocean temperature, the negative correlation between multidecadal net downward surface heat flux anomalies and AMV is interpreted as a result of negligible oceanic forcing with stochastic atmospheric noise as the main AMV driver (Cane et al., 2017; Clement et al., 2016).

However, when realistic oceanic damping is included in the equation for SST anomalies, the negative correlation/regression between net downward surface heat flux and SST anomalies at low frequencies indicates an essential role of ocean dynamics in AMV (Zhang, 2017). The slab ocean models without oceanic damping also overestimate the amplitude of the SST response to atmospheric-induced surface heat flux forcing (Garuba et al., 2018). The phase relationship between the atmospheric circulation mode (e.g., winter NAO) and the North Atlantic SST at multidecadal timescales is also very different between the slab ocean models and the CGCMs, with ocean dynamics playing a central role in connecting the winter NAO with multidecadal subpolar SST anomalies in CGCMs (Delworth et al., 2017).

In addition to the discrepancy in the relationship between multidecadal surface heat flux anomalies and AMV, the hypothesis that AMV is a red noise process forced by stochastic atmospheric white noise likewise cannot explain many other observed key elements of AMV reviewed in section 2, including the observed Atlantic dipole SST pattern associated with AMV and the observed anticorrelation between multidecadal tropical North Atlantic surface and subsurface temperature variations associated with AMV. The observed monopolar AMV SST pattern with high spatial coherence over the entire North Atlantic can be simulated in CGCMs showing a relatively strong linkage/correlation between the AMOC and AMV, whereas in slab ocean models the SST anomalies associated with AMV over the midlatitude western North Atlantic have an opposite sign with those over other regions of the North Atlantic (Sun et al., 2018). This red noise forcing mechanism is incompatible with high coherence among observed subpolar North Atlantic SST, SSS, upper ocean heat and salt content at multidecadal (but not at interannual) timescales, and decadal persistence of observed subpolar North Atlantic SST and SSS variations and much higher multidecadal power (above a red noise level) in their spectra (Zhang, 2017). Hence, the red noise mechanism as found in slab ocean models implies no decadal predictability other than the simple short persistence, and the most predictable component of the North Atlantic SST persists much longer with much higher predictability in CGCMs than in slab ocean models (Figures 5e–5g), due to the important role of ocean dynamics in CGCMs (Yan et al., 2018).

3.2. Observational and Modeling Evidence for the AMOC-AMV Linkage

3.2.1. Linkage Indicated by Observed AMOC Fingerprints

The AMOC strength/index generally refers to the maximum value of the meridional overturning streamfunction (i.e., the maximum Atlantic meridional volume transport) at a specific latitude. Direct continuous full-depth observations of the AMOC strength at 26°N were first established in 2004 by the U.K.-U.S. RAPID program (e.g., Cunningham et al., 2007; Kanzow et al., 2007; McCarthy et al., 2012; Smeed et al., 2014, 2018; Srokosz & Bryden, 2015). Since there are no direct continuous observations of the AMOC before 2004, it is necessary to reconstruct historical multidecadal AMOC variability using longer, observed AMOC fingerprints to understand the linkage of AMOC with the observed AMV. As discussed above, the AMOC-induced change in tropical North Atlantic subsurface temperature is anticorrelated with tropical North Atlantic SST and can be used as an AMOC fingerprint to infer past AMOC changes (Zhang, 2007). This is because the weakening of NADW formation and AMOC leads to surface cooling associated with the southward shift of the ITCZ (to be discussed in detail in section 4.1) and subsurface warming associated with the thermocline deepening as simulated in a CGCM. The observed detrended tropical North Atlantic surface and subsurface temperature anomalies also exhibit anticorrelated multidecadal variations and the inferred historical multidecadal AMOC variability from this observed AMOC fingerprint (i.e., detrended multidecadal tropical North Atlantic subsurface temperature anomaly) is closely linked to the observed AMV signal (Zhang, 2007).

The leading mode of detrended subsurface (e.g., 400 m) temperature (or upper ocean heat content) anomalies in the extratropical North Atlantic has been proposed as another independent AMOC fingerprint (Zhang, 2008). Low-frequency AMOC variability associated with changes in NADW formation leads to opposite-sign anomalous horizontal gyre circulations and related dipole subsurface temperature (or upper ocean heat content) pattern with opposite-sign anomalies in the subpolar gyre and the Gulf Stream region, as simulated in CGCMs' control simulations (Yan et al., 2017, 2018; Zhang, 2008). A stronger AMOC at northern high latitudes is triggered by a stronger NADW formation; a few years later, it leads to a warmer, weaker, and contracted subpolar gyre coupled with a westward shift of the North Atlantic Current path and a colder stronger northern recirculation gyre coupled with a southward shift of the Gulf Stream path. Hence, meridional shifts of the Gulf Stream path are anticorrelated with AMOC strength at multidecadal timescales (Joyce & Zhang, 2010; Nye et al., 2011; Sanchez-Franks & Zhang, 2015; Yeager, 2015; Zhang, 2008). The

coupling between the AMOC and the horizontal gyre circulations involves the interaction between the deep flow of NADW and the complicated bathymetry in the North Atlantic Ocean (Yeager, 2015; Zhang, 2008; R. Zhang, Delworth, et al., 2011; Zhang & Vallis, 2007). The observed extratropical AMOC fingerprint exhibits a similar dipole pattern (Figure 6a) and historical multidecadal AMOC variability inferred from this observed extratropical AMOC fingerprint (weaker AMOC from mid-1960s to mid-1990s and stronger AMOC before and afterward) is also closely linked to the observed AMV signal (Yan et al., 2017; Zhang, 2008). This is consistent with the observed anticorrelated relationship between AMV and multidecadal variations in the subpolar gyre strength (Hátún et al., 2009).

3.2.2. Linkage Indicated by Directly Observed AMOC Changes Over the Recent Decade

The directly observed AMOC at 26°N from the RAPID program exhibits a significant downward shift over the recent decade since 2004, which has been widely interpreted as arising from intrinsic decadal/multidecadal AMOC variability and a reversal from the previous AMOC strengthening (e.g., Jackson et al., 2016; Robson, Hodson, et al., 2014; Robson et al., 2016; Smeed et al., 2014, 2018; Yan et al., 2017, 2018). The total reduction of the directly observed AMOC at 26°N between 2004–2009 and 2009–2014 is 2.9 Sv and is statistically significant (Frajka-Williams et al., 2016). The directly observed AMOC downward shift at 26°N over the recent decade is reproduced in an eddy-permitting data-constrained ocean state estimate (Jackson et al., 2016) but is less evident in a relatively coarse-resolution data-constrained ocean state estimate, in which the AMOC variability is indistinguishable from a stationary Gaussian red noise process (Wunsch & Heimbach, 2013). This directly observed AMOC weakening is consistent with that inferred and predicted using the observed extratropical AMOC fingerprint (Mahajan, Zhang, Delworth, Zhang, et al., 2011; Smeed et al., 2018; Yan et al., 2017, 2018) and the observed decline in AMV (Robson et al., 2016; Yan et al., 2017) over this period. The recent observed cooling trend in the subpolar North Atlantic upper ocean temperature since 2005 (Figure 6b) is closely linked to the observed decline in the AMOC, which is supported by both observations and the control simulation of a high resolution CGCM (Robson et al., 2016). The recent cooling trend since 2005 in the subpolar North Atlantic is also accompanied by a warming trend over the Gulf Stream region (Figure 6b). Such a dipole pattern is consistent with an AMOC decline indicated by the extratropical AMOC fingerprint (Figure 6a; Yan et al., 2017; Smeed et al., 2018) and the directly observed AMOC weakening at 26°N from the RAPID program since 2004 (Figure 6c; e.g., Frajka-Williams et al., 2016; Smeed et al., 2018). In addition to the buoyancy-driven component, the AMOC also includes a wind-driven component that is closely coupled to horizontal gyres on seasonal timescales (e.g., Yang, 2015). Observations reveal an abrupt substantial weakening in the Ekman (i.e., the direct wind-driven) component of the AMOC during 2009–2010, which recovers soon thereafter (Figure 6c; Frajka-Williams et al., 2016; Smeed et al., 2018). Hence, over the recent decade since 2004, there is no significant downward trend in the Ekman component of the AMOC, and the observed decadal AMOC decline is in the non-Ekman AMOC component associated mainly with the reduced southward NADW flow at the depth range of 3,000–5,000 m (Figure 6c; Frajka-Williams et al., 2016; Smeed et al., 2018).

The recent cooling trend in the subpolar North Atlantic is mainly caused by the reduced ocean heat transport at the southern boundary of the region around 46°N associated with the decreased northward North Atlantic Current and the increased southward Labrador Current (Piecuch et al. (2017). In this analysis of an ocean state estimate, changes in the horizontal currents are interpreted as a direct response to the anomalous local wind stress curl through the Sverdrup balance (Sverdrup, 1947). However, the above change in the North Atlantic Current and the Labrador Current is near the western boundary of the Atlantic Ocean and near a region with strong ocean currents and strong interactions between the deep flow of NADW and the continental slope where it is known that the Sverdrup balance does not apply (e.g., Pedlosky, 2013; Wunsch & Roemmich, 1985; Yeager, 2015; Zhang & Vallis, 2007). A weaker AMOC can lead to changes in the horizontal circulation, especially a reduction in the northward North Atlantic Current and an increase in the southward Labrador Sea Current in an eddy-permitting CGCM (R. Zhang, Delworth, et al., 2011). The changes in the horizontal currents are due to the bottom vortex stretching effect induced by the interaction between the anomalous deep flow of NADW and the bathymetry over this region—an anomalous case of the joint effect of baroclinicity and relief (JEBAR; Sarkisyan & Ivanov, 1971; Holland & Hirschman, 1972; Myers et al., 1996). As a consequence, the AMOC variability can modulate the variability of the horizontal gyre circulations in the North Atlantic (Kwon & Frankignoul, 2014; Zhang, 2008; R. Zhang, Delworth, et al., 2011). Late-twentieth-century fluctuations in the strength of the intergyre gyre, at the

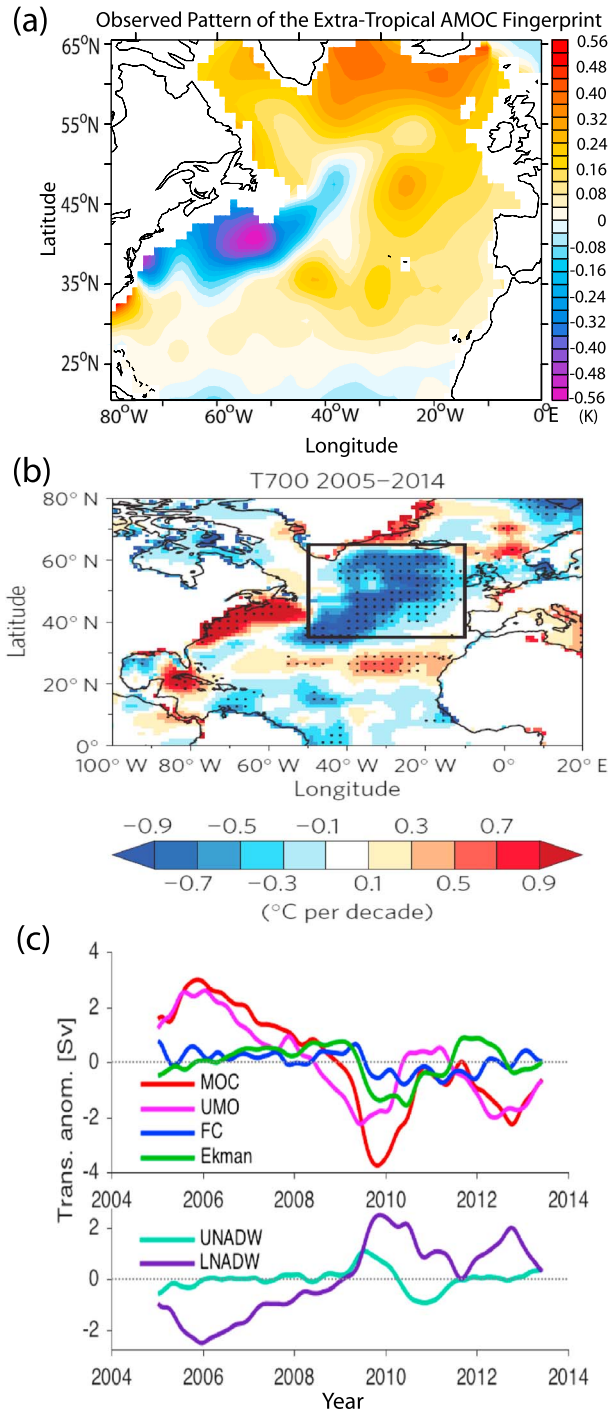

Figure 6. The observed extratropical AMOC fingerprint, recent upper ocean temperature trend, and AMOC anomalies. (a) The spatial pattern of the observed extratropical AMOC fingerprint updated from Zhang (2008), that is, the first empirical orthogonal function (EOF1) of observed detrended subsurface ocean temperature anomalies (K) at 400 m in the extratropical North Atlantic, derived from an objectively analyzed ocean temperature data set over the period 1955–2017 (Levitus et al., 2012). (b) Observed 0- to 700-m averaged temperature trend over 2005–2014 from Robson et al. (2016). Reprinted by permission from Springer Customer Service Centre GmbH: Springer Nature, Nature Geoscience, A reversal of climatic trends in the North Atlantic since 2005, Robson et al., Copyright 2016. The stippling shows where the trend is statistically significant. (c) The 1.5-year low-pass-filtered AMOC anomaly (MOC) and components from the RAPID program (MOC = UMO + FC + Ekman ≈−(UNADW + LNADW); UMO = upper mid-ocean transport; FC = Florida Current; Ekman = direct wind-driven transport; UNADW and LNADW = deep mid-ocean transports at 1,100–3,000 m and 3,000–5,000 m, respectively; positive means northward), from Frajka-Williams et al. (2016) under a CC BY 3.0 license.

interface between the subtropical and subpolar regions of the North Atlantic, were almost entirely buoyancy-driven in a realistic forced ocean model simulation decomposed into buoyancy- and momentum-forced components (Yeager et al., 2015; Yeager & Danabasoglu, 2014). The recent spindown of AMOC and associated subpolar cooling is associated with a predictable, buoyancy-forced weakening of the subpolar gyre and associated heat transport due to the bottom vortex stretching effect that breaks the wind-driven Sverdup balance in this region (Yeager et al., 2015).

3.2.3. Linkage Indicated by Other Indirect Observations of AMOC Components

Other indirect observations of overturning-related circulation components shed light on AMOC variability prior to 2004. The North Brazil Current is a major pathway of the northward upper limb of the AMOC in the tropical Atlantic. At multidecadal timescales, the geostrophic transport of the North Brazil Current calculated from historical hydrographic data since 1950s is significantly correlated with the observed Labrador Sea Water thickness but lags it by a few years and significantly correlated with the observed AMV index at zero time lag (D. Zhang, Msadek, et al., 2011). Both the North Brazil Current transport and AMV lag changes of the NADW formation at northern high latitudes by several years due to the southward propagation of the AMOC signal (which will be discussed in section 3.2.5), and thus, the North Brazil Current transport and AMV are positively correlated around zero time lag. The SST pattern associated with low-frequency variations in the North Brazil Current resembles the observed Atlantic dipole pattern associated with AMV and is consistent with that simulated in a CGCM's control simulation, supporting the important role of AMOC in AMV and associated Atlantic dipole SST pattern.

At basin scale, multidecadal changes in the AMOC and associated heat transport across midlatitudes—leading to steric changes of sea level—are inferred from the difference between sea level anomalies observed at U.S. east coast tide gauges, south and north of Cape Hatteras. These changes are strongly linked to the observed AMV, especially the warming shift in the subpolar North Atlantic in the 1990s (McCarthy et al., 2015).

3.2.4. Linkage Indicated by Modeling Results

The linkage between multidecadal AMOC variability and AMV has been found in many unforced CGCM control simulations (e.g., Ba et al., 2014; Brown et al., 2016; Danabasoglu et al., 2012; Delworth & Mann, 2000; Drews & Greatbatch, 2016, 2017; Keenlyside et al., 2016; Kim, Yeager, Chang, & Danabasoglu, 2018; Knight et al., 2005; Latif et al., 2004, 2006; Park et al., 2016; Park & Latif, 2008; Roberts et al., 2013; Sun et al., 2018; Wu et al., 2018; Yan et al., 2017, 2018) and forced historical simulations of the twentieth century (e.g., Medhaug & Furevik, 2011; Zhang & Wang, 2013). The simulated correlation between the AMOC and AMV varies considerably among CGCMs (Ba et al., 2014; Keenlyside et al., 2016; Medhaug & Furevik, 2011; Tandon & Kushner, 2015; Wu et al., 2018; Yan et al., 2018; Zhang & Wang, 2013). The linkages are more diverse in forced historical simulations than in unforced control simulations due to the interference with simulated response to external radiative forcing (Tandon & Kushner, 2015). The spread in the strength of the AMOC-AMV linkage in unforced control simulations is likely related to model biases, such as the underestimation of low-frequency AMOC variability in many CGCMs (Yan et al., 2018).

In many CGCMs, the anomalous Atlantic meridional heat transport induced by multidecadal AMOC variability plays a crucial role in the simulated linkage with AMV (e.g., Danabasoglu et al., 2012; Knight et al., 2005; Wills et al., 2019; Zhang & Zhang, 2015). Similar results are also found in OGCM simulations forced by atmospheric reanalysis data, with simulated AMV-related SST and upper ocean heat content anomalies in the subpolar North Atlantic primarily induced by multidecadal AMOC variations, which are forced by the anomalous surface buoyancy fluxes at northern high latitudes and propagate southward (Figures 7a and 7b; e.g., Robson, Sutton, Lohmann, et al., 2012; Yeager & Danabasoglu, 2014). Such results indicate that the simulated warming in the subpolar North Atlantic in the mid-1990s was directly forced by the enhanced Atlantic meridional heat transport convergence associated with the enhanced AMOC strength (Danabasoglu et al., 2016; Grist et al., 2010; Lohmann et al., 2009; Robson, Sutton, Lohmann, et al., 2012; Yeager et al., 2012). In an OGCM simulation, over the subpolar North Atlantic region, the majority fraction of the increased Atlantic meridional heat transport convergence is balanced by the enhanced ocean heat content, and a relative small fraction is released to the atmosphere through the enhanced upward surface heat flux (Robson, Sutton, Lohmann, et al., 2012). It is important to quantify this partitioning in future observational studies.

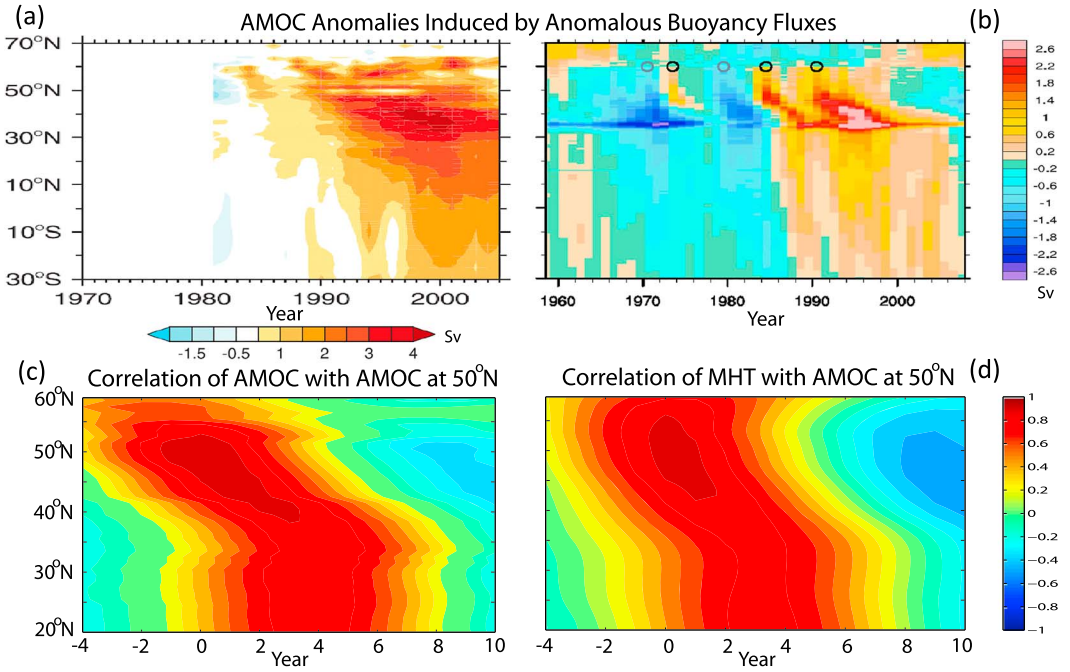

Figure 7. Simulated AMOC anomalies associated with changes in NADW and their southward propagation. (a, b) AMOC variations induced by the anomalous buoyancy fluxes as a function of latitude and time in two different OGCMs forced by atmospheric reanalysis data. The black (gray) circles in (b) denote the approximate origins of positive (negative) AMOC anomalies at northern high latitudes. Panel (a) is adapted from Robson, Sutton, Lohmann, et al. (2012), © Copyright 2012 AMS; (b) is adapted from Yeager and Danabasoglu (2014), © Copyright 2014 AMS. (c, d) Cross correlations of the AMOC anomaly at 50°N with the AMOC anomalies (c) and Atlantic meridional heat transport (MHT) anomalies (d) at different latitudes and time lags from a CGCM 1,000-year control simulation (anomalies are 10-year low-pass filtered and positive time lags indicate the AMOC anomaly at 50°N leads), adapted from Zhang and Zhang (2015).

3.2.5. Southward Propagation of AMOC and AMV Signal

Previous studies have suggested that AMOC anomalies have little or no simultaneous meridional coherence across the North Atlantic (Bingham et al., 2007; Lozier, 2010, 2012; Lozier et al., 2010; Wunsch & Heimbach, 2013). The lack of simultaneous meridional coherence in low-frequency AMOC anomalies associated with NADW formation is due to the existence of interior pathways of NADW at midlatitudes (Zhang, 2010), as has been observed (Bower et al., 2009); low-frequency AMOC anomalies induced by changes in high-latitude deep water formation thus propagate southward with a slow advection speed at midlatitudes and with a fast coastal Kelvin wave speed at lower latitudes (Figure 7c). At low frequencies, Atlantic meridional heat transport anomalies are closely correlated with AMOC anomalies induced by changes in high-latitude deep water formation (Figure 7d); hence, their meridional convergences/divergences are stronger at midlatitudes (which directly leads to the dipole upper ocean heat content anomaly) but much weaker at lower latitudes. Other mechanisms are involved in linking low-frequency AMOC anomalies at northern high latitudes with the tropical AMV signal (Zhang & Zhang, 2015).

Recent observational and modeling studies suggest that coupled air-sea feedbacks, such as the wind-evaporation-SST feedback, cloud feedback, or dust feedback, are essential for the propagation of the AMOC-induced AMV SST signal from the subpolar to the tropical North Atlantic along the horseshoe pathway (Figure 8a) and for amplifying the tropical AMV signal by modulating the net downward surface heat flux (Bellomo et al., 2016; Brown et al., 2016; Smirnov & Vimont, 2012; Wang et al., 2012; Yuan et al., 2016). In particular, the wind-evaporation-SST feedback involves the interaction between surface wind speed and SST anomalies through anomalous evaporation and is characterized by a horseshoe-shaped pattern for the propagated SST anomalies (e.g., Chang et al., 1997; Smirnov & Vimont, 2012; Xie & Philander, 1994). The warm midlatitude SST anomaly induces a cyclonic circulation over lower latitudes and weakens the trade winds, leading to reduced dust emission over the Sahara and dust transport toward the tropical Atlantic and reduced low cloud cover over the tropical North Atlantic (Figure 8a); both feedbacks

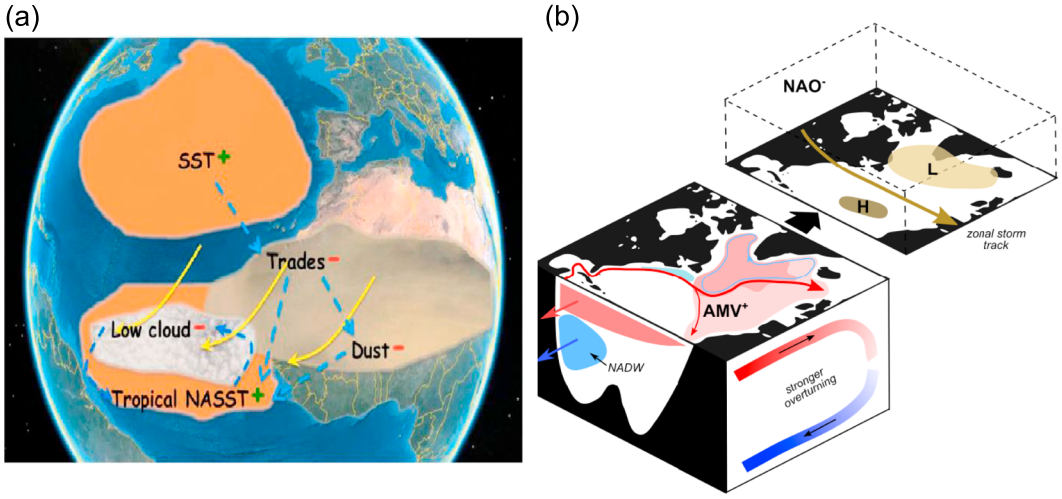

Figure 8. Schematic diagrams for the air-sea feedbacks associated with a positive AMV. (a) The warm midlatitude SST anomaly induces a cyclonic circulation over lower latitudes and weakens trade winds, which reduce dust emission over the Sahara and dust transport toward the tropical Atlantic and reduce low cloud cover over the tropical North Atlantic. Both feedbacks contribute to the warm tropical AMV signal from Yuan et al. (2016). (b) A positive AMV phase associated with a stronger AMOC is characterized by a warm anomaly over the subpolar gyre and a cold anomaly over the northern recirculation gyre north of the Gulf Stream, and the decreased meridional SST gradient leads to a negative winter NAO response (i.e., weaker subtropical high and subpolar low over the North Atlantic) from Sutton et al. (2018), © Copyright 2018 AMS.

contribute to the warm tropical AMV signal (Yuan et al., 2016). In CGCMs with relatively stronger low-frequency AMOC variability, there is a significant positive correlation between AMOC strength and the net downward surface heat flux over the tropical North Atlantic, which is consistent with the above coupled air-sea feedbacks and indicates the indirect influence of AMOC on the tropical AMV SST signal (Yan et al., 2018). Most CGCMs are still not capable of simulating these feedbacks and the associated tropical AMV SST signal adequately (e.g., Martin et al., 2014; Yuan et al., 2016).

3.2.6. Role of Ocean-Atmosphere Coupling in Multidecadal AMOC Variability and Its Relationship With AMV

One crucial question is: What is the role of ocean-atmosphere coupling in multidecadal AMOC variability and the relationship between multidecadal AMOC variability and AMV? Modeling studies have not reached a consensus on whether multidecadal AMOC variability associated with changes in NADW formation is a dynamic ocean response to the atmospheric forcing (e.g., Danabasoglu, 2008; Delworth & Greatbatch, 2000; Dong & Sutton, 2005; Eden & Jung, 2001; Griffies & Tziperman, 1995; Mecking et al., 2014) or an ocean-atmosphere coupled mode of variability (e.g., Timmermann et al., 1998; Vellinga & Wu, 2004; Weaver & Valcke, 1998).

There is, however, a consensus that anomalous surface buoyancy fluxes over NADW formation sites are critical contributors to changes in NADW formation and associated multidecadal AMOC variability. Numerous modeling results suggest that Labrador Sea deep water formation is sensitive to winter NAO-induced anomalous surface heat flux. In these simulations, AMOC variability is dominated by changes in the Labrador Sea deep water formation; thus, a positive winter NAO associated with stronger westerlies can induce enhanced surface heat loss and stronger deep water formation over the Labrador Sea, leading a positive phase in AMOC and associated AMV by about a decade (e.g., Danabasoglu et al., 2012; Delworth et al., 2016, 2017; Delworth & Greatbatch, 2000; Delworth & Zeng, 2016; Eden & Jung, 2001; Kwon & Frankignoul, 2012; Latif & Keenlyside, 2011; Medhaug et al., 2012; Ortega et al., 2017; Otterå et al., 2010; Robson, Sutton, Lohmann, et al., 2012; Yeager & Danabasoglu, 2014). Meanwhile, both observational and modeling studies have shown that a positive AMV (associated with a stronger AMOC) can also induce a negative winter NAO response in the atmosphere as illustrated in the schematic diagram Figure 8b (to be discussed in detail in section 4.3), which will weaken the Labrador Sea deep water formation and associated AMOC strength. Hence, there might be important coupled interactions between the NAO,

AMOC, and AMV (e.g., Grossmann & Klotzbach, 2009; Farneti & Vallis, 2011; J. Li, Sun, & Jin, 2017; Sutton et al., 2018; Sun et al., 2018).

In reality, multidecadal AMOC variability may also be affected by changes in the Nordic Seas deep water formation and associated overflow transport variability, which is not well represented in standard CGCMs, and may not necessarily be dominated by changes in the Labrador Sea deep water formation alone (e.g., Ba et al., 2014; Hawkins & Sutton, 2007; Lohmann et al., 2014; Lozier et al., 2019; Pickart & Spall, 2007; Smeed et al., 2014, 2018). The influence of the winter NAO on deep water formation in the Nordic Seas is opposite to that in the Labrador Sea because the former is favored by cold and dry air masses during negative winter NAO associated with fewer storms, while the latter is favored by positive winter NAO associated with more storms (e.g., Dickson et al., 1996; Drinkwater et al., 2014; Grossmann & Klotzbach, 2009; Marsh, 2000; Medhaug et al., 2012). The Nordic Seas overflows are governed by the density difference between the Nordic Seas source waters and the ambient interior waters on the Atlantic side of the Greenland-Iceland-Scotland ridge, and an explicit Nordic Seas overflow parameterization based on this density difference has been implemented in a widely used CGCM (Danabasoglu et al., 2010). In the CGCM simulation with parameterized overflows, although the Nordic Seas source water density leads the AMOC by a few years, its variability is too weak and the density difference is dominated by that of the ambient interior waters on the Atlantic side of the Greenland-Iceland-Scotland ridge, which lags the AMOC by several years. Hence, the simulated Nordic Seas overflow product water also lags the AMOC by several years (Danabasoglu et al., 2012). Only when the low-frequency variability of the Nordic Seas source water density is much stronger than that of the ambient interior water density on the Atlantic side of the Greenland-Iceland-Scotland ridge, it is possible for the Nordic Seas overflows to lead the AMOC.

Both observational and modeling studies suggest that NADW formation and AMOC strength can also be affected by anomalous freshwater/sea ice exported from the polar region into the North Atlantic (e.g., Delworth et al., 1997; Dima & Lohmann, 2007; Frankcombe et al., 2010; Frankcombe & Dijkstra, 2011; Grossmann & Klotzbach, 2009; Hawkins & Sutton, 2007; Hodson et al., 2014; Holland et al., 2001; Ionita et al., 2016; Jungclaus et al., 2005; Oka et al., 2006; Ortega et al., 2017; Yang & Neelin, 1993, 1997; Zhang & Vallis, 2006), as occurred during the observed Great Salinity Anomaly events (Belkin et al., 1998; Dickson et al., 1988, 1996). The AMOC and associated AMV could also affect the Arctic freshwater export through their impacts on the oceanic/atmospheric circulation changing the Arctic salinity and Fram Strait freshwater/sea ice export, and this coupled Arctic-North Atlantic interaction might also be an important driver for multidecadal AMOC variability (e.g., Dima & Lohmann, 2007; Frankcombe et al., 2010; Frankcombe & Dijkstra, 2011; Jungclaus et al., 2005).

3.2.7. Relationship With Observed Key Elements of AMV

The simulated linkage between multidecadal AMOC variability and AMV is consistent with all observed key elements of AMV reviewed in section 2. For example, over the entire Atlantic, the observed dipole SST pattern associated with AMV is similar to the simulated AMOC-induced dipole patterns in SST and surface air temperature at multidecadal timescales in the control simulations of CGCMs (e.g., Park & Latif, 2008; Roberts et al., 2013). This dipole SST pattern also resembles that following an abrupt change in the AMOC and associated Atlantic meridional heat transport in CGCMs (e.g., Dahl et al., 2005; Dong & Sutton, 2002, 2007; LeGrande et al., 2006; Stouffer et al., 2006; Timmermann et al., 2007; Vellinga & Wood, 2002; Zhang & Delworth, 2005). Over the North Atlantic, the observed high spatial coherence of the SST pattern associated with AMV also exists in CGCMs' control simulations showing a relatively strong linkage between the AMOC and AMV (e.g., Sun et al., 2018). The observed relatively strong subpolar AMV SST signal is consistent with direct forcing by multidecadal AMOC variability and associated anomalous meridional heat transport convergence (e.g., Danabasoglu et al., 2016; Grist et al., 2010; Robson, Sutton, Lohmann, et al., 2012; Yeager et al., 2012; Zhang & Zhang, 2015); the observed relatively weak, lagged tropical AMV SST signal is consistent with the southward propagation of AMV SST signal from the extratropics into the tropics along the horseshoe pathway through coupled air-sea feedbacks, such as wind-evaporation-SST feedback, cloud feedback, or dust feedback (e.g., Bellomo et al., 2016; Brown et al., 2016; Smirnov & Vimont, 2012; Wang et al., 2012; Yuan et al., 2016).

The observed coherence between AMV and multidecadal upward surface turbulent heat flux variations over the midlatitude North Atlantic Ocean (Gulev et al., 2013) is consistent with that found in many CGCMs' control simulations and can be explained by invoking a role for ocean dynamics, especially the anomalous ocean

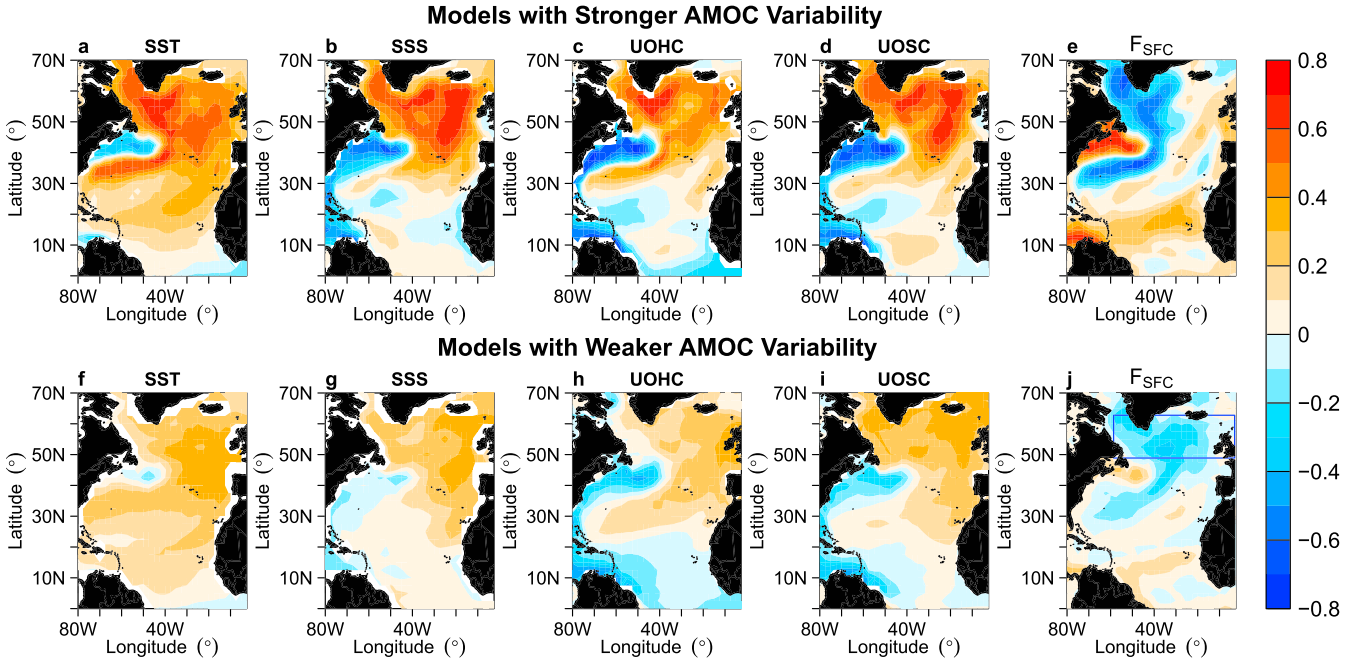

Figure 9. Multimodel ensemble mean correlation maps between the AMOC index at 26°N and the North Atlantic SST, SSS, 0- to 700-m upper ocean heat content (UOHC), 0- to 700-m upper ocean salt content (UOSC), and net downward surface heat flux (F_{SFC}) in control simulations of Coupled Model Intercomparison Project Phase 5 (CMIP5) CGCMs with relatively stronger (upper panels) and weaker (lower panels) low-frequency AMOC variability from Yan et al. (2018). All variables are 10-year low-pass filtered.

heat transport convergence induced by multidecadal AMOC variability (Drews & Greatbatch, 2016, 2017; O'Reilly et al., 2016; Yan et al., 2018; Zhang, 2017; Zhang et al., 2016). The observed coherence among subpolar North Atlantic SST, SSS, and upper ocean heat and salt content anomalies at low frequencies, which is closely linked to the observed extratropical AMOC fingerprint, is also found in many modeling studies, and these simulated coherent variations are attributable to multidecadal AMOC variability (e.g., Robson et al., 2016; Robson, Sutton, Lohmann, et al., 2012; Yan et al., 2018; Yeager & Danabasoglu, 2014; Zhang, 2008, 2017). The correlation between the AMOC and AMV-related subpolar signal in SST, SSS, upper ocean heat and salt content, and net downward surface heat flux is much stronger (weaker) in CGCMs with relatively stronger (weaker) low-frequency AMOC variability (Figure 9). However, most CGCMs underestimate the amplitude of low-frequency AMOC variability, leading to underestimation of the linkage/correlation between the AMOC and AMV as well (Yan et al., 2018).

Observed AMV-related anticorrelated multidecadal variations between upper and deep subpolar North Atlantic temperature have been linked to multidecadal AMOC variability in an OGCM hindcast forced with atmospheric reanalysis data and in a CGCM control simulation (Kim, Yeager, & Danabasoglu, 2018). The observed anticorrelation between multidecadal tropical North Atlantic surface and subsurface temperature variations associated with AMV resembles the response to AMOC changes simulated in CGCMs (Chiang et al., 2008; Zhang, 2007) and recorded in paleo proxies (Parker et al., 2015; Schmidt et al., 2012; Wurtzel et al., 2013). The anticorrelation is also present in many CGCMs and is linked to multidecadal AMOC variability (Wang & Zhang, 2013). The decadal persistence in the auto-correlations of the observed subpolar North Atlantic SST and SSS variations and the corresponding enhanced power at low frequencies in their spectra (i.e., higher than that expected from a red noise process) is also manifested in a CGCM that exhibits enhanced low-frequency power in AMOC variability (Zhang, 2017).

3.2.8. Relationship Between AMOC, AMV, and Atlantic Decadal Predictability and Prediction

Decadal predictability and prediction studies are powerful tools for understanding the mechanisms of the observed AMV, and they support the close linkage between AMV and multidecadal AMOC variability. Many recent studies have demonstrated that multidecadal AMOC variability is a significant source for the enhanced decadal predictability and prediction skills of AMV signal (e.g., Hermanson et al., 2014; Matei

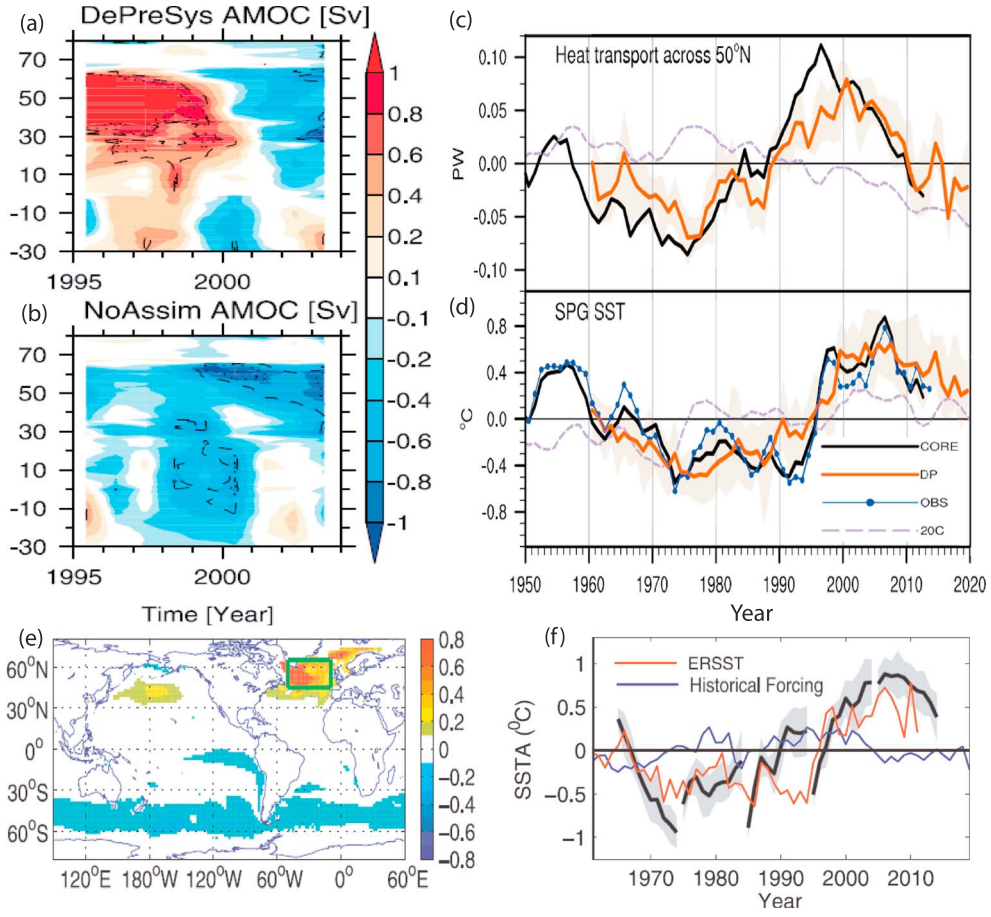

Figure 10. Results from decadal prediction experiments. (a, b) The latitude-time evolution of AMOC anomalies (Sv) for the hindcasts starting in 1994 from the U.K. Met Office's Decadal Prediction System (DePreSys) hindcast initialized with observed ocean states (a) and from the NoAssim hindcast with changes in external radiative forcings but no initialization in ocean states (b), adapted from Robson, Sutton, and Smith (2012). Black contours: significant anomalies with $p \leq 0.05$ (dashed) and $p \leq 0.01$(dotted). (c, d) Atlantic meridional heat transport anomalies across 50°N (c) and SST anomalies in central subpolar gyre (SPG; d) from the National Center for Atmospheric Research (NCAR) decadal prediction (DP) experiments with initialized ocean states, adapted from Yeager et al. (2015). Orange line: ensemble mean; shading: spread; blue dotted line: observation; black lines: OGCM simulation forced by atmospheric reanalysis data (CORE); purple dashed lines: ensemble mean of uninitialized twentieth-century historical simulations (20C) using the same CGCM as DP. (e, f) Pattern of the most predictable component in SST internal residuals (differences between initialized predictions and uninitialized historical simulations) from the Geophysical Fluid Dynamics Laboratory (GFDL) experiments (e) and predicted SST over the subpolar North Atlantic (green box in e) with initializations every 10 years from 1965 (f), adapted from Yang et al. (2013), © Copyright 2013 AMS. Black line: ensemble mean; gray shading: spread; red lines: observations from ERSST; blue lines: uninitialized historical simulations using the same CGCM.

et al., 2012; Msadek et al., 2014; Robson, Sutton, & Smith, 2012, 2014; Trenary & DelSole, 2016; Yan et al., 2018; Yang et al., 2013; Yeager et al., 2012, 2015, 2018; Yeager & Robson, 2017; Zhang, 2017; Zhang & Zhang, 2015). In particular, recent CGCM decadal prediction experiments using observationally based ocean initial conditions exhibit a positive AMOC anomaly at northern high latitudes in the mid-1990s (Figure 10a), whereas uninitialized hindcasts including changes in external radiative forcings do not have this positive AMOC anomaly (Figure 10b). As a result, initialized experiments simulated an increase in the Atlantic meridional heat transport into the subpolar region (Figure 10c) and successfully predicted the observed decadal warming shift in the subpolar North Atlantic (Figures 10d–10f), whereas uninitialized hindcasts cannot predict the observed positive AMV shift (Figures 10d and 10f; e.g., Robson, Sutton, & Smith, 2012; Yeager et al., 2012, 2015, 2018; Matei et al., 2012; Yang et al., 2013; Hermanson et al., 2014; Msadek et al., 2014). Similarly, initializing a negative anomaly in the AMOC and associated Atlantic meridional heat transport at northern high latitudes leads to a successful prediction of the observed decadal cooling shift in the subpolar North Atlantic in the 1960s (Robson, Sutton, & Smith, 2014) and over the last decade (Hermanson et al., 2014; Yeager et al., 2015).

The southward propagation of AMOC anomalies from NADW formation sites at northern high latitudes to the subtropics with a slow advection speed (Figure 7c) is crucial for inducing the anomalous Atlantic meridional heat transport convergence and the associated enhanced decadal predictability of the temperature signal in the subpolar North Atlantic (Zhang & Zhang, 2015). In experiments that prohibit the southward propagation of AMOC anomalies, there is no predictable temperature signal in the subpolar North Atlantic. The subpolar North Atlantic is a critical region for driving the predictability of the tropical AMV signal through the coupled air-sea feedbacks (Dunstone et al., 2011). The Atlantic decadal predictability is much higher in CGCMs with relatively stronger low-frequency AMOC variability, providing further evidence for the critical role of AMOC in AMV and associated Atlantic decadal predictability (e.g., Collins et al., 2006; Griffies & Bryan, 1997a, 1997b; Yan et al., 2018).

The enhanced Atlantic decadal prediction skill in the above-mentioned decadal prediction experiments is achieved primarily by initializing AMOC anomalies instead of predicting AMOC anomalies at northern high latitudes. In principle, multidecadal AMOC anomalies themselves should be predictable at the decadal timescale due to their long persistence and lagged response to the surface heat and freshwater buoyancy flux forcing affecting NADW formation. In many CGCM control simulations, the AMOC indeed exhibits enhanced decadal potential predictability, which is sensitive to the amplitudes of simulated multidecadal AMOC variability in individual models and the initial oceanic conditions (e.g., Branstator & Teng, 2014; Collins et al., 2006; Griffies & Bryan, 1997a, 1997b; Hawkins & Sutton, 2008; Hermanson & Sutton, 2010; Msadek et al., 2010; Persechino et al., 2013; Pohlmann et al., 2004; Teng et al., 2011). However, it is challenging for current climate models to simulate realistic multidecadal AMOC variability and its linkages with surface heat and freshwater buoyancy flux forcing. An improved understanding and modeling of the linkages between AMOC and surface heat and freshwater buoyancy fluxes over NADW formation sites is important to advance the prediction of AMOC, AMV, and associated climate impacts in the real climate system at relatively longer lead times.

3.3. Summary

There is strong observational and modeling evidence that multidecadal AMOC variability is a key driver for observed AMV, consistent with all observed key elements of AMV reviewed in section 2 and that it is an important source for the enhanced decadal predictability and prediction skills of AMV. It is crucial to use multivariate metrics to understand the observed AMV, and the mechanisms proposed for AMV should be able to account for all observed key elements of AMV. The hypothesis that changes in external radiative forcing or stochastic atmospheric forcing is a prime driver of AMV disagrees with many observed key elements of AMV reviewed in section 2 and is inconsistent with hindcast experiments with and without ocean state initialization (section 3.2.8). Multidecadal variability in the AMOC and associated Atlantic meridional heat transport have leading order contributions for the subpolar North Atlantic SST and upper ocean heat content anomalies at low frequencies and should not be neglected in any mathematical representations of the system. A mechanism that invokes multidecadal AMOC variability as a critical driver of the observed AMV does not mean that only ocean dynamics is involved, as it includes coupled air-sea feedbacks in response to the AMOC-induced changes in subpolar North Atlantic, which are very important for the propagation of AMV SST signal from the subpolar to the tropical North Atlantic along the horseshoe pathway.

4. Climate Impacts of Multidecadal AMOC Variability and AMV

This section reviews observational and modeling studies of the impacts of multidecadal AMOC variability and AMV on various regional- and hemispheric-scale climate phenomena with important societal and economic implications. Not all studies draw a direct connection between multidecadal AMOC variability and the specific climate impacts, for example, AMOC variability is explicitly simulated in CGCMs but not in uncoupled AGCMs. However, the synthesis of related studies with a wide range of different approaches on a particular climate phenomenon offers a compelling body of evidence for the role of multidecadal AMOC variability in AMV-related climate impacts.

4.1. Impact on ITCZ and Related Phenomena

The ITCZ is a band of converging trade winds and rising air that produces intense rainfall in the tropics. Statistical analyses of observational and reanalysis data sets suggest that AMV is correlated with

multidecadal fluctuations of ITCZ position and Sahel summer rainfall (Folland et al., 1986; Martin & Thorncroft, 2014a; Ward, 1998), rainy season (March to May) rainfall over northeast Brazil (Folland et al., 2001), and Atlantic major hurricane frequency (Goldenberg et al., 2001; Gray, 1990; Klotzbach et al., 2015; Klotzbach & Gray, 2008; Landsea, 2005; Landsea et al., 1999) during the twentieth century. AMV is anticorrelated with multidecadal variability of hurricane season vertical wind shear over the Atlantic hurricane main development region (MDR; Gray, 1990; Landsea et al., 1999; Goldenberg et al., 2001; Wang et al., 2006; Nigam & Guan, 2011). Strong (weak) vertical wind shear can suppress (enhance) the axisymmetric organization of deep convection and thus the formation and intensification of Atlantic hurricanes (Gray, 1968) during a negative (positive) AMV phase. As discussed below, the multidecadal variability of hurricane season vertical wind shear over the MDR is closely linked to the AMV-related ITCZ shifts.

These observational analyses are supported by modeling studies. For example, in the extended control simulation of a CGCM (Knight et al., 2006), AMV is correlated with multidecadal variations of wet season ITCZ position, Sahel and North East Brazilian rainfall, and anticorrelated with multidecadal variations of hurricane season vertical wind shear over the Atlantic hurricane MDR, consistent with observational analyses. The causal linkage between AMV and multidecadal ITCZ shifts and related phenomena is shown in a hybrid CGCM, in which the prescribed positive AMV phase is associated with an implied increase of the Atlantic meridional heat transport across the equator induced by AMOC strengthening and a reduced atmospheric meridional heat transport across the equator in compensation (Zhang & Delworth, 2006). The prescribed positive AMV phase leads to an anomalous anticlockwise Hadley circulation (i.e., the meridional atmospheric circulation in the tropics), a northward shift of the ITCZ, enhanced summer monsoon rainfall over the Sahel and India (Figures 11a and 11b), and reduced hurricane season vertical wind shear over the MDR for Atlantic hurricanes. The simulated response has a comparable amplitude to observations. These results are consistent with another CGCM simulation of the compensation between anomalous ocean and atmosphere meridional heat transport across the equator and associated change in the Hadley circulation/ITCZ shift induced by an abrupt AMOC change (Zhang & Delworth, 2005). These results are also supported by idealized modeling studies of the ITCZ response to interhemispheric asymmetric thermal forcing associated with implied changes in the meridional ocean heat transport (Broccoli et al., 2006; Kang et al., 2008) and more recent observational and modeling studies linking the asymmetric mean ITCZ location to the AMOC and associated ocean heat transport (Frierson et al., 2013; Marshall et al., 2014). AMV explains a significant portion of multidecadal variability in global Hadley circulation, ITCZ position, and interhemispheric tropospheric temperature contrast in observations (Green et al., 2017), consistent with modeling results of an essential role of the AMOC, AMV, and associated ocean heat transport in modulating multidecadal ITCZ migrations.

The linkage between AMV and multidecadal fluctuations of ITCZ position and Sahel summer monsoon rainfall is also found in AGCM experiments forced by prescribed SST anomalies associated with the observed AMV pattern (i.e., AGCM-AMV experiments; Mohino et al., 2011), in the internal variability component of CGCM simulations with varying external forcings (Han et al., 2016; Ting et al., 2011, 2014), and in CGCM simulations with the North Atlantic SST restored to the estimated internal component of the observed AMV pattern (i.e., CGCM-AMV experiments; Figures 11c and 11d; Ruprich-Robert et al., 2017). The decadal prediction skill of Sahel rainfall depends crucially on the simulated AMV and associated linkage with the Sahel rainfall (Gaetani & Mohino, 2013; García-Serrano et al., 2015; Martin & Thorncroft, 2014b; Mohino et al., 2016; Monerie et al., 2018; Mueller et al., 2014; Sheen et al., 2017; Yeager et al., 2018). Initializing a weaker AMOC is crucial for predicting the cooling in the subpolar AMV signal and associated southward shift of the ITCZ in the 1960s (Robson, Sutton, Lohmann, et al., 2012) and vice versa in the 1990s (Msadek et al., 2014; Robson et al., 2013; Robson, Sutton, & Smith, 2012). The AMV-induced multidecadal variability in the ITCZ position and Sahel rainfall is also reflected in the observed SSS variability over the tropical North Atlantic, which is anticorrelated with the observed Sahel rainfall at multidecadal timescales (Friedman et al., 2017).

The observed AMV SST signal is identified as the primary driver for the anticorrelated multidecadal variations in hurricane season vertical wind shear over the Atlantic hurricane MDR in AGCM-AMV experiments (Latif et al., 2007; Sutton & Hodson, 2007; Wang et al., 2008a). This mechanism/relationship has been attributed mostly to internal variability associated with Atlantic meridional heat transport variations rather than changes in external radiative forcing, using combined observational and modeling analyses (Zhang &

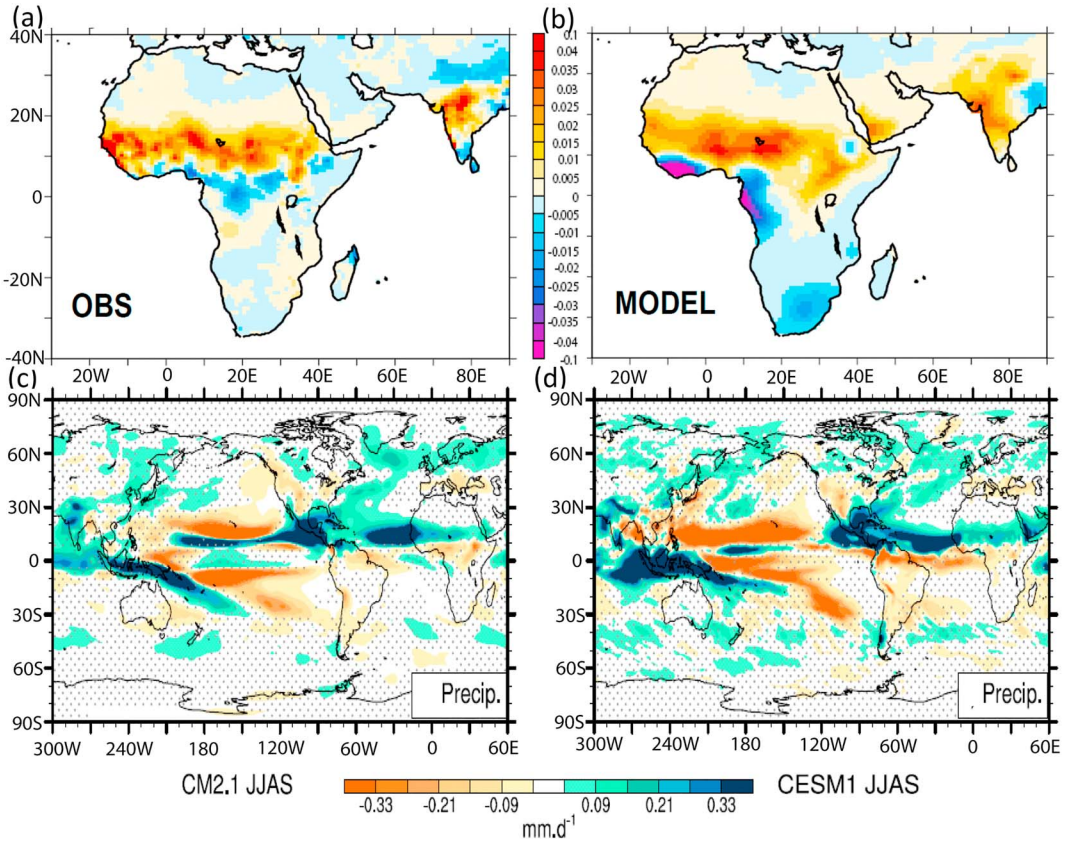

Figure 11. Summer (JJAS) precipitation anomalies associated with AMV. (a, b) Observed (OBS) and modeled regression of 10-year low-pass-filtered summer precipitation on the standardized AMV index, normalized by the standard deviation of the first principal component of 10-year low-pass-filtered summer precipitation anomalies over the region, respectively, adapted from Zhang and Delworth (2006). (c, d) Simulated summer precipitation response to the prescribed AMV-like forcing in two CGCMs, Geophysical Fluid Dynamics Laboratory (GFDL) CM2.1 and National Center for Atmospheric Research (NCAR) CESM1, and stippled regions are below the 95% significant level, adapted from Ruprich-Robert et al. (2017), © Copyright 2017 AMS.

Delworth, 2009). The subpolar North Atlantic variability is critical for the multiyear predictability and prediction of the hurricane season vertical wind shear over the Atlantic hurricane MDR and associated tropical storm frequency (Dunstone et al., 2011; Smith et al., 2010). Initialized decadal prediction experiments also predicted a reduction of Atlantic tropical storms over the most recent decade due to reduced AMOC and associated ocean heat transport convergence (Hermanson et al., 2014).

Based on some CGCM historical simulations with aerosol indirect effects included as discussed in section 3.1 , changes in anthropogenic sulfate aerosols have been proposed as the prime driver for anticorrelated changes in AMV and associated Atlantic tropical cyclone frequency (Booth et al., 2012; Dunstone et al., 2013). However, as discussed earlier, the simulated aerosol indirect effects might be overestimated, and this mechanism is inconsistent with many observations (Figure 4; Zhang et al., 2013). The observed decline of the Atlantic major hurricane frequency over the period 2005–2015 (Figures 12a and 12b) is associated with the directly observed AMOC weakening rather than the observed modest decrease in anthropogenic sulfate aerosols over the North Atlantic over this period (Yan et al., 2017). These results, from both observations and a CGCM control simulation with improved AMOC structure, reveal an essential role of the inferred AMOC variability in AMV, multidecadal variability of hurricane season vertical wind shear over the Atlantic hurricane MDR (Figures 12c and 12d), and associated Atlantic major hurricane frequency. There is an increase in the hurricane season vertical wind shear over the Atlantic hurricane MDR when the AMOC declines (Figures 12c and 12d), favoring the reduction of the Atlantic major hurricane frequency, consistent with earlier modeling studies showing that AMV leads to anticorrelated changes in the

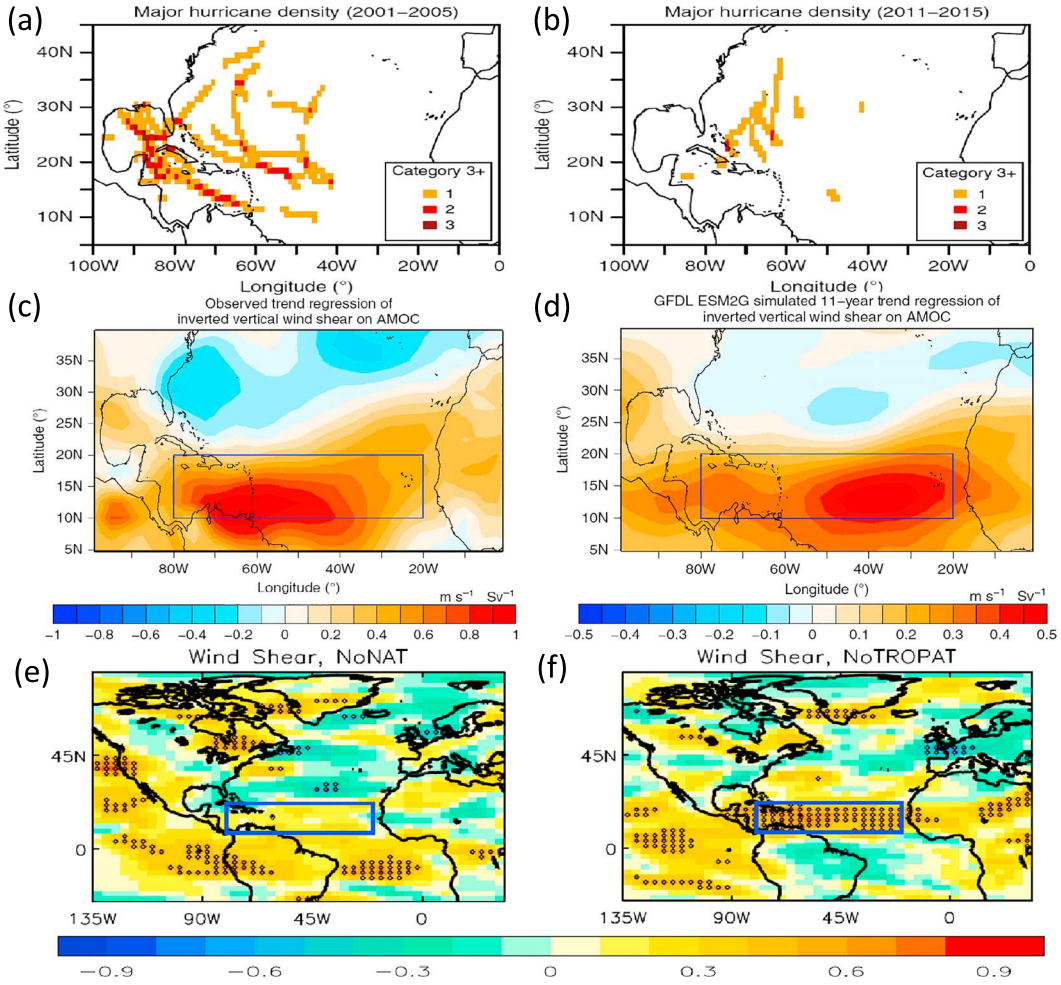

Figure 12. Atlantic major hurricane frequency and the linkage with AMOC through the hurricane season (JJASON) vertical wind shear over the Atlantic hurricane Main Development Region (MDR). (a, b) Observed Atlantic major hurricane track density maps (i.e., total number of major hurricanes that occurred at each grid box for the periods 2001–2005 and 2011–2015, respectively. (c, d) Observed and modeled 11-year trends of inverted hurricane season vertical shear of zonal wind (m/s) regressed on the corresponding 11-year trends of AMOC index at 26°N (Sv). The observed AMOC index at 26°N is reconstructed from the extratropical AMOC fingerprint. The modeled results are from the control simulation of a CGCM—Geophysical Fluid Dynamics Laboratory (GFDL) ESM 2G. The regressions are derived from all available 11-year segments sampled from the observation and the control simulation respectively. Positive values represent an increase in hurricane season vertical wind shear when AMOC declines. (e, f) Predictability skill for hurricane season vertical shear of zonal wind at years 2 to 6 for experiments with ocean assimilation removed from the extratropical North Atlantic (NoNAT, e) or from the tropical Atlantic (NoTROPAT, f), stippled regions have correlations significant at the 95% level. The blue boxes in (c–f) denote the Atlantic hurricane MDR. (a–d) are adapted from Yan et al. (2017) under a CC BY 4.0 license and (e, f) are adapted from Dunstone et al. (2011).

hurricane season vertical wind shear over the MDR (e.g., Latif et al., 2007; Sutton & Hodson, 2007; Wang et al., 2008a; Zhang & Delworth, 2006). The suggested remote influence of the AMOC-induced subpolar North Atlantic variability on the hurricane season MDR vertical wind shear at multidecadal timescales (Yan et al., 2017) is consistent with previous decadal predictability and prediction studies (Dunstone et al., 2011; Hermanson et al., 2014; Smith et al., 2010). The multiyear predictability skill of hurricane season vertical wind shear over the MDR is lost when ocean is not initialized in the extratropical North Atlantic (Figure 12e) but remains when ocean is initialized in the extratropical North Atlantic but not in the tropical Atlantic (Figure 12f). This result indicates the importance of initializing subpolar ocean states, and the tropical vertical wind shear response to subpolar ocean states is closely related to the responses in Hadley circulation and ITCZ position (Dunstone et al., 2011).

4.2. Impact on Pacific Climate Variability

Many observational and modeling studies indicate that AMV may have substantial impacts on climate variability in the Pacific, where the Pacific Decadal Oscillation (PDO) or Pacific Decadal Variability (PDV) is the

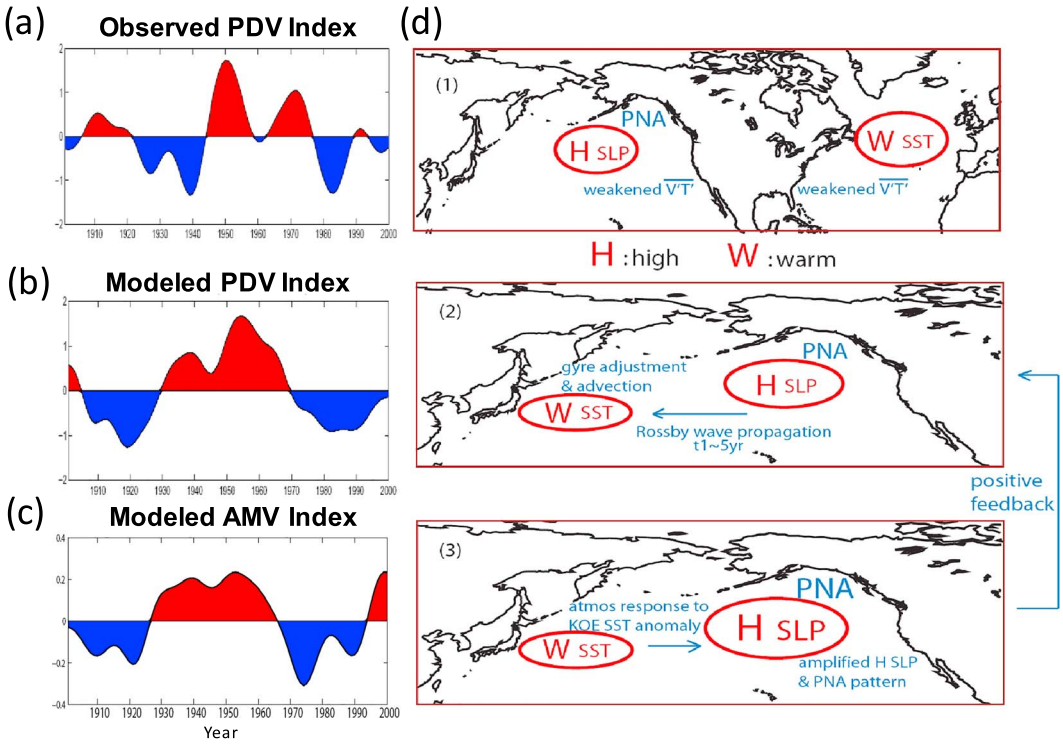

Figure 13. Observed and simulated PDV and AMV indices and the schematic diagram of the impact of AMV on PDV, adapted from Zhang and Delworth (2007). (a) Observed PDV index, a positive phase corresponds to warm anomalies over the western and central North Pacific. (b) Modeled PDV index in response to the prescribed AMV-like forcing. PDV indices in (a, b) are 10-year low-pass filtered. (c) Modeled AMV index induced by the prescribed AMV-like forcing. (d) Schematic diagram: a positive AMV phase leads to a weakening in midlatitude winter storm track and Aleutian low and associated Pacific/North America (PNA) pattern (1) and thus warming over the western North Pacific through the westward oceanic Rossby wave propagation (2), which leads to even stronger SLP anomalies and PNA pattern and the coupled air-sea interaction over the North Pacific provides a positive feedback (3).

leading mode of the North Pacific SST variability (Deser et al., 2012; Mantua et al., 1997). Observational statistical analyses suggest that the multidecadal component of PDV lags AMV by a decade and the lagged relationship provides a potential for the prediction of future PDV changes (Chylek, Dubey, et al., 2014; d'Orgeville & Peltier, 2007; S. Wu, Liu, et al., 2011; Zhang & Delworth, 2007), though these results are limited by short observational records. Here the sign of the PDV index is chosen so that a positive PDV phase corresponds to an anomalous warming over the western and central North Pacific (d'Orgeville & Peltier, 2007; Zhang & Delworth, 2007). Observational statistical analyses also indicate that at multidecadal timescales PDV leads the negative AMV by ~17 years (d'Orgeville & Peltier, 2007). However, when the externally forced signal is removed, the correlation when PDV leads the negative AMV becomes much weaker and thus is not robust, whereas the correlation when AMV leads PDV remains unaffected (Frankignoul et al., 2017; Marini & Frankignoul, 2014).

The causal linkage between AMV and PDV is simulated in a hybrid CGCM with prescribed AMV-related surface heat flux anomalies associated with implied changes in the Atlantic meridional heat transport and AMOC, whereby AMV contributes to the multidecadal component of PDV (with AMV leading PDV by several years, Figures 13a–13c) and the associated Pacific/North America pattern (Zhang & Delworth, 2007). The positive (negative) AMV phase associated with the enhanced (reduced) Atlantic meridional heat transport leads to a weakening (strengthening) in the atmospheric meridional eddy heat transport, midlatitude winter storm track, and Aleutian low and thus leads to the warming (cooling) over the western North Pacific through westward oceanic Rossby wave propagation, which further weakens the Aleutian low (Figure 13d). Hence, AMV provides a source of multidecadal variability to the Pacific through atmospheric teleconnections amplified by the ocean dynamics and coupled air-sea feedbacks in the North Pacific (Figure 13d; Zhang & Delworth, 2007). This teleconnected impact of AMV is seen in recent multimodel CGCM-AMV experiments (e.g., Ruprich-Robert et al., 2017) and is consistent with the simulated impact of AMOC weakening on the cooling over the western and central North Pacific through the extratropical

atmospheric bridge in CGCMs (e.g., Wu et al., 2008; Zhang & Delworth, 2005; Zhang & Zhao, 2015). In addition to the above extratropical pathway for the impact of AMV on PDV, a tropical pathway for this teleconnected impact has also been proposed, which will be discussed later in this section. The relative contributions of the two different pathways are likely sensitive to the details of model and forcing structure.

AMV also has significant impacts on the tropical Pacific variability. In CGCM-AMV experiments, the positive AMV phase leads to stronger trade winds and Walker circulation (i.e., the zonal atmospheric circulation in the tropics) and La Niña-like cooling over the eastern tropical Pacific (Dong et al., 2006; Kucharski et al., 2016; Ruprich-Robert et al., 2017), similar to the changes induced by a weakening of the AMOC in CGCMs but with an opposite sign (e.g., Dong & Sutton, 2002; Zhang & Delworth, 2005). The AMV-induced anomalous atmospheric circulation over the tropical Pacific is also found in AGCM-AMV experiments (Sutton & Hodson, 2007). Initializing ocean states in the North Atlantic plays a vital role in predicting the positive AMV phase and associated response in the Pacific, that is, the La Niña-like SST pattern observed in the equatorial Pacific, during the late 1990s (Chikamoto et al., 2012). The teleconnection is also consistents with simulated enhanced trade wind and surface cooling over the central and eastern equatorial Pacific forced by the specified observed surface warming over the tropical North Atlantic in recent decades (Li et al., 2016; McGregor et al., 2014). The tropical AMV signal is important for generating the out-of-phase SST response in the central tropical Pacific in a CGCM forced by the idealized tropical AMV signal (Zanchettin et al., 2016), whereas the subpolar AMV signal plays an essential role in triggering the tropical AMV signal and the subsequent teleconnection between the tropical Atlantic and Pacific in observations (Chafik et al., 2016). The strengthened Walker circulation and La Niña-like condition over the equatorial Pacific induced by the positive AMV phase can further lead to an increase in the vertical wind shear and a reduction of the tropical cyclone frequency over the western North Pacific (Zhang et al., 2018), as well as a northward shift in the Pacific ITCZ (Levine et al., 2018).

AMV further influences the North Pacific through the tropical pathway. For example, in an AGCM-AMV experiment, descending motion over the central tropical Pacific induced by the positive AMV phase can excite a Rossby wave train that extends into the extratropics, weakening the Aleutian low and enhancing the subtropical high over the eastern North Pacific in winter (Lyu et al., 2017). In CGCM-AMV experiments, the AMV-induced response in both the tropical and North Pacific (e.g., anomalous SST over the central tropical Pacific and the Pacific/North America pattern revealed by anomalous 500-mb geopotential height over the North Pacific) is mainly due to the tropical AMV forcing (Figures 14a–14d); the North Pacific response is relayed and amplified by the tropical Pacific response through the Rossby wave propagation into the North Pacific (Figures 14a and 14b; Ruprich-Robert et al., 2017).

The above tropical pathway for the teleconnection between the North Atlantic and the North Pacific (Lyu et al., 2017; Ruprich-Robert et al., 2017) is consistent with the response induced by the tropical North Atlantic surface cooling associated with AMOC weakening in previous studies (Okumura et al., 2009; Zhang & Zhao, 2015). In CGCM experiments forced by a multimodel SST cold bias (related to weak AMOC bias) in either the extratropical North Atlantic or the tropical North Atlantic, there is a cooling response over the western and central North Pacific (Figures 14e and 14g) and associated anomalous 500-mb geopotential height response over the North Pacific (Pacific/North America pattern, Figures 14f and 14h). This result suggests that both the extratropical and tropical pathways for the teleconnection between the North Atlantic and the North Pacific are possible (Figures 14e–14h; Zhang & Zhao, 2015). On the other hand, the simulated impact of the AMOC weakening on the North Pacific (i.e., the strengthening of the Aleutian low and midlatitude westerlies and surface cooling over the northwestern Pacific) in a CGCM almost disappears when the air-sea coupling over the extratropical North Atlantic is disabled but it is mostly unaffected when the air-sea coupling over the tropical North Atlantic is disabled (Wu et al., 2008). That is, the extratropical pathway dominates the teleconnection. Hence, the relative contribution of the two different pathways for the North Atlantic and North Pacific teleconnection might be sensitive to the different models and the detailed structure of the Atlantic forcing used in various experiments.

Similar spatiotemporal features of a global scale multidecadal climate mode appear in both observations and a CGCM control simulation (Barcikowska et al., 2017). The center of action of this multidecadal climate mode is over the Atlantic and resembles AMV. A positive AMV phase is teleconnected with warming over the western tropical Pacific and North Pacific through both extratropical and tropical pathways, as also

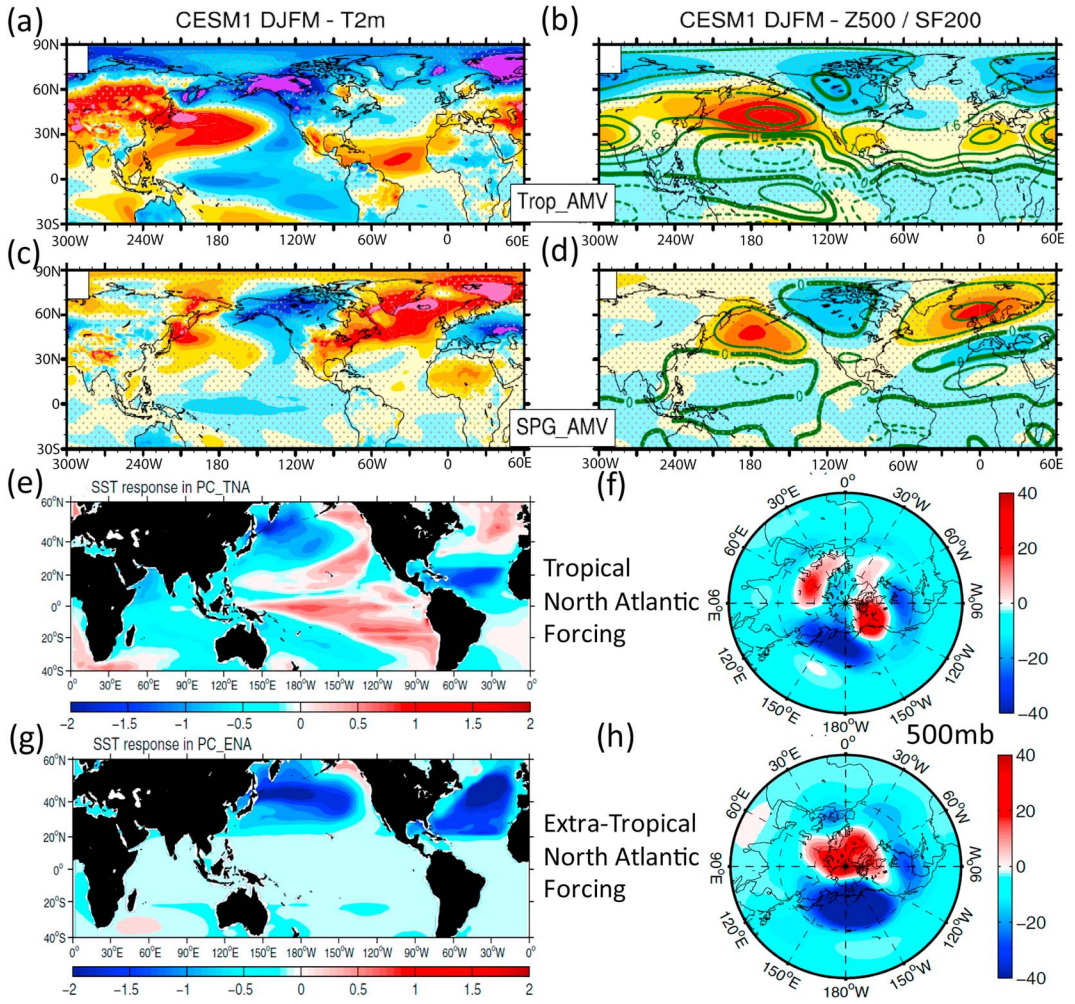

Figure 14. Simulated surface temperature and geopotential height response over the Pacific to the prescribed Atlantic forcing. (a–d) Simulated winter (DJFM) response in surface air temperature (a, c), 500-mb geopotential height (shading) and 200-mb streamfunction (SF, contour; b, d) to the prescribed tropical (a, b) or subpolar (c, d) component of AMV-like forcing (positive minus negative) in a CGCM—National Center for Atmospheric Research (NCAR) CESM1. Stippled regions are below the 95% significant level, adapted from Ruprich-Robert et al. (2017), © Copyright 2017 AMS. (e–h) Simulated response in SST (e, g) and 500-mb geopotential height (f, h) to the prescribed tropical (e, f) or extratropical (g, h) SST forcing (associated with an AMOC weakening) in the same CGCM (NCAR CESM1), adapted from Zhang and Zhao (2015).

simulated in an AGCM-AMV experiment (Sun et al., 2017). This multidecadal climate mode is closely linked to multidecadal AMOC variability and associated tropical AMOC fingerprint (i.e., the anticorrelation between multidecadal tropical North Atlantic surface and subsurface temperature anomalies) in the CGCM, suggesting an essential role of the AMOC as a pacemaker for the interbasin teleconnected multidecadal climate mode (Barcikowska et al., 2017).

Observational and modeling studies also show that AMV has modulated the amplitude of the El Niño–Southern Oscillation (ENSO) variability (a large-scale climate variability over the tropical Pacific peaking at interannual timescales) at multidecadal timescales (Dong et al., 2006; Kang et al., 2014; Levine et al., 2017; Ruprich-Robert et al., 2017). A positive AMV phase leads to a reduced ENSO variability through the background cooling over the central equatorial Pacific (Dong et al., 2006; Kang et al., 2014; Levine et al., 2017), consistent with CGCM simulations in which the weakening of the AMOC leads to an enhanced ENSO variability due to changes in the background state in the tropical Pacific (Dong & Sutton, 2007; Timmermann et al., 2007) and an enhanced ENSO-south Asian summer monsoon interaction (Lu et al., 2008) through atmospheric teleconnections. In an AGCM-AMV experiment, the positive AMV phase leads

to a weakening of the Aleutian low and a strengthening of the subtropical high over the eastern North Pacific, which extends southwestward to the central equatorial Pacific through the wind-evaporation-SST feedback and strengthens the trade wind over the central equatorial Pacific (Yu et al., 2015). This change in the background state results in more frequent occurrence of the central Pacific type of El Niño events, that is, a westward shift of the warm SST anomaly associated with El Niño events from the eastern Pacific to the central Pacific. Hence, the shift of El Niño events to the central Pacific type in recent decades can be partly attributed to the shift of AMV to a positive phase in mid-1990s (Yu et al., 2015).

4.3. Impact on Extratropical Atmospheric Circulation

Bjerknes' (1964) seminal paper hypothesized that variations in the Atlantic meridional heat transport associated with the AMOC can induce anticorrelated atmospheric meridional heat transport anomalies at low frequencies, if variations in the ocean heat storage and the top-of-atmosphere radiative fluxes are small. This anticorrelation between oceanic and atmospheric meridional heat transport anomalies is often referred to as Bjerknes compensation. Bjerknes compensation exists in the northern extratropics at decadal timescales in a CGCM's control simulation in which the decadal oceanic meridional heat transport is dominated by the AMOC variability (Shaffrey & Sutton, 2006). Similar results appear in many other CGCMs' control simulations at decadal timescales (e.g., Farneti & Vallis, 2013; Jungclaus & Koenigk, 2010; Koenigk & Brodeau, 2014; Van der Swaluw et al., 2007) and Bjerknes compensation becomes stronger at multidecadal timescales (e.g., Zhang, 2015; Outten & Esau, 2017; D. Li, Zhang, & Knutson, 2018).

In addition to the above hypothesis, Bjerknes (1964) also proposed that (as introduced in section 1) at low frequencies, AMOC variability plays an active role in the AMV-like SST anomaly and associated NAO-like SLP anomaly over the North Atlantic through air-sea coupling. The NAO index is often defined as the leading mode of SLP anomalies over the North Atlantic sector north of 20°N or the normalized SLP difference between the station-based subtropical high and the subpolar low; a positive NAO index is associated with stronger westerlies over the midlatitude North Atlantic (Hurrell, 1995). Many more subsequent observational analyses have consistently suggested that AMV is associated with multidecadal variations of the winter NAO, with a positive AMV index leading a negative winter NAO index by a few years and vice versa (Deser & Blackmon, 1993; Gastineau & Frankignoul, 2015; Hodson et al., 2014; Kushnir, 1994; Omrani et al., 2014, 2016; Peings et al., 2016; Peings & Magnusdottir, 2014; Sutton & Hodson, 2003; Ting et al., 2014; Zhang & Vallis, 2006).

In AGCM simulations forced by observed global SST and sea ice extent data, the pattern of the multidecadal winter atmospheric response over the North Atlantic region resembles the winter NAO, and the anticorrelated AMV signal has been identified as a critical contributor to the winter NAO response (Sutton & Hodson, 2003). Bjerknes' hypothesis is further supported by recent studies showing that the natural variability of the AMOC leads AMV-like SST anomalies and the anticorrelated multidecadal winter NAO signal (weak but significant) in some CGCMs' unforced control simulations (Frankignoul et al., 2015; Gastineau et al., 2013, 2016; Gastineau & Frankignoul, 2012; Msadek et al., 2011; Ortega et al., 2017) as well as the internal variability component of externally forced simulations (Ting et al., 2014). In these control simulations, an intensification of the AMOC leads to a positive AMV phase, an enhanced heat loss over the subpolar North Atlantic, a southward shift of lower tropospheric baroclinicity, a weakened eddy activity in the North Atlantic storm track and thus a negative winter NAO response. The winter NAO response has also been simulated in AGCM experiments (Gastineau et al., 2016; Msadek et al., 2011) forced by the prescribed AMV signal simulated in CGCMs, and the above-identified mechanism is consistent with an observational analysis (Gastineau & Frankignoul, 2015). However, the amplitude of the simulated winter NAO signal associated with AMV in CGCM simulations is much weaker than observed (Ting et al., 2014). Initializing the ocean component of CGCMs with a weak AMOC state, that is, a negative AMOC anomaly, is crucial for predicting the cooling in the subpolar AMV signal and associated positive winter NAO response in the 1960s (Robson, Sutton, & Smith, 2014).

Some recent AGCM-AMV experiments suggest that the observed AMV can induce a winter NAO response with an amplitude comparable to that observed (Figure 15a) at low frequencies (Omrani et al., 2014). A realistic winter NAO response to AMV exists in a high-top AGCM with well-resolved stratosphere (Figure 15b) but not in a low-top AGCM (Figure 15c) that has poorly resolved stratosphere and implements a sponge layer in the upper levels that inhibits the upward propagation of planetary waves (Omrani et al., 2014). In

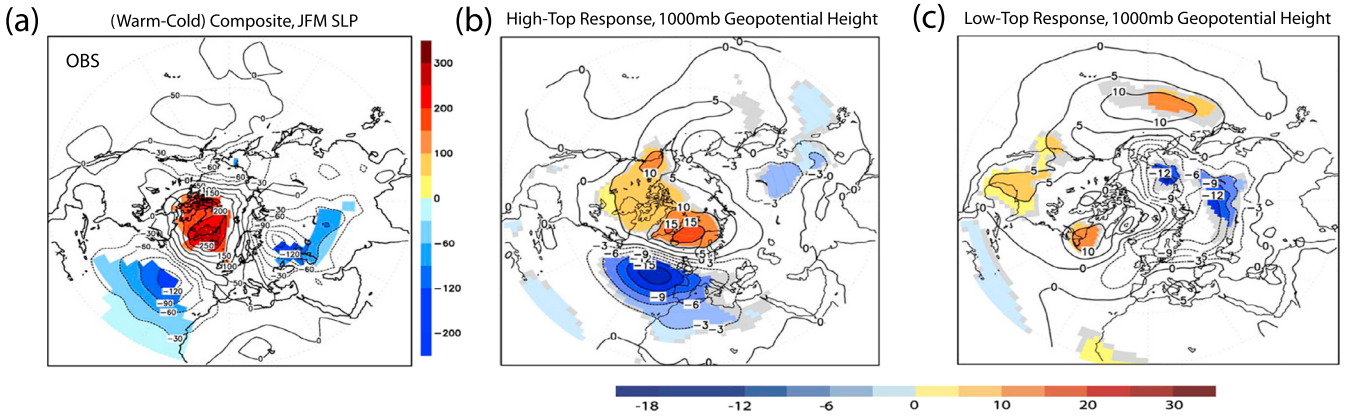

Figure 15. Observed and simulated winter NAO response associated with AMV, adapted from Omrani et al. (2014). (a) Observed winter (JFM) SLP anomalies (in pascals) associated with AMV (positive minus negative AMV phase), regions with anomalies significant at the 90% level are shaded. (b, c) Simulated winter 1,000-mb geopotential height (m) response to the prescribed SST anomalies associated with a positive AMV phase in high-top (b) and low-top (c) AGCMs (MPI-ECHAM5), respectively, regions significant at the 95% (90%) level are shaded in color (gray). Reprinted by permission from Springer Customer Service Centre GmbH: Springer Nature, Climate Dynamics, Stratosphere key for wintertime atmospheric response to warm Atlantic decadal conditions, Omrani et al., Copyright 2014.

this high-top AGCM experiment, a positive AMV not only leads to the reduced baroclinicity/eddy activity and weakened westerly winds but also induces an increase in the upward propagation of planetary waves and thus the weakening of the stratospheric polar vortex and warming in high-latitude stratosphere. The stratosphere warming signal further propagates downward to the troposphere and enhances the negative NAO response in winter. A similar mechanism also appears in CGCMs with well-resolved stratosphere (Omrani et al., 2016), and this mechanism might be sensitive to the strength and structure of the background westerly winds that control the upward propagation of planetary waves (Keenlyside & Omrani, 2014; Omrani et al., 2014). A realistic winter NAO response to the observed AMV is also simulated in a different low-top AGCM (Peings & Magnusdottir, 2014, 2016). This low-top AGCM result is different from Omrani et al. (2014) and might be due to the turbulent mountain stress parameterization included in this low-top AGCM, which can improve the upward propagation of planetary waves into the stratosphere and the frequency of sudden stratospheric warming events (Peings & Magnusdottir, 2016) that are often underestimated in low-top AGCMs (Charlton-Perez et al., 2013). The stratosphere-troposphere interaction could amplify the winter NAO response but remains also sensitive to the details of the surface forcing (Peings & Magnusdottir, 2016).

Some AGCM simulations suggest that the tropical AMV signal is the primary driver of the winter NAO response (Davini et al., 2015), while many other observational and modeling studies found that the extratropical AMV signal is also very important in forcing the winter NAO response (Frankignoul et al., 2015; Gastineau et al., 2016; Gastineau & Frankignoul, 2012; Msadek et al., 2011; Omrani et al., 2014; Peings & Magnusdottir, 2016; Ruprich-Robert et al., 2017). The phase of the NAO is closely linked to the frequency of atmospheric blocking events (a quasi-stationary high-pressure system) over the Euro-Atlantic region (Davini et al., 2012; Rimbu et al., 2014; Woollings et al., 2008, 2010) and the North Atlantic jet stream (Hurrell, 1995; Simpson et al., 2018), and AMV is positively correlated with multidecadal variations of late winter North Atlantic jet stream (Simpson et al., 2018) and winter atmospheric blocking frequency over the Euro-Atlantic region (Häkkinen et al., 2011; Rimbu et al., 2014) in observations. Consistently, in AGCM simulations a positive AMV leads to more frequent winter blocking episodes over the Euro-Atlantic region along with a negative winter NAO response (Davini et al., 2015; Peings & Magnusdottir, 2014), which could promote more winter cold extremes over Europe (Cattiaux et al., 2010; Rimbu et al., 2014).

4.4. Impact on Climate Over Europe, North America, and Asia

Both observational and modeling studies suggest that AMV has a significant impact on the climate over Europe, North America, and Asia. The positive AMV can lead to warmer and wetter summers over western Europe, in both observations and AGCM-AMV experiments (Figures 16a–16d; Sutton & Hodson, 2005). A

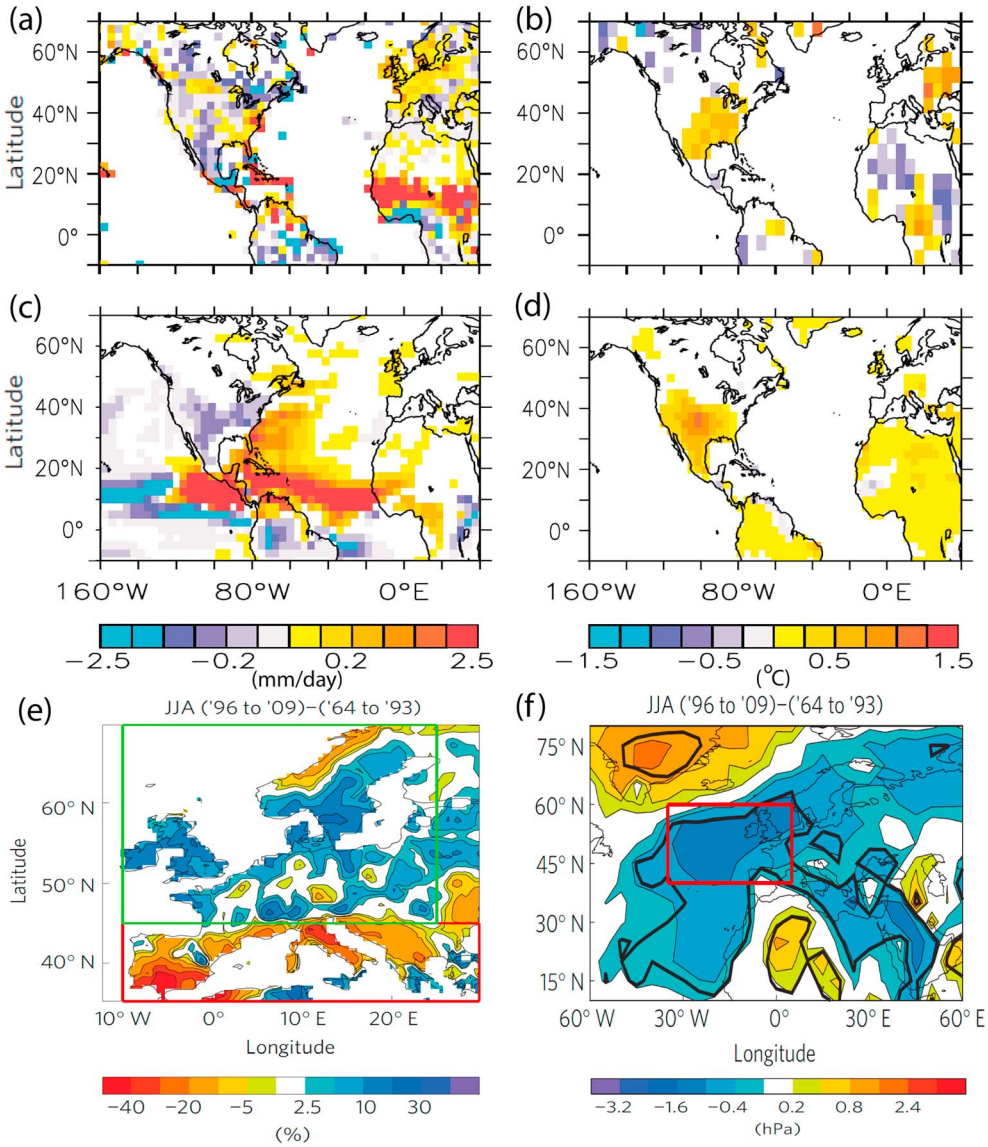

Figure 16. Observed and simulated summer (JJA) climate associated with AMV (positive minus negative AMV phase). (a–d) Observed (a, b) and simulated (c, d) summer precipitation (a, c, mm/day) and surface air temperature (b, d, °C) associated with AMV, adapted from Sutton and Hodson (2005). Reprinted with permission from AAAS. (e, f) Observed detrended summer anomalies in precipitation (e, % of the climatology) and SLP (f, mb) between the warm AMV phase (1996–2009) and the cold AMV phase (1964–1993), adapted from Sutton and Dong (2012). Reprinted by permission from Springer Customer Service Centre GmbH: Springer Nature, Nature Geoscience, Atlantic Ocean influence on a shift in European climate in the 1990s, Sutton and Dong, Copyright 2012. In (a–d), regions not significant at the 90% level are shaded white. Solid black contours in (f) indicate the 90% significant level.

similar relationship between AMV (associated with multidecadal AMOC variability) and western European summer climate exists in a CGCM (Knight et al., 2006). More recent observational analyses (Sutton & Dong, 2012) reveal that a shift toward the positive AMV phase during the 1950s and the 1990s is associated with a shift toward wetter summers over western and northern Europe, drier summers over southern Europe (Figure 16e), and lower SLP over western Europe (Figure 16f), indicating that AMV is the critical driver for the decadal shifts in summertime European climate. The observed dipole summer precipitation response over Europe (noted above) is also simulated in CGCM-AMV experiments (Ruprich-Robert et al., 2017). Observational analyses additionally suggest that AMV is anticorrelated with glacier surface mass balance (Huss et al., 2010) and spring snowfall (Zampieri et al., 2013) in the Alps at multidecadal timescales,

consistent with the observed warmer spring/summer temperature over Europe during the positive AMV phase (Sutton & Dong, 2012). Initializing the ocean states properly in climate prediction simulations is critical for predicting the positive shift in AMV and associated European summer climate shifts in the 1990s (Msadek et al., 2014; Robson et al., 2013; Robson, Sutton, & Smith, 2012; Yeager et al., 2018) and the early twentieth century (Mueller et al., 2014).

In CGCM control simulations, models with strong correlations between AMV and multidecadal surface turbulent heat flux anomalies over the midlatitude North Atlantic have also similarly strong summer warming over Europe during the positive AMV phase; in contrast, the positive AMV simulated in slab ocean models cannot lead to a warmer summer over Europe (O'Reilly et al., 2016). These results agree with previous observational and modeling studies (Knight et al., 2006; Sutton & Dong, 2012; Sutton & Hodson, 2005) and are supported by more recent observational analyses (Ghosh et al., 2017) showing coherent multidecadal variations in European summer temperature and midlatitude North Atlantic surface turbulent heat fluxes associated with AMV. These studies (Ghosh et al., 2017; O'Reilly et al., 2016) reveal the essential role of ocean dynamics and associated anomalous surface turbulent heat fluxes in AMV's impact on European summer temperature. Consistently, across multiple CGCM simulations whose variability is purely internal, the teleconnection between AMV and European summer temperature is stronger in models with greater AMV persistence, variance, and basin-scale spatial coherence (Qasmi et al., 2017) than otherwise. In contrast, the observed multidecadal variations of European winter temperature are not correlated with the observed AMV, because the thermodynamic response is masked by the anticorrelated dynamic NAO response to AMV in winter (Yamamoto & Palter, 2016).

AMV is anticorrelated with the central U.S. rainfall and river flows and positively correlated with the central U.S. drought frequency at multidecadal timescales in observations (Enfield et al., 2001; McCabe et al., 2004). In an AGCM-AMV experiment (Sutton & Hodson, 2005, 2007), AMV is an essential driver of multidecadal summer climate variability over North America: A positive AMV phase leads to warmer and drier summer climate (Figures 16a–16d) and lower SLP over central North America as observed. However, different sets of AGCM-AMV simulations appear to show different responses to AMV over central North America: One set has a consistency in the precipitation response but agrees less on the surface temperature response (Schubert et al., 2009), whereas another set agrees in the summer surface temperature and SLP response but not in the summer precipitation response (Hodson et al., 2010).

Observational analyses (Hu & Feng, 2008; Liu et al., 2015; Nigam et al., 2011; Wang et al., 2006) reveal the important role of AMV in driving regional atmospheric circulation and summer precipitation changes over North America; this linkage is also found in AGCM-AMV and CGCM-AMV experiments (Hu et al., 2011; Ruprich-Robert et al., 2018; Wang et al., 2008b). In particular, the positive AMV phase weakens the North Atlantic subtropical high pressure system and leads to a weaker low-level southerly flow and reduced moisture transport from the Gulf of Mexico into the U.S. Great Plains and thus below-normal precipitation and drier conditions over central North America. In a high-resolution regional atmospheric model, the strengthened (weakened) low-level southerly flow from the Gulf of Mexico into the U.S. Great Plains during the negative (positive) AMV phase enhances (reduces) precipitation (Veres & Hu, 2013). In both observations and AGCM-AMV experiments, the positive AMV phase can reduce the multidecadal mean as well as the variance of the ENSO-related winter precipitation over the southwest United States through a reduced moisture supply to this region (Lee et al., 2018).

AMV has been used as an important predictor for the surface air temperature and precipitation over the southwestern United States in observation-based multiple linear regression analyses (Chylek, Dubey, et al., 2014), consistent with initialized decadal predictions (Msadek et al., 2014; Robson et al., 2013; Robson, Sutton, & Smith, 2012). A similar AMV impact on the central North American summer climate is also simulated in CGCM-AMV experiments (Ruprich-Robert et al., 2018). In these simulations, a positive AMV favors increased summer heat waves over northern Mexico and the southern United States directly and indirectly from the La Niña-like Pacific response to AMV forcing.

A positive AMV phase can also lead to stronger southeast and east Asian summer monsoons through a coupled air-sea feedback over the Indo-western Pacific region, as shown in a CGCM-AMV experiment (Lu et al., 2006). This finding is consistent with changes induced by a weakening of the AMOC in CGCMs but with an opposite sign (Zhang & Delworth, 2005). The simulated warmer east Asian summer surface air

temperature and enhanced precipitation response to a positive AMV phase agrees with the station observations in China. A delayed withdrawal of the Indian monsoon rainfall is associated with the increased tropospheric meridional temperature contrast between Asia and the Indian Ocean during a positive AMV phase (Lu et al., 2006). This is consistent with observational analyses (Goswami et al., 2006), AGCM-AMV experiments (Li et al., 2008; Wang et al., 2009), and a CGCM control simulation with AMV linked to multidecadal AMOC variability (Luo et al., 2011). Observational analyses (Feng & Hu, 2008; Wang et al., 2009) and AGCM-AMV experiments (Wang et al., 2009) suggest that a positive AMV phase leads to enhanced summer warming over the Tibetan Plateau and enhanced meridional temperature contrast between the Tibetan Plateau and the tropical Indian Ocean, which contributes to increased Indian summer monsoon rainfall. A positive AMV phase also leads to warmer and wetter winters over northeast China at multidecadal timescales in both observations and AGCM-AMV experiments (Li & Bates, 2007; Wang et al., 2009). The east China winter climate response to AMV is further amplified by air-sea coupling in AGCM-AMV experiments coupled to a slab ocean (Zhou et al., 2015). The atmospheric Rossby wave propagation from the North Atlantic to Asia is involved in the teleconnection between AMV and Asian climate (Li et al., 2008; Luo et al., 2011; Wang et al., 2009). The primary source of the multiyear prediction skill (and skill enhancement over uninitialized but externally forced simulations) of summer surface air temperature over the northeast Asia comes from AMV and associated atmospheric Rossby wave propagation (Monerie et al., 2018; Yeager et al., 2018).

4.5. Impact on Polar and High Latitude Climate

Substantial multidecadal variations in Arctic surface air temperature have been observed over the twentieth century (Bengtsson et al., 2004; Johannessen et al., 2004; Polyakov, Alekseev, et al., 2003; Semenov & Bengtsson, 2003) and anticorrelated multidecadal sea ice variability is also found in Arctic marginal seas based on Russian historical observational records over the twentieth century (Polyakov, Bekryaev, et al., 2003). Both observational and modeling studies suggest that the Arctic sea ice change is crucial for the anticorrelated Arctic surface air temperature change at multidecadal timescales (Bengtsson et al., 2004; Johannessen et al., 2004; Screen & Simmonds, 2010; Semenov & Latif, 2012; Serreze et al., 2009). The observed AMV is highly correlated with the observed multidecadal surface air temperature variations over the Arctic (Chylek et al., 2009, 2010) and the Atlantic-Arctic boundary (Wood et al., 2010). The AMOC and AMV are significantly correlated with the Arctic surface air temperature and anticorrelated with the Arctic sea ice extent at multidecadal timescales in a CGCM control simulation (Mahajan, Zhang, & Delworth, 2011), consistent with observational analyses; the strongest linkage is found in winter. The simulated winter Arctic sea ice decline associated with an intensified AMOC and a positive AMV phase (Figure 17a) resembles the satellite-observed winter Arctic sea ice decline pattern over the recent decades (Figure 17b), suggesting a possible role of the AMOC and AMV in the recently observed winter Arctic sea ice decline. Similar anticorrelations between AMV/AMOC and the Arctic sea ice extent exist in control simulations of multiple CGCMs, and in all these models, the anticorrelations are stronger in winter than in summer (Day et al., 2012).

Winter Arctic sea ice, especially in the Barents Sea, is strongly influenced by the Atlantic heat transport across the Barents Sea opening at multidecadal timescales (e.g., Årthun et al., 2012; Delworth et al., 2016; D. Li, Zhang, & Knutson, 2017; Smedsrud et al., 2013; Yeager et al., 2015; Zhang, 2015). The multidecadal variability of the Atlantic water temperature in the Barents Sea has also been observed over the twentieth century and is correlated with the observed AMV index (Årthun et al., 2018; Drinkwater et al., 2014; Levitus et al., 2009). At multidecadal timescales, the AMOC and associated Atlantic heat transport across the Arctic Circle lead the Atlantic inflow temperature in the Barents Sea, as well as the Atlantic heat transport across the Barents Sea opening by several years; furthermore, they contribute to the anticorrelated variations in both Barents Sea winter sea ice extent and Arctic summer sea ice extent in a CGCM's extended control simulation (Zhang, 2015). If the AMOC and associated Atlantic heat transport into the Arctic were to weaken in the near future due to natural variability, there might be a hiatus in the decline of September Arctic sea ice (Zhang, 2015). Similar results appear in other CGCMs with different mean states of Arctic sea ice; models with thicker mean Arctic sea ice exhibit stronger Arctic sea ice thickness response to the anomalous Atlantic heat transport associated with multidecadal AMOC variability (D. Li, Zhang, & Knutson, 2018).

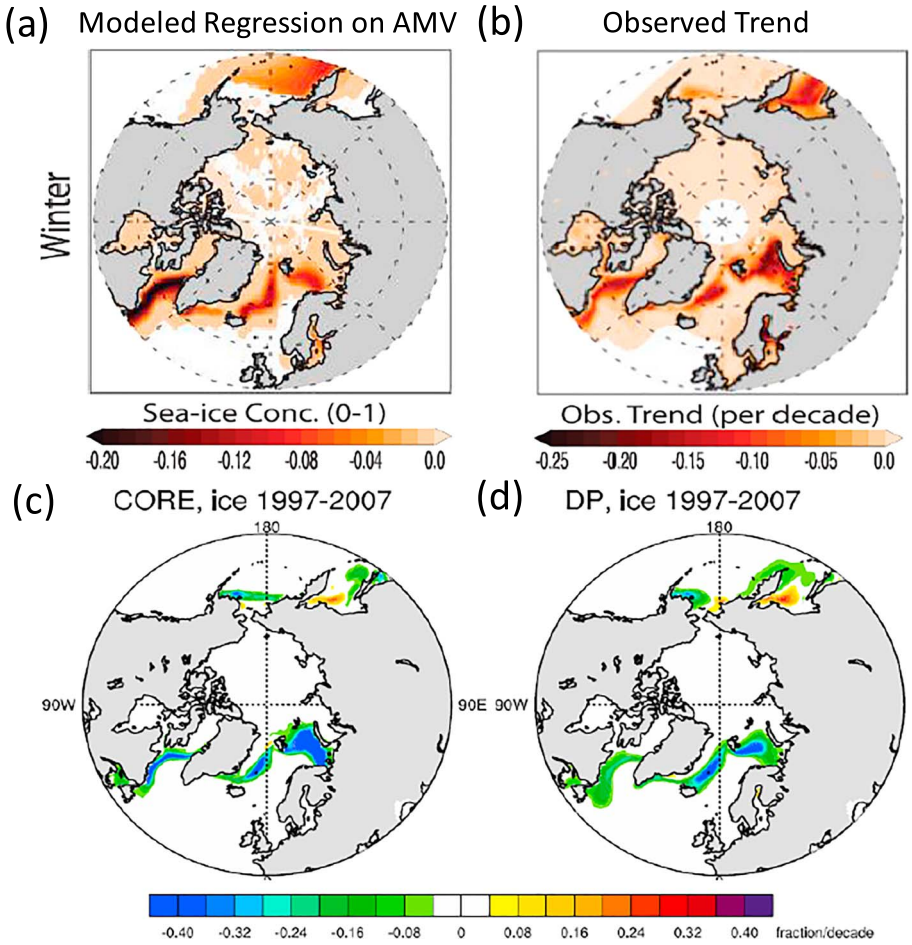

Figure 17. Observed and simulated winter Arctic sea ice concentration changes. (a) Simulated regression of 10-year low-pass-filtered winter Arctic sea ice concentration (%) on the standardized AMV index from the control simulation of a CGCM—Geophysical Fluid Dynamics Laboratory (GFDL) CM2.1. (b) Observed trend (1979–2008) of winter Arctic sea ice concentration (% per decade). (c, d) Simulated trends (1997–2007) of winter Arctic sea ice concentration (% per decade) from the National Center for Atmospheric Research (NCAR) OGCM forced with atmospheric reanalysis data (CORE; c) and from the ensemble mean of NCAR decadal prediction (DP) experiments with initialized ocean states (d). Panels (a, b) are adapted from Mahajan, Zhang, and Delworth (2011), © Copyright 2011 AMS. Panels (c, d) are adapted from Yeager et al. (2015).

In addition to ocean processes, AMV-related stratosphere-troposphere coupling may drive changes in the polar vortex and air temperatures; specifically, the recent warm AMV phase appears to have led to weakening of the polar vortex, Arctic warming, and decreased winter sea ice extent in the Barents Sea (F. Li. Orsolini, et al., 2018). The PDV could also induce changes in the polar vortex and have important impacts on Arctic surface warming (Svendsen et al., 2018). Both AGCM and CGCM experiments suggest that a combination of AMV and PDV phases could have contributed substantially to the early-twentieth-century Arctic surface warming, while the contribution in the fully coupled system is stronger (Tokinaga et al., 2017). Atmospheric teleconnections arising from the imposition of AMV-like SST anomalies in CGCM-AMV experiments are also shown to drive low-frequency Arctic sea ice fluctuations (Castruccio et al., 2019). Specifically, positive AMV phases lead to thinner and less extensive sea ice cover in the Arctic through both dynamic and thermodynamic effects, without any oceanic heat transport changes. The dynamic effects include a weakening of the Beaufort Sea High and an increased prevalence of an Arctic Dipole-like SLP pattern in late winter/early spring with the resulting anomalous winds driving anomalous ice motions. The thermodynamic effect includes warmer surface temperatures in response to increased low cloud cover.

Multidecadal AMOC variability is a significant driver for the decadal predictability of Arctic sea ice thickness in the Atlantic sector (Koenigk et al., 2012). Initializing with a weak AMOC is critical for predicting the shift

to a cool subpolar AMV signal and associated enhanced winter Arctic sea ice cover over the Atlantic side in the 1960s (Robson, Sutton, & Smith, 2014) and vice versa in the 1990s (Msadek et al., 2014; Yeager et al., 2015). The predicted decadal winter Arctic sea ice decline since the late 1990s (Figure 17d) is very similar to that simulated in the OGCM hindcast (Figure 17c) due to a strengthening in the AMOC (Figure 7b) and associated Atlantic meridional heat transport (Figures 10c; Yeager et al., 2015). Initialized decadal predictions also suggest that a weakening of the AMOC that began in the early 21st century will continue and result in a slowdown in the rate of winter sea ice loss in the Atlantic sector of the Arctic in the near future (Yeager et al., 2015).

Pronounced multidecadal surface air temperature variability over the Greenland ice sheet has also been observed during the twentieth century (e.g., Chylek et al., 2006; Box, 2013; Box et al., 2009; Drinkwater et al., 2014) and is significantly correlated with the observed AMV index (Drinkwater et al., 2014). Many observational studies suggest that the warming of the subpolar AMV signal in the mid-1990s contributed to the rapid mass loss of the Greenland ice sheet over the recent decades (Holland et al., 2008; Howat et al., 2008; Seale et al., 2011; Straneo et al., 2010; Straneo & Heimbach, 2013). The observed number and season length of icebergs drifting south of 48°N in the western North Atlantic over the twentieth century also exhibit multidecadal variations (Peterson et al., 2015). These variations can be attributed to a combination of changes in the NAO, Labrador Sea SST, and the surface mass balance of Greenland (Bigg et al., 2014)—the relative importance of these factors has varied at low frequencies throughout the twentieth century (Zhao et al., 2016). At multidecadal timescales, the observed season length of icebergs off eastern Newfoundland is significantly anticorrelated with the observed AMV index over the twentieth century, that is, during a positive (negative) AMV phase the length of iceberg season is shorter (longer; Peterson et al., 2015).

The observed multidecadal variations in Arctic surface air temperature, which are highly correlated with the observed AMV index, are also anticorrelated with the observed multidecadal variations in Antarctic surface air temperature, suggesting an essential role of multidecadal AMOC variability and associated AMV in the observed bipolar seesaw over the twentieth century (Chylek et al., 2010). A bipolar seesaw pattern similar to that observed also appears in the most predictable AMV-like pattern in decadal prediction experiments with initialized ocean states (Figure 10e; Yang et al., 2013) and is associated with multidecadal AMOC variability in a CGCM control simulation (Zhang et al., 2017).

4.6. Impact on Hemispheric-Scale Surface Temperature

Observational analyses reveal a clear AMV imprint on global mean surface temperature (Schlesinger & Ramankutty, 1994). Multidecadal AMOC variability, which is closely linked to AMV, is significantly correlated with multidecadal variations of global and Northern Hemisphere mean surface temperature in the control simulation of a CGCM (Knight et al., 2005). The linkage between the AMOC and surface temperature is strongest in the Northern Hemisphere. In a hybrid CGCM with prescribed AMV-related surface heat flux anomalies associated with implied changes in the Atlantic meridional heat transport and AMOC, AMV could contribute to multidecadal Northern Hemispheric mean surface temperature fluctuations similarly to those of observations over the twentieth century, in addition to the long-term warming trend (Zhang et al., 2007). A substantial AMV impact on the Northern Hemisphere surface temperature is simulated in an AGCM coupled to a slab ocean and forced by prescribed AMV-related surface heat flux anomalies over the North Atlantic-Arctic sector (diagnosed from a CGCM control simulation; Semenov et al., 2010).

The AMV imprint on global and Northern Hemisphere mean surface temperature has also been identified in many studies with different statistical analysis methods applied to both observations and modeling results (Barcikowska et al., 2017; Chen et al., 2017; Chen & Tung, 2017; Cheung et al., 2017; Chylek, Klett, et al., 2014; Chylek et al., 2016; DelSole et al., 2011; Kravtsov et al., 2014; Kravtsov & Spannagle, 2008; Steinman et al., 2015; Stolpe et al., 2017; Tung & Zhou, 2013; Z. Wu, Huang, et al., 2011; Wyatt et al., 2012; Zhou & Tung, 2013). These statistical studies are consistent with the above-mentioned AGCM/hybrid CGCM experiments (Semenov et al., 2010; Zhang et al., 2007), illustrating that the enhanced surface heat flux released from the ocean to the atmosphere during a positive AMV and AMOC phase leads to the hemispheric-scale anomalous surface warming and vice versa. Multidecadal AMOC variability is a key player in AMV's impact on global and Northern Hemisphere mean surface temperature in CGCMs' control simulations (Barcikowska et al., 2017; Park et al., 2016; Stolpe et al., 2017; Wu et al., 2018; Yan et al., 2018), consistent with the simulated impact of multidecadal AMOC change or collapse on global and Northern

Hemisphere mean surface temperature in CGCMs' internally perturbed or externally forced simulations (Delworth et al., 2016; Delworth & Zeng, 2016; Drijfhout, 2015; Stolpe et al., 2018). The linkage between AMV and the Northern Hemisphere mean surface temperatures is stronger (weaker) in CGCMs with relatively stronger (weaker) low-frequency AMOC variability (Yan et al., 2018). The impact of the AMOC on the Northern Hemisphere mean surface temperature is stronger in some CGCMs with the mean state North Atlantic SSS biases artificially corrected than otherwise (Park et al., 2016; Wu et al., 2018).

4.7. Summary and Discussion

This synthesis of many recent observational and modeling studies consistently suggests an essential role of the AMOC in AMV-related regional and hemispheric-scale climate impacts. In particular, the AMOC-induced anomalous Atlantic meridional heat transport and surface heat fluxes released into the atmosphere over middle- to high-latitude North Atlantic is critical for the impacts of AMV on many climate phenomena. Initializing observed ocean states, especially the AMOC anomalies, is essential in predicting observed AMV decadal shifts and many associated climate impacts in CGCM decadal prediction experiments.

Some important issues in understanding AMV-related climate impacts remain unresolved. For example, observational analyses reveal a decadal time lag between PDV and AMV. However, such decadal time lag that is longer than the Rossby wave propagation timescale (Figure 13d) is not well understood and simulated in modeling studies. Furthermore, observational records are too short to test the robustness of the lagged relationship between PDV and AMV. Some regional climate impacts (e.g., the North American climate response to AMV, the linkage between PDV and AMV) are primarily found in AGCM/hybrid CGCM simulations with the prescribed, observation-based AMV-like forcing but are absent in many unforced CGCM simulations. Some simulated AMV-related climate impacts (e.g., ITCZ and NAO) are often much weaker in CGCMs than those found in AGCM/hybrid CGCM simulations forced by the observed AMV-like forcing.

Some of these challenging issues are very likely related to the deficiencies in simulating the pattern and amplitude of the observed AMV (especially in the tropical North Atlantic), the pattern and amplitude of the observed AMV-related anomalous surface heat fluxes released into the atmosphere over middle- to high-latitude North Atlantic, and the associated timescale and amplitude of AMOC variability in current CGCMs. Meanwhile, the simulations using different AGCMs, but forced by the same observed SST anomalies associated with AMV, do not necessarily produce the same pattern and amplitude of AMV-related surface heat flux anomalies as in observations of the real world, which are crucial for many climate impacts of AMV. By studying the atmospheric response to the anomalous ocean heat transport convergence prescribed in the extratropical North Atlantic using an AGCM coupled to a slab ocean, Sutton and Mathieu (2002) have shown that the atmospheric response to the specified SST anomalies in a given AGCM does not necessarily provide a reliable understanding of the role of the extratropical ocean in climate in the real world. That is, the influence of the extratropical ocean on climate is mainly through surface heat flux anomalies, not through SST anomalies (Sutton & Mathieu, 2002).

5. Paleoclimate Evidence of AMV, Multidecadal AMOC Variability, and Associated Climate Linkages

The brevity of available instrumental data limits our understanding of AMV. Paleoclimate proxy-derived reconstructions of AMV-related signals that extend beyond the instrumental era provide an important basis for understanding the nature and stationarity in time of AMV and associated climate impacts. This section briefly reviews the paleoclimate reconstructions of AMV and inferred linkages with multidecadal AMOC variability and associated regional- and hemispheric-scale climate phenomena.

5.1. Paleoclimate Proxies for AMV and Multidecadal AMOC Variability

5.1.1. AMV Reconstructions Primarily Based on Terrestrial Proxies

The large spatial scale of AMV, and its diverse set of associated climate impacts, means that it can, in principle, be reconstructed using both terrestrial and marine proxies. A reasonable paleo reconstruction of AMV, however, needs to be carefully calibrated to the instrumental AMV record. A pioneering reconstructed AMV index using tree ring records from regions that are influenced by AMV is strongly correlated with the instrumental AMV index and exhibits robust multidecadal variability extending back to the sixteenth century (Gray et al., 2004). Another, longer (past 1,500 years), terrestrial-dominated reconstruction of the AMV

index (Mann et al., 2009) includes multiproxy records (tree rings, ice cores, corals, speleothems, sediments, etc.) with broad spatial coverage, although some proxy records included have a realtively low temporal (decadal) resolution. This reconstruction has few spatial degrees of freedom before the seventeenth century and as such may not be able to resolve AMV well in space. It is calibrated against the instrumental records and is broadly comparable with AMV reconstruction from Gray et al. (2004). The more recent J. Wang, Yang, et al. (2017) AMV reconstruction using terrestrial proxy records (tree rings, ice cores, etc.) over the past 1,200 years has both broad spatial coverage and high temporal (annual) resolution. It is largely consistent with the instrumental AMV index and the reconstructions of Gray et al. (2004) and Mann et al. (2009) during their respective overlapping periods. However, this reconstruction exhibits a stronger and more persistent AMV signal before the sixteenth century compared with the reconstruction of Mann et al. (2009), which is likely related to the higher temporal resolution of J. Wang, Yang, et al. (2017). The reconstruction exhibits a broad band of enhanced multidecadal variability significantly above a red noise background (Figure 18a), inconsistent with the mechanism that AMV is a direct SST response induced by the atmospheric white noise (section 3.1; Clement et al., 2015, 2016; Cane et al., 2017).

The analyzed AMV index from the Last Millennium Reanalysis (Hakim et al., 2016; Steiger et al., 2014), which employs data assimilation to reconstruct climate fields from a diverse set of terrestrial-dominated proxy time series (Ahmed et al., 2013), has an extremely high correlation ($r = 0.97$) and very similar amplitude to reconstructed multidecadal global mean surface temperature anomalies over the last 2,000 years from this reanalysis (Singh et al., 2018), including the instrumental period. The global-scale spatial pattern of surface temperature regressed on this analyzed AMV index is centered over the northern North America and Europe, whereas the much weaker signal in the Atlantic Ocean is indistinguishable from that in other ocean basins (Singh et al., 2018). The above results suggest that this mode mainly reflects the global mean surface temperature and does not represent AMV. Many studies have pointed out the importance of removing the global-scale signal in the AMV definition (e.g., Frajka-Williams et al., 2017; Frankignoul et al., 2017; Sutton et al., 2018; Trenberth & Shea, 2006; Yan et al., 2019). When the component regressed on the global-scale signal is removed, there is essentially not much AMV signal in this reanalysis, in contrast to the pronounced multidecadal variations exhibited in the instrumental AMV index (Figure 2).

5.1.2. AMV Reconstructions Based on Marine Proxies

Studies focusing on North Atlantic marine proxy records also reveal persistent multidecadal variability prior to the instrumental period, at least back to the eighteenth century (e.g., Kilbourne et al., 2008, 2014; Saenger et al., 2009; Svendsen et al., 2014; Vásquez-Bedoya et al., 2012). A Caribbean SST reconstruction based on the average of SST-related proxy records from four Caribbean sites correlates significantly with local instrumental SST anomaly, as well as with the instrumental AMV index, during their overlapping period (Kilbourne et al., 2014). The extended Caribbean SST reconstruction back to the fourteenth century exhibits significant power at multidecadal timescales above a red noise background. However, it does not correlate well with the two terrestrial-dominated AMV reconstructions (Gray et al., 2004; Mann et al., 2009) prior to the instrumental period. Another marine-based AMV reconstruction since 1781 (Svendsen et al., 2014) is estimated through an optimally weighted average of five published marine coral-based proxy records for SST from the western tropical North Atlantic, where large and long-lived massive growing coral colonies exist. The reconstructed AMV signal, which correlates with the instrumental AMV index, is stationary and persists over the entire period (Svendsen et al., 2014). It is comparable with the two terrestrial-dominated AMV reconstructions (Gray et al., 2004; Mann et al., 2009) but lags them by about 11–12 years. It exhibits stronger multidecadal variability than the reconstruction from Kilbourne et al. (2014).

The choice and weighting of proxies can substantially affect marine-based AMV reconstructions. For example, the coral growth record from the Yucatan peninsula in the Atlantic Warm Pool (Vásquez-Bedoya et al., 2012) compares well with the instrumental local SST and AMV index and all three terrestrial-dominated AMV reconstructions (Gray et al., 2004; Mann et al., 2009; J. Wang, Yang, et al., 2017) since 1775. This record has the largest weight in the Svendsen et al. (2014) reconstruction, which uses an optimally weighted average of records, but has a much smaller weight in the Kilbourne et al. (2014) reconstruction which uses equal weighting across all records. In contrast to this coral growth record, the Sr/Ca ratio records included in both Kilbourne et al. (2014) and Svendsen et al. (2014) reconstructions have difficulties in representing SST and

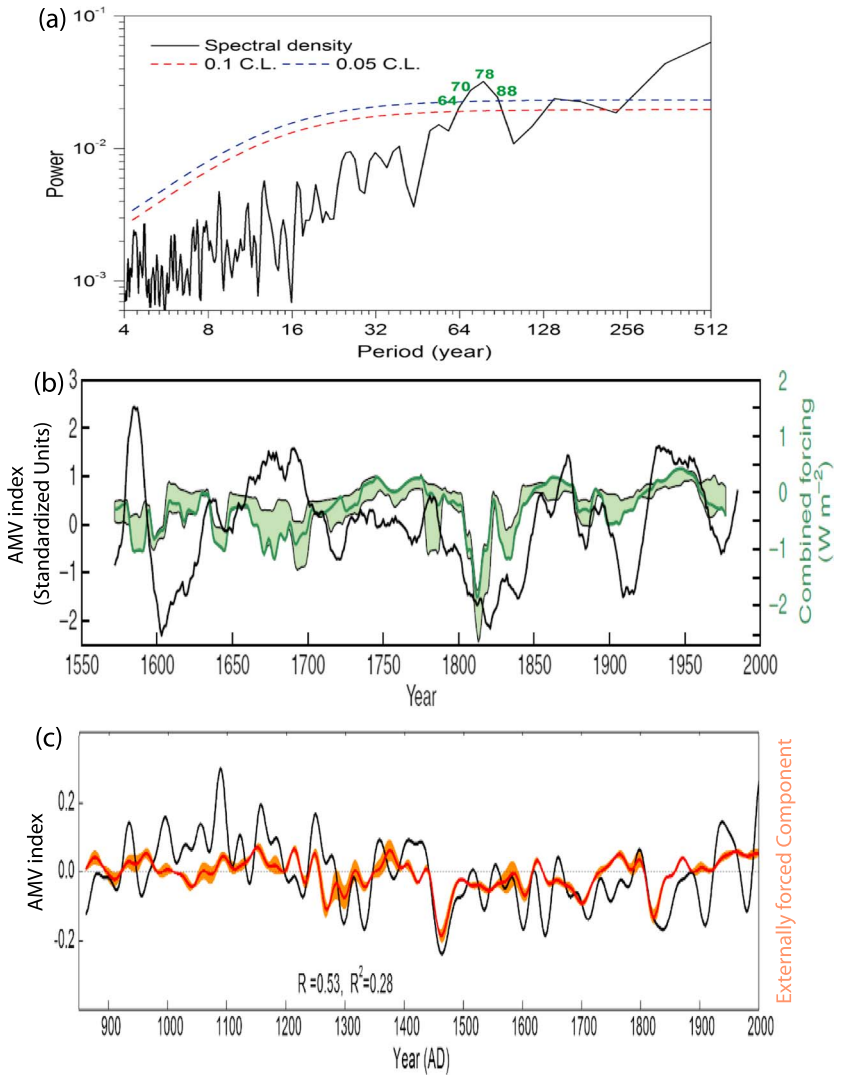

Figure 18. Reconstructed AMV index and the comparison with reconstructed combined solar and volcanic forcings. (a) The spectral density of the reconstructed North Atlantic basin-averaged SST over the period 800–2010, from J. Wang, Yang, et al. (2017). The 95%/90% confidence level (C.L.) is tested against a red noise background (dashed blue/red lines). The band at multidecadal timescales that is significant above the 90% confidence level (dashed red line) is marked with green numbers. (b) The normalized Gray et al. (2004) AMV reconstruction (black line, left axis) and one reconstruction (solid green line) and the spread of nine possible reconstructions (light green shading) of combined solar and volcanic forcings (right axis) since the mid-sixteenth century (11-year running mean) from Knudsen et al. (2014) under a CC BY 3.0 license. (c) The J. Wang, Yang, et al. (2017) AMV reconstruction and the composite (red) and spread (orange) of four reconstructions of externally forced component of AMV based on multiple linear regressions (30-year low-pass filtered), along with the correlation between the reconstructed AMV and the composite of reconstructed externally forced component of AMV and the variance explained, adapted from J. Wang, Yang, et al. (2017). Panels (a, c) are reprinted by permission from Springer Customer Service Centre GmbH: Springer Nature, Nature Geoscience, Internal and external forcing of multidecadal Atlantic climate variability over the past 1,200 years, J. Wang, Yang, et al., Copyright 2017.

compare poorly with instrumental SST records (Vásquez-Bedoya et al., 2012) and thus degrade the two reconstructions that use multiproxy marine based records. In addition to the location, type, and weighting of proxies, differences between reconstructions also arise due to temporal resolution, dating uncertainties, and differences in analysis methods.

The above marine-based AMV reconstructions are all from the tropical North Atlantic. Recently, a combined marine record of growth rates and Mg/Ca ratios from a coralline alga collected off the Labrador coast in the western extratropical North Atlantic has been used as a proxy for local SST over the past six centuries (Moore

et al., 2017). The correlation of this record with the instrumental local SST over the twentieth century is ~0.5. The record exhibits amplified multidecadal variability along with a centennial warming trend after 1825 compared to the prolonged cold period before. This is interpreted as an evidence for an amplification of AMV since the end of the Little Ice Age (Moore et al., 2017). However, as also shown in Moore et al. (2017), there is no evidence of such an amplification of AMV in the Svendsen et al. (2014) AMV reconstruction from the tropical North Atlantic or in the terrestrial Gray et al. (2004) AMV reconstruction with much broader spatial coverage. The Mann et al. (2009) AMV reconstruction has a reduced amplitude during the seventeenth to eighteenth centuries, but the amplitude increases again during the fifteenth to sixteenth centuries (Moore et al., 2017). The prolonged cold period and the reduced multidecadal variability off the Labrador coast before 1825 might reflect a local change due to the enhanced transport of cold fresh Arctic water into this region through the Canadian Arctic Archipelago (i.e., enhanced Arctic influence and reduced North Atlantic influence), as indicated by many surrounding regional paleo evidence (Keigwin et al., 2003).

5.1.3. External Forcing and Paleoclimate AMV

Several studies have analyzed paleoclimate data to investigate whether AMV is internally or externally driven. Correlations between the Gray et al. (2004) and Mann et al. (2009) AMV reconstructions and reconstructed combined solar and volcanic forcing are enhanced since 1775 (Knudsen et al., 2014). The AMOC is suggested to be important for linking changes in external forcing with AMV, based on the spatial cross-covariance pattern between the North Atlantic SST and the combined solar and volcanic forcing at different time lags over the instrumental period (Knudsen et al., 2014). However, the amplitude of the reconstructed combined external forcing (solar and volcanic) anomalies after the early nineteenth century is on the same order as the range of their reconstruction uncertainties and much smaller than the extreme low anomaly associated with the Dalton Minimum of solar activity and the 1815 Tambora volcanic eruption (Figure 18b). Meanwhile, the amplitude of the reconstructed AMV does not exhibit an apparent change throughout the entire period since 1775 (Figure 18b), inconsistent with the nonstationary anomalies in the combined external forcing.

Over the past 12 centuries, the reconstructed solar and volcanic forcing do correlate with the much longer J. Wang, Yang, et al. (2017) AMV reconstruction, but their combined contribution explains less than one third (28%) of the total AMV variance (Figure 18c); the reconstructed AMV is dominated by internal variability (J. Wang, Yang, et al., 2017. The internal variability component of the J. Wang, Yang, et al. (2017) AMV reconstruction also reveals significant signals at multidecadal timescales above a red noise background and its amplitude during the preindustrial period, especially before the Little Ice Age, is on the same order as that found in the instrumental AMV index.

5.1.4. Paleo Proxies for Multidecadal AMOC Variability and Linkage With AMV

Because the AMOC is composed of many separate pathways and dynamical regimes, reconstructions of AMOC variability at multidecadal timescales are challenging. The near-bottom flow speed of the Iceland Scotland Overflow Water (ISOW), one major deep component of the AMOC, has been reconstructed over the past 230 years using the sortable silt mean grain size from a marine sediment core in the Iceland Basin (Boessenkool et al., 2007). Higher values in this proxy (i.e., larger mean grain size) indicate relatively stronger near-bottom flow speeds and vice versa. The reconstructed ISOW speed exhibits pronounced multidecadal variability over the past 230 years and generally covaries with the instrumental AMV index during their overlapping period.

The reconstruction of ISOW speed has been extended to the past 600 years using the sortable silt mean grain size from a different sediment core in the Iceland Basin with a high accumulation rate (Mjell et al., 2016). Their reconstructed ISOW exhibits coherent variations with that reconstructed by Boessenkool et al. (2007) during their overlapping period, and the multidecadal variability extends back to the past ~600 years. Periods of stronger ISOW are associated with warmer periods in the North Atlantic as indicated by the AMV reconstructions (Gray et al., 2004; Mann et al., 2009; Svendsen et al., 2014). The precise phasing between the ISOW vigor and various AMV reconstructions is challenging to determine because of dating uncertainties in ISOW speed reconstructions. Using new constraints on the core top age of the sediment core, the ISOW vigor and the Gray et al. (2004) AMV reconstructions vary coherently during their overlapping period (Figure 19; Ulysses Ninnemann and Nil Irvali, personal communication, 2018). The result indicates the existence of a persistent relationship between AMV and one major deep component of the AMOC prior to the instrumental period.

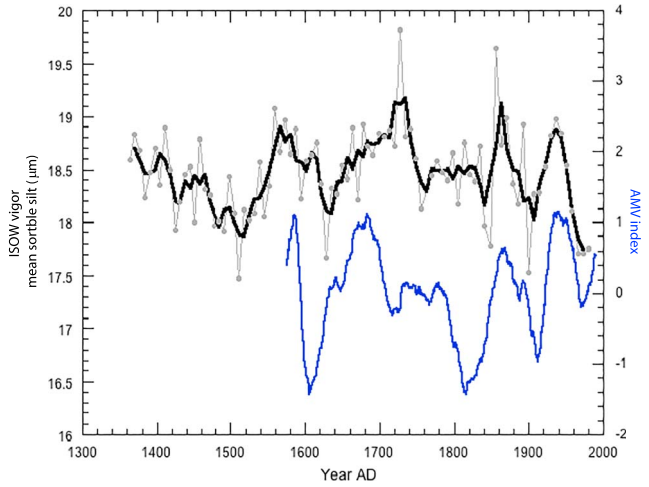

Figure 19. The multidecadal variability observed in the Iceland Scotland Overflow Water (ISOW) compared with the Gray et al. (2004) AMV reconstruction, adapted from Mjell et al. (2016). At top, the detrended sortable silt (SS) data from core GS06-144-09MC-D (thin gray line with three-point smoothing in black), is a proxy for changes in the bottom water flow speed along the southward flow path of ISOW interpreted to reflect changes in the strength of ISOW (Langehaug et al., 2016; Mjell et al., 2016). The age model for the SS record uses published dates from Mjell et al. (2016) but is updated with new constraints on the core top age using the carbon isotope Suess effect (Irvali et al., in preparation/personal communication). The bottom curve illustrates multidecadal changes in North Atlantic climate based on a 20-year smoothing of the detrended tree ring based AMV reconstruction by Gray et al. (2004; blue curve). There is still uncertainty in the age model such that the precise phasing of climate and deep southward transport still needs further work to resolve. Figure provided by Ulysses Ninnemann and Nil Irvali (personal communication, 2018).

An indirect proxy for the AMOC may be obtained using $\delta^{18}O$ ratios from shells of the long-lived marine bivalve *Arctica Islandica*. Samples have been used to reconstruct temperatures within the inner North Icelandic Irminger Current, continuously over the last millennium (Reynolds et al., 2016). The relative warmth of the North Icelandic Irminger Current covaries with the AMOC; variability in this proxy thus indicates a leading role for the AMOC in Northern Hemisphere climate variability on multidecadal timescales. Specimens collected from the Tiree Passage, located on the western fringes of the Hebridean continental shelf, northwest Scotland, provides a proxy for mean summer temperature variability associated with changes in subpolar gyre dynamics and the North Atlantic Current over 1799–2010 (Reynolds et al., 2017).

5.2. Paleo Proxies for Associated Climate Linkages

Here we briefly review studies investigating climate linkages associated with AMV prior to the instrumental period using paleoclimate proxy records, and the comparison with the climate impacts of AMV inferred from instrumental records and climate model simulations (section 4).

5.2.1. Linkage With ITCZ and Related Phenomena

Multidecadal West African monsoon and regional ITCZ migrations reconstructed using sediment cores from Lake Bosumtwi, Ghana, exhibit a significant coherent relationship with the Gray et al. (2004) AMV reconstruction during their overlapping period (Shanahan et al., 2009). The sediment record indicates that significant multidecadal variability persisted over the past three millennia, suggesting that multidecadal ITCZ migrations and long-lasting episodes of wet/dry conditions over West Africa were a regular feature prior to the instrumental period and possibly indicating an AMV influence. Reconstructions indicate that periods of high precipitation over West Africa (suggestive of a northward ITCZ shift) are associated with periods of positive AMV, consistent with observations over the instrumental period and climate model simulations (section 4.1).

Spectral analyses of tropical Atlantic precipitation proxy records from the Yucatan Peninsula and the Cariaco Basin, which are linked to AMV and associated Atlantic ITCZ during the instrumental period, indicate a significant quasi-persistent AMV-related tropical Atlantic ITCZ signal over the past 8,000 years that is not dominated by the reconstructed solar forcing (Knudsen et al., 2011). The comparison of tree ring-based Indian summer monsoon rainfall reconstructions (Borgaonkar et al., 2010; Pant et al., 1988; Shi et al., 2014) with AMV reconstructions (Gray et al., 2004; Mann et al., 2009; Svendsen et al., 2014) suggests that the observed and modeled impact of AMV on Indian summer monsoon rainfall (e.g., Goswami et al., 2006; Li et al., 2008; Lu et al., 2006; Luo et al., 2011; Wang et al., 2009; Zhang & Delworth, 2006) persists back to around 1800 (Sankar et al., 2016). Prior to 1800, the large spread among tree ring reconstructions for Indian summer monsoon rainfall makes it very difficult to assess the relationship with AMV, and data with improved quality are needed to be conclusive (Sankar et al., 2016).

5.2.2. Linkage With Pacific Climate Variability

To study the linkage between AMV and multidecadal variability in the North Pacific beyond the instrumental period, the Gray et al. (2004) AMV reconstruction is compared with a low-pass-filtered marine record (1818–1967) of Mg/Ca ratios from a coralline alga collected in the western Bering Sea-Aleutian Island region, a proxy for local SST (Hetzinger et al., 2012). This proxy record is positively correlated with the local instrumental SST record, the instrumental AMV index, and the Gray et al. (2004) AMV reconstruction during their respective overlapping periods. The implied linkage between AMV and multidecadal variability in the northern North Pacific prior to the instrumental period is consistent with the teleconnection observed during the instrumental period (d'Orgeville & Peltier, 2007). Despite this evidence, preinstrumental relationships between AMV and PDV remain unclear (compared to the relationship discussed in section 4.2 for the

twentieth century), because paleo reconstructions of PDV index over the last several centuries differ substantially among themselves prior to the instrumental period (Newman et al., 2016).

5.2.3. Linkage With Extratropical Atmospheric Circulation

At multidecadal timescales over the nineteenth and twentieth centuries, the instrumental winter NAO index is significantly anticorrelated with the speed of ISOW (one major deep component of the AMOC) reconstructed from the marine sediment core in the Iceland Basin since 1824 (Boessenkool et al., 2007). Because the reconstructed ISOW speed generally covaries with the instrumental AMV index, the result is consistent with the anticorrelated relationship between AMV and multidecadal winter NAO variability observed over the instrumental period (section 4.3). The relationship between the reconstructed multidecadal ISOW speed (Mjell et al., 2016) and winter NAO (Trouet et al., 2009) over the past 600 years appears anticorrelated during the fifteenth century, but it does not hold during the sixteenth to eighteenth centuries (Mjell et al., 2016). Meanwhile, periods of stronger ISOW are associated with warmer periods in the North Atlantic in AMV reconstructions. Hence, the results suggest that the relationship between reconstructed AMV (or multidecadal ISOW speed) and multidecadal variability of winter NAO reconstructed from precipitation/drought proxies (Trouet et al., 2009) over the past several centuries is more complicated than that found during the instrumental period. The impact of AMV on multidecadal winter NAO variability might be sensitive to the background atmospheric state (Keenlyside & Omrani, 2014; Omrani et al., 2014), which could have been very different and contributed to a more complicated AMV and NAO relationship in the past. However, the large spread in winter NAO reconstructions prior to the instrumental period (Cook et al., 2002; Glueck & Stockton, 2001; Luterbacher et al., 2002; Ortega et al., 2015; Trouet et al., 2009) limits the ability to assess this hypothesis. If the location of the background jet stream shifted in the past, the contemporary definition of the NAO index implicitly used in these paleo reconstructions might not be accurate.

5.2.4. Linkage With Climate over Europe, North America, and Asia

The Gray et al. (2004) AMV reconstruction varies in phase with the extended instrumental summer air temperature record from the Greater Alpine Region (Auer et al., 2007) at multidecadal timescales since 1765, consistent with the observed anticorrelated relationship between glacier surface mass balance in the Swiss Alps and the AMV index during the instrumental period (Huss et al., 2010). Compared with the long-observed record of glacier length change in the Alps (since 1765; Holzhauser & Zumbühl, 1999), the local minima in AMV and Alpine air temperature are followed by glacial advances with a decadal time lag, suggesting that AMV had an impact on the Alpine glacier changes over the last 250 years (Huss et al., 2010). The rock magnetic properties of sedimentary records over the last 2,500 years from two high Alpine lakes are substantially influenced by climate conditions (Hirt et al., 2003; Lanci et al., 1999, 2001), and the only spectral peak in each record that is significantly above a red noise background is at multidecadal timescales (Lanci & Hirt, 2015). There is also high coherence between the two independent sedimentary records at multidecadal timescale, and this frequency band is quite similar to that found for the instrumental AMV index and cannot be explained by variations of the total solar irradiance (Lanci & Hirt, 2015). The multidecadal climate signal recorded in the two lake sediments also varies in phase with the instrumental AMV index over the last 110 years and consistently suggests that AMV played a significant role in the past multidecadal variability of the Alpine climate (Lanci & Hirt, 2015). The above linkage between AMV and the central European climate during the preindustrial period agrees with that observed over the instrumental period and simulated in climate models (section 4.4).

The imprint of AMV signal is detectable in North American climate proxies. Across western North America since late sixteenth century, fire scars on tree rings tends to be synchronous over a vast region (from the southwest to the northern Rockies) that experiences drought conditions (reconstructed from tree rings) during the positive AMV phase inferred from the Gray et al. (2004) AMV reconstruction; this evidence suggests that AMV drives broad patterns in drought and thus wildfire synchrony over the western North America at multidecadal timescales during the preindustrial period (Kitzberger et al., 2007). Reconstructions of the Palmer Drought Severity Index (based on tree ring records) averaged over the Great Plains or southwest North America are significantly anticorrelated with the Gray et al. (2004) AMV reconstruction, and drought over the two regions is associated with a positive AMV phase (Feng et al., 2011). These results are consistent with the observed and simulated impact of AMV on the North American drought (section 4.4).

Moisture availability in northeastern Asia reconstructed using regional high resolution tree ring widths since 1568 exhibits coherent multidecadal variations with the instrumental AMV index and the Gray et al. (2004) AMV reconstruction during their respective overlapping periods (Wang et al., 2011). The linkage seen in this proxy record is consistent with previously observed and modeled results of warmer and wetter conditions over northeast China during the positive AMV phase (Li & Bates, 2007; Wang et al., 2009; Zhou et al., 2015) and decadal prediction experiments (Monerie et al., 2018). The tree ring-based summer surface temperature reconstruction over the eastern Tibetan Plateau is significantly correlated with local instrumental records as well as with the instrumental AMV index and has a fragile direct relationship with solar forcing at multidecadal timescales but a robust in-phase relationship with the Mann et al. (2009) AMV reconstruction over the last millennium (J. Wang, Yang, & Ljungqvist, 2015). This result suggests a vital role of AMV in multidecadal summer surface temperature variability over the eastern Tibetan Plateau, consistent with that observed over the instrumental period (Feng & Hu, 2008; Wang et al., 2009) and simulated in climate models (Wang et al., 2009).

5.2.5. Linkage With Polar and High Latitude Climate

Pronounced multidecadal Arctic temperature variability associated with AMV is evident in ice core records from Greenland and the Canadian Arctic since the fourteenth century (Chylek et al., 2011). A robust AMV-related climate signal with a significant peak around 70-year exists in the ice core records from Greenland and Canadian Arctic throughout the past 1,200 years (Zhou et al., 2016). Spectral analyses of ice core records from Greenland and the Canadian Arctic show a significant, quasi-persistent, AMV-related climate signal over the Arctic region during the last ~8,000 years that is not explained by solar forcing (Knudsen et al., 2011). These Arctic ice core records are closely linked to the AMV index during the instrumental period, consistent with AMV-related multidecadadal variability in Arctic surface air temperature observed during the twentieth century and simulated in climate models (section 4.5).

Historical records of Arctic sea ice from the North Icelandic shelf over the Holocene (Moros et al., 2006) and the western Nordic Seas since 1200 (Macias Fauria et al., 2010) have been synthesized to infer winterspring Arctic sea ice conditions, and they exhibit persistent multidecadal variability prior to the instrumental period (Miles et al., 2014). Over the twentieth century, these reconstructed multidecadal sea ice fluctuations are consistent with the observed sea ice records from the Russian Arctic seas (Polyakov, Alekseev, et al., 2003). The reconstructed multidecadal variations of winter Arctic sea ice at the Atlantic side are anticorrelated with the instrumental AMV index and the Gray et al. (2004) AMV reconstruction during their overlapping periods, consistent with the impact of AMV on multidecadal winter Arctic sea ice variability found in climate models (e.g., Day et al., 2012; Mahajan, Zhang, & Delworth, 2011) and decadal prediction experiments (Msadek et al., 2014; Robson, Sutton, & Smith, 2014; Yeager et al., 2015).

5.2.6. Linkage With Hemispheric-Scale Surface Temperature

The reconstructed Northern Hemisphere mean surface temperature spanning the past 1,500 years by Mann et al. (2009) correlated well with their AMV reconstruction at multidecadal timescales. However, this result might be limited by the low spatial degree of freedom in their reconstruction, especially before the seventeenth century. There is a significant correlation between the J. Wang, Yang, et al. (2017) AMV reconstruction and a composite of Northern Hemisphere summer temperature-sensitive tree ring records, as well as a composite of published Northern Hemisphere mean surface temperature reconstructions over the past 1,200 years. Both the reconstructed AMV index and Northern Hemisphere mean surface temperature are dominated by internal variability at multidecadal timescales, and thus a significant correlation also exists even after estimates of external forced components are removed from both reconstructions. The suggested linkage between AMV and the Northern Hemisphere mean surface temperature through internal climate variability over the extended reconstruction period is consistent with that observed over the twentieth century and simulated in climate models (section 4.6).

5.3. Summary and Discussion

Paleo reconstructions largely indicate that AMV is a persistent phenomenon that retains enhanced power at low frequencies significantly above the background red noise level through the preindustrial period. The reconstructed AMV is not primarily driven by external forcing. Paleo proxies also support the existence of the AMOC-AMV linkage over the past several centuries. Various climate linkages associated with AMV in modern climate, such as the linkages with the Atlantic ITCZ, Western African Monsoon, climate over

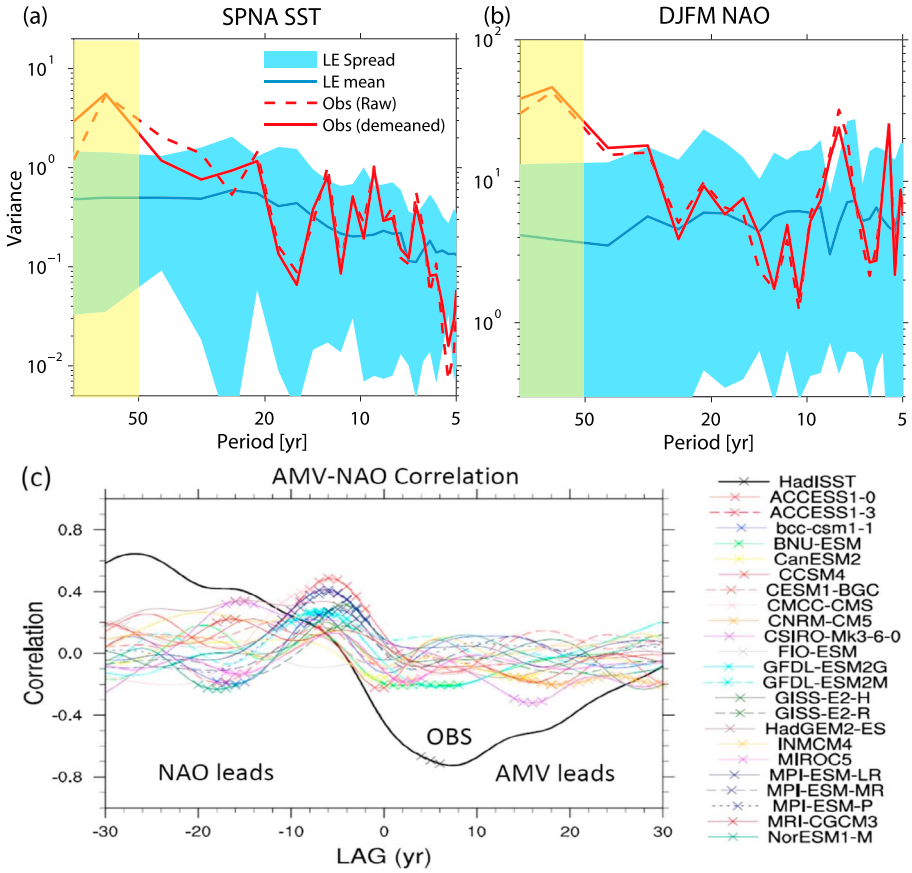

Figure 20. Climate model biases in AMV, low-frequency winter NAO, and their correlations. (a, b) Power spectra of the annual subpolar North Atlantic SST (a) and winter (DJFM) NAO (b) from the large ensemble of a CGCM's historical simulations—National Center for Atmospheric Research (NCAR) CESM-LE, adapted from Kim, Yeager, Chang, and Danabasoglu (2018), © Copyright 2018 AMS. Blue shading: ensemble spread; blue line: ensemble mean; solid red line: observations; red dashed line: observations with the simulated externally forced response removed. The simulated externally forced response is removed from each ensemble member. The yellow shading highlights the low frequency band where the model substantially underestimates the observed variance. (c) Lead-lag correlations between the basin-wide SST-based AMV index and the decadal winter NAO index (with the high-frequency component removed) in individual CMIP5 models and observations (black line). Negative (positive) lags indicate that the winter NAO precedes (follows) AMV. Crosses indicate where the correlation is significant at the 95% level. Adapted from Peings et al. (2016).

Europe, North America, Asia, and Arctic, as well as Northern Hemisphere mean surface temperature, also appear to be imprinted in paleo proxy records prior to the instrumental period. These linkages are largely consistent with the climate impacts of AMV and multidecadal AMOC variability indicated in instrumental records and simulated in climate models that are reviewed in section 4. There are, however, substantial uncertainties in reconstructions of PDV and NAO, making it challenging to assess their relationship with AMV in the past.

6. Conclusions and Challenging Issues

Understanding the linkage between the AMOC and AMV and associated climate impacts is crucial for interpreting the past record and for predicting future climate change and variability. In this review, we have synthesized paleo evidence, modern observations, and climate simulations to provide a comprehensive picture of our current understanding of this linkage. The following summarizes our key findings:

1. The observed key elements of AMV are critical for understanding the mechanisms of AMV and its linkage with the AMOC. The observed AMV is associated with a dipole SST pattern over the entire (North and South) Atlantic and a monopolar pattern over the North Atlantic with high spatial coherence. As

AMV evolves, subpolar SST signals propagate into the tropical North Atlantic along a horseshoe-shaped pathway. The observed AMV is correlated with multidecadal variations in the ocean-driven surface turbulent heat fluxes over the midlatitude North Atlantic. There is a high coherence among observed subpolar North Atlantic SST, SSS, and upper ocean heat and salt content variations but only at low frequencies (decadal and longer timescales). Multidecadal variations in upper and deep subpolar North Atlantic temperature are anticorrelated. Tropical North Atlantic surface and subsurface temperature variations associated with observed AMV are significantly anticorrelated. The observed subpolar North Atlantic SST and SSS exhibit decadal persistence and much higher multidecadal power in their spectra than that expected from a red noise process, consistent with the significant multidecadal variability above the background red noise level found in many extended paleo proxies of AMV-related signals.

2. Observational and modeling results are consistent with a central role for multidecadal AMOC variability in AMV. In particular, this AMOC-AMV linkage is consistent with all the above observed key elements of AMV and underlies the enhanced decadal predictability and prediction skills of AMV. Multidecadal variability in the AMOC and associated Atlantic meridional heat transport are leading-order contributors to the subpolar North Atlantic SST and upper ocean heat content anomalies at low frequencies and should not be neglected in any mathematical representations of the system. Coupled air-sea feedbacks in response to changes in the subpolar North Atlantic are important for the propagation of AMV SST signal from the subpolar to the tropical North Atlantic along the horseshoe pathway. The hypothesis that changes in external radiative forcing or stochastic atmospheric forcing is the primary driver of AMV disagrees with many observed key elements of AMV. It is also inconsistent with the paleo evidence that AMV has enhanced multidecadal power significantly above a red noise background and is not dominated by the external forcing. It is critical to use multivariate metrics to understand the key drivers of the observed AMV.
3. There is an essential role for AMOC in many AMV-related regional and hemispheric-scale climate phenomena, such as the ITCZ, Sahel/Indian monsoons, Atlantic Hurricanes, ENSO, PDV, NAO, climate over Europe, North America, and Asia, Arctic sea ice and surface air temperature, and Northern Hemisphere/global mean surface temperature. In particular, AMOC-induced anomalous Atlantic meridional heat transport and surface heat flux released into the atmosphere over middle- to high-latitude North Atlantic are crucial for many AMV-related climate impacts. Initializing the AMOC anomalies at northern high latitudes is critical in predicting the observed AMV decadal shifts and associated climate impacts.
4. Paleo reconstructions largely indicate that AMV is a phenomenon that existed prior to the instrumental period, with enhanced power at multidecadal timescales significantly above a red noise background and not dominated by solar and volcanic forcing. Paleo proxies indicate that the linkage between AMV and multidecadal AMOC variability also existed in the preindustrial era. Various climate linkages associated with AMV, such as the linkages with the ITCZ, Western African Monsoon, climate over Europe, North America, Asia, and Arctic, as well as Northern Hemisphere mean surface temperature, are also imprinted in paleo proxy records prior to the instrumental period and are consistent with the climate impacts of AMV and multidecadal AMOC variability indicated in instrumental records and simulated in climate models.

Despite the above key findings, our understanding of the linkage between the AMOC and AMV and associated climate impacts is hindered by substantial biases in most climate models. Most CGCMs have difficulty simulating observed pattern and amplitude of AMV and associated impacts. For example, the amplitudes of internal variability in subpolar North Atlantic SST and associated winter NAO in a CGCM's historical simulation are much weaker than observed at multidecadal timescales (Figures 20a and 20b), which are linked to the underestimated low-frequency internal AMOC variability (Kim, Yeager, Chang, & Danabasoglu, 2018). Correcting the mean state North Atlantic SSS and AMOC biases in CGCMs might improve the pattern and amplitude of AMV-related SST and surface turbulent heat fluxes (Drews & Greatbatch, 2016, 2017; Park et al., 2016). The impact of AMV on the anticorrelated multidecadal variability in winter NAO is substantially underestimated in most CGCMs (e.g., Peings et al., 2016; Ting et al., 2014), due to the underestimated internally generated AMV signal and associated surface turbulent heat flux anomalies (Peings et al., 2016). This is consistent with the underestimation of internal multidecadal winter NAO/North Atlantic jet stream variability in many CGCMs' historical simulations (Kravtsov, 2017; X. Wang, Li, Sun, & Liu, 2017; Kim,

Yeager, Chang, & Danabasoglu, 2018; Simpson et al., 2018; Xu et al., 2018). At low frequencies, most CGCMs simulate a stronger-than-observed positive correlation when the winter NAO index leads AMV by ~5 years despite their underestimated amplitudes, and the observed strong anticorrelation with the winter NAO index is almost absent when AMV leads by several years (Figure 20c; Peings et al., 2016). The impact of AMV on the European summer surface air temperature is underestimated in many CGCMs (Qasmi et al., 2017), especially in those CGCMs that have particularly weak correlations between AMV and multidecadal surface turbulent heat flux anomalies over the midlatitude North Atlantic (O'Reilly et al., 2016).

Most current CGCMs lack both the critical trade wind speed response to the midlatitude AMV signal and the positive low cloud feedback over the tropical Atlantic (Figure 8a; Martin et al., 2014; Yuan et al., 2016). As a result, the tropical AMV SST signal and its teleconnection with the subpolar AMV SST signal simulated in most CGCMs are much weaker than observed; the North American precipitation response to AMV is mostly absent, in additional to the much weaker than observed Sahel rainfall response to AMV (Kavvada et al., 2013; Kim, Yeager, Chang, & Danabasoglu, 2018; Martin et al., 2014; Ruiz-Barradas et al., 2013; Sheffield et al., 2013; Yuan et al., 2016). The tropical Atlantic is a region with substantial mean state model biases in CGCMs (e.g., Cabos et al., 2017; Farneti, 2017; Harlaß et al., 2018; Koseki et al., 2018; McGregor et al., 2018; Richter et al., 2014; Xu et al., 2014). CGCMs with smaller mean state SST biases in the tropical Atlantic simulate a more realistic subpolar-tropical AMV teleconnection and thus stronger tropical AMV signal and associated climate impacts (e.g., ITCZ shift, changes in the vertical wind shear over the Atlantic hurricane MDR; Martin et al., 2014). Mean state SST biases in the tropical Atlantic in most CGCMs also weaken the tropical Pacific response to tropical Atlantic warming in recent decades (McGregor et al., 2018). Enhanced horizontal and vertical resolutions in the atmosphere and ocean components in CGCMs may partially alleviate the tropical Atlantic mean state biases (e.g., Harlaß et al., 2018; Xu et al., 2014) and improve teleconnections between the subpolar and the tropical AMV signal and associated coupled air-sea feedbacks.

The simulated AMOC-AMV linkage varies considerably among CGCMs (Ba et al., 2014; Keenlyside et al., 2016; Medhaug & Furevik, 2011; Wu et al., 2018; Yan et al., 2018; Zhang & Wang, 2013). The diverse AMOC-AMV linkage in unforced CGCM simulations is likely affected by the spread of mean state model biases in the North Atlantic (Ba et al., 2014; Brown et al., 2016; Menary et al., 2015; Wang et al., 2014; Wu et al., 2018). Artificially improving the mean state North Atlantic SSS and AMOC structure in some CGCMs leads to a stronger AMOC-AMV linkage (Park et al., 2016). The AMOC-AMV linkage depends on the amplitudes of low-frequency AMOC variability (Figure 9) and thus is likely much weaker in most CGCMs than in the real world due to the underestimated low-frequency AMOC variability (Yan et al., 2018). The underestimated low-frequency AMOC variability amplifies the relative role of external radiative forcing or stochastic atmospheric forcing in AMV (Kim, Yeager, Chang, & Danabasoglu, 2018). The low-frequency winter Arctic sea ice variability in CGCMs is much weaker than observed, likely related to the underestimated low-frequency variability in AMOC, Atlantic heat transport and surface winds (D. Li, Zhang, & Knutson, 2017, 2018). The linkage between AMV and Northern Hemisphere mean surface temperature is also weak in most CGCMs' unforced simulations due to the underestimated low-frequency AMOC variability (Yan et al., 2018). This is consistent with evidence that internal low-frequency variability of Northern Hemisphere surface air temperature is underestimated in many CGCMs' historical simulations (Wang et al., 2017) and that the CGCMs with smaller mean state biases in the North Atlantic SST/SSS and AMOC structure may have stronger AMOC-AMV linkage and higher multiyear predictability in the Northern Hemisphere surface air temperature (Wu et al., 2018).

The above model deficiencies are a serious challenge when using the current CGCMs for understanding and attributing observed AMV and AMV-related climate impacts during the industrial era. On the other hand, they also pose great opportunities for future research. For example:

1. It is essential to improve CGCMs' mean state AMOC structure and North Atlantic SST and SSS for more realistic simulations of low-frequency AMOC variability and for achieving more realistic linkages between the AMOC and AMV and associated climate impacts and much higher Atlantic decadal predictability. The CGCMs coupled with an isopycnal-coordinate ocean component or including an overflow parameterization are promising in simulating a more realistic mean state AMOC structure and associated North Atlantic SST due to improved Nordic Seas overflows.

2. It is important to understand the relative roles of Labrador Sea versus northeastern North Atlantic deep water formation versus Nordic Seas overflows in low-frequency AMOC variability, both by using long-sustained observations and improved climate models.
3. The improvements of the anticorrelated relationship between AMV and winter NAO as well as the coupled Arctic-North Atlantic interaction at multidecadal timescales in CGCMs might be critical for improving the amplitude of multidecadal variability in surface heat and freshwater buoyancy fluxes over NADW formation sites and thus the amplitude of multidecadal AMOC variability. The strength of two-way ocean-atmosphere coupling remains uncertain and is an important area for future research.
4. Currently, enhanced Atlantic decadal prediction skill is achieved primarily by initializing AMOC anomalies instead of predicting AMOC anomalies at northern high latitudes. A better understanding of the linkages between surface heat and freshwater buoyancy fluxes over NADW formation sites and the AMOC is important for predicting AMOC anomalies at northern high latitudes and for improving prediction at longer lead times.
5. The pattern and amplitude of AMOC-driven multidecadal fluctuations in surface heat flux released into the atmosphere over the middle- to high-latitude North Atlantic, which are crucial for many AMV-related climate impacts (e.g., ITCZ, vertical wind shear over the Atlantic hurricane MDR, winter NAO, and European summer climate), are poorly simulated in CGCMs and should be targeted for future understanding and improvements.
6. It is essential to apply realistic AMV-related surface heat flux anomalies associated with the anomalous ocean heat transport convergence to simulate more realistic climate impacts of AMV in hybrid CGCMs and to compare results across different models with similar surface heat flux anomalies.
7. The propagation of the subpolar AMV SST signal into the tropics and associated coupled air-sea feedbacks are significantly hampered by the substantial mean state SST biases in the tropical Atlantic in most CGCMs and are likely to be improved in CGCMs with enhanced horizontal and vertical resolutions in the atmosphere and ocean components due to partially reduced tropical Atlantic mean state biases. Mechanisms for the propagation of the subpolar AMV SST signal into the tropical North Atlantic deserve more detailed investigations.
8. Simulated AMV-related climate impacts (e.g., ITCZ, vertical wind shear over the Atlantic hurricane MDR, winter NAO, and European and North American summer climate) are much weaker or absent in unforced CGCM simulations than those found in AGCM/hybrid CGCM simulations forced by the observed AMV-like forcing. It is important to understand the key factors causing the deficiencies in modeling these climate impacts in unforced CGCM simulations for future improvements.
9. The observed decadal time lag between PDV and AMV is not well understood and needs to be better simulated in climate models. The observational records are too short to test the robustness of the lagged relationship between PDV and AMV. Improved paleo reconstructions of PDV with substantial smaller uncertainties might help to assess its relationship with AMV in the past.
10. Many paleo reconstructions are focused on terrestrial and marine surface temperature signals and direct proxies of AMOC strength are limited. Paleo reconstructions using other marine signals (e.g., subpolar North Atlantic SSS and subsurface North Atlantic temperature, coastal sea level, and current speed) might provide valuable information to compare with modern observations and modeling results, particularly with respect to AMV and multidecadal AMOC variability, and should be encouraged.

Given the substantial modeling biases and the difficulties in addressing these biases in current CGCMs, it would be valuable to employ a hierarchy of models. A better understanding of the linkages also requires the expansion of high-resolution paleo records and sustained long-term instrumental observations in the future. More comprehensive uncertainty quantification in paleoclimate reconstructions of both AMV and AMOC would facilitate the understanding of their linkage over the past. Deficiencies in modeling the observed AMOC, AMV, and associated climate impacts, especially the underestimated linkage between the AMOC and AMV and associated climate impacts in most current CGCMs, lead to a substantial degree of uncertainty in current studies but also indicate a great potential for future improvements in understanding and predicting AMV and associated climate impacts. With such improvements, decadal prediction skill associated with multidecadal AMOC variability can ultimately be extended beyond the subpolar North Atlantic to the tropical North Atlantic, the South Atlantic, and the Pacific, as well as the surrounding continents, cryosphere, and atmosphere.

Glossary

AGCM	atmosphere general circulation model
AGCM-AMV experiment	AGCM (or AGCM coupled to a slab ocean outside the North Atlantic) experiment forced by prescribed SST anomalies associated with the observed AMV
AMOC	Atlantic Meridional Overturning Circulation
AMO	Atlantic Multidecadal Oscillation
AMV	Atlantic Multidecadal Variability
CGCM	coupled general circulation model
CGCM-AMV experiment	CGCM experiment with the Atlantic (or North Atlantic) SST restored to the observed AMV (or estimated internal component of the observed AMV)
CMIP3	Coupled Model Intercomparison Project, phase 3
CMIP5	Coupled Model Intercomparison Project, phase 5
ENSO	El Niño–Southern Oscillation
ERSST	U.S. National Oceanic and Atmospheric Administration's Extended Reconstructed SST
HADISST	Hadley Centre Sea Ice and Sea Surface Temperature data set
ISOW	Iceland Scotland Overflow Water
ITCZ	Intertropical Convergence Zone
JEBAR	Joint Effect of Baroclinicity and Relief
MDR	main development region
NADW	North Atlantic Deep Water
NAO	North Atlantic Oscillation
OGCM	ocean general circulation model
PDO	Pacific Decadal Oscillation
PDV	Pacific Decadal Variability
RAPID	Rapid Climate Change, a program to understand the causes of sudden changes in the Earth's climate and monitor the AMOC at 26°N
SLP	sea level pressure
SSS	sea surface salinity
SST	sea surface temperature

Acknowledgments
We thank the joint support from the US AMOC Science Team and the U.K.-U.S. RAPID program for this review paper. The HADISST data set used in Figure 2 can be downloaded from https://www.metoffice.gov.uk/hadobs/hadisst/data/download.html. Y. -O. K. is supported by the National Science Foundation (NSF; OCE-1242989) and Department of Energy (DE-SC0019492). S. G. Y. is partially supported by the NSF Collaborative Research EaSM2 grant OCE-1243015. G. D. and S. G. Y. are supported by the National Center for Atmospheric Research, which is a major facility sponsored by the National Science Foundation under Cooperative Agreement 1852977. D. E. A. was supported by an NSF postdoctoral fellowship. We would like to thank Ulysses Ninnemann and Nil Irvali for providing Figure 19. We thank Mike Winton and Xiaoqin Yan for the internal review of the manuscript.

References

Ahmed, M., Anchukaitis, K. J., Asrat, A., Borgaonkar, H. P., Braida, M., Buckley, B. M., et al. (2013). Continental-scale temperature variability during the past two millennia. *Nature geoscience*, *6*(5), 339.

Alley, R. B. (2007). Wally was right: Predictive ability of the North Atlantic "conveyor belt" hypothesis for abrupt climate change. *Annual Review of Earth and Planetary Sciences*, *35*(1), 241–272. https://doi.org/10.1146/annurev.earth.35.081006.131524

Årthun, M., Bogstad, B., Daewel, U., Keenlyside, N. S., Sandø, A. B., Schrum, C., & Ottersen, G. (2018). Climate based multi-year predictions of the Barents Sea cod stock. *PloS one*, *13*(10), e0206319. https://doi.org/10.1371/journal.pone.0206319

Årthun, M., Eldevik, T., Smedsrud, L. H., Skagseth, Ø., & Ingvaldsen, R. B. (2012). Quantifying the influence of Atlantic heat on Barents Sea ice variability and retreat. *Journal of Climate*, *25*(13), 4736–4743. https://doi.org/10.1175/JCLI-D-11-00466.1

Auer, I., Böhm, R., Jurkovic, A., Lipa, W., Orlik, A., Potzmann, R., et al. (2007). HISTALP—Historical instrumental climatological surface time series of the Greater Alpine Region. *International Journal of Climatology*, *27*(1), 17–46. https://doi.org/10.1002/joc.1377

Ba, J., Keenlyside, N. S., Latif, M., Park, W., Ding, H., Lohmann, K., et al. (2014). A multi-model comparison of Atlantic multidecadal variability. *Climate Dynamics*, *43*(9-10), 2333–2348. https://doi.org/10.1007/s00382-014-2056-1

Ba, J., Keenlyside, N. S., Park, W., Latif, M., Hawkins, E., & Ding, H. (2013). A mechanism for Atlantic multidecadal variability in the Kiel Climate Model. *Climate Dynamics*, *41*(7-8), 2133–2144. https://doi.org/10.1007/s00382-012-1633-4

Barcikowska, M. J., Knutson, T. R., & Zhang, R. (2017). Observed and simulated fingerprints of multidecadal climate variability and their contributions to periods of global SST stagnation. *Journal of Climate*, *30*(2), 721–737. https://doi.org/10.1175/JCLI-D-16-0443.1

Belkin, I. M., Levitus, S., Antonov, J., & Malmberg, S. A. (1998). "Great salinity anomalies" in the North Atlantic. *Progress in Oceanography*, *41*(1), 1–68. https://doi.org/10.1016/S0079-6611(98)00015-9

Bellomo, K., Clement, A. C., Murphy, L. N., Polvani, L. M., & Cane, M. A. (2016). New observational evidence for a positive cloud feedback that amplifies the Atlantic Multidecadal Oscillation. *Geophysical Research Letters*, *43*, 9852–9859. https://doi.org/10.1002/2016GL069961

Bellomo, K., Murphy, L. N., Cane, M. A., Clement, A. C., & Polvani, L. M. (2018). Historical forcings as main drivers of the Atlantic multidecadal variability in the CESM large ensemble. *Climate Dynamics*, *50*(9-10), 3687–3698. https://doi.org/10.1007/s00382-017-3834-3

Bellucci, A., Mariotti, A., & Gualdi, S. (2017). The role of forcings in the twentieth-century North Atlantic multidecadal variability: The 1940–75 North Atlantic cooling case study. *Journal of Climate*, *30*(18), 7317–7337. https://doi.org/10.1175/JCLI-D-16-0301.1

Bengtsson, L., Semenov, V. A., & Johannessen, O. M. (2004). The early twentieth-century warming in the Arctic—A possible mechanism. *Journal of Climate*, *17*(20), 4045–4057. https://doi.org/10.1175/1520-0442(2004)017<4045:TETWIT>2.0.CO;2

Bigg, G. R., Wei, H. L., Wilton, D. J., Zhao, Y., Billings, S. A., Hanna, E., & Kadirkamanathan, V. (2014). A century of variation in the dependence of Greenland iceberg calving on ice sheet surface mass balance and regional climate change. *Proceedings of the Royal Society A: Mathematical, Physical and Engineering Sciences*, *470*(2166), 20130662. https://doi.org/10.1098/rspa.2013.0662

Bingham, R. J., Hughes, C. W., Roussenov, V., & Williams, R. G. (2007). Meridional coherence of the North Atlantic meridional overturning circulation. *Geophysical Research Letters*, *34*, L23606. https://doi.org/10.1029/2007GL031731

Bjerknes, J. (1964). Atlantic air-sea interaction. In *Advances in Geophysics*, (Vol. 10, pp. 1–82). NewYork and London: Academic Press.

Boessenkool, K. P., Hall, I. R., Elderfield, H., & Yashayaev, I. (2007). North Atlantic climate and deep-ocean flow speed changes during the last 230 years. *Geophysical Research Letters*, *34*, L13614. https://doi.org/10.1029/2007GL030285

Booth, B. B., Dunstone, N. J., Halloran, P. R., Andrews, T., & Bellouin, N. (2012). Aerosols implicated as a prime driver of twentieth-century North Atlantic climate variability. *Nature*, *484*(7393), 228–232. https://doi.org/10.1038/nature10946

Borgaonkar, H. P., Sikder, A. B., Ram, S., & Pant, G. B. (2010). El Niño and related monsoon drought signals in 523-year-long ring width records of teak (Tectona grandis LF) trees from south India. *Palaeogeography, Palaeoclimatology, Palaeoecology*, *285*(1-2), 74–84. https://doi.org/10.1016/j.palaeo.2009.10.026

Bower, A. S., Lozier, M. S., Gary, S. F., & Böning, C. W. (2009). Interior pathways of the North Atlantic meridional overturning circulation. *Nature*, *459*(7244), 243–247. https://doi.org/10.1038/nature07979

Box, J. E. (2013). Greenland ice sheet mass balance reconstruction. Part II: Surface mass balance (1840–2010). *Journal of Climate*, *26*(18), 6974–6989. https://doi.org/10.1175/JCLI-D-12-00518.1

Box, J. E., Yang, L., Bromwich, D. H., & Bai, L. S. (2009). Greenland ice sheet surface air temperature variability: 1840–2007. *Journal of Climate*, *22*(14), 4029–4049. https://doi.org/10.1175/2009JCLI2816.1

Branstator, G., & Teng, H. (2014). Is AMOC more predictable than North Atlantic heat content? *Journal of Climate*, *27*(10), 3537–3550. https://doi.org/10.1175/JCLI-D-13-00274.1

Broccoli, A. J., Dahl, K. A., & Stouffer, R. J. (2006). Response of the ITCZ to Northern Hemisphere cooling. *Geophysical Research Letters*, *33*, L01702. https://doi.org/10.1029/2005GL024546

Broecker, W. S., Peteet, D. M., & Rind, D. (1985). Does the ocean–atmosphere system have more than one stable mode of operation? *Nature*, *315*(6014), 21–26. https://doi.org/10.1038/315021a0

Broecker, W. S., Takahashi, T., & Li, Y. H. (1976, December). Hydrography of the central Atlantic—I. The two-degree discontinuity. In *Deep Sea Research and Oceanographic Abstracts*, (Vol. 23, No. 12, pp. 1083–1104). Amsterdam: Elsevier.

Brown, P. T., Lozier, M. S., Zhang, R., & Li, W. (2016). The necessity of cloud feedback for a basin-scale Atlantic Multidecadal Oscillation. *Geophysical Research Letters*, *43*, 3955–3963. https://doi.org/10.1002/2016GL068303

Bryan, K. (1962). Measurements of meridional heat transport by ocean currents. *Journal of Geophysical Research*, *67*(9), 3403–3414. https://doi.org/10.1029/JZ067i009p03403

Buckley, M. W., & Marshall, J. (2016). Observations, inferences, and mechanisms of the Atlantic Meridional Overturning Circulation: A review. *Reviews of Geophysics*, *54*, 5–63. https://doi.org/10.1002/2015RG000493

Cabos, W., Sein, D. V., Pinto, J. G., Fink, A. H., Koldunov, N. V., Alvarez, F., et al. (2017). The South Atlantic Anticyclone as a key player for the representation of the tropical Atlantic climate in coupled climate models. *Climate Dynamics*, *48*(11-12), 4051–4069. https://doi.org/10.1007/s00382-016-3319-9

Cane, M. A., Clement, A. C., Murphy, L. N., & Bellomo, K. (2017). Low-pass filtering, heat flux, and Atlantic multidecadal variability. *Journal of Climate*, *30*(18), 7529–7553. https://doi.org/10.1175/JCLI-D-16-0810.1

Castruccio, F. S., Ruprich-Robert, Y., Yeager, S. G., Danabasoglu, G., Msadek, R., & Delworth, T. L. (2019). Modulation of Arctic sea ice loss by atmospheric teleconnections from Atlantic multi-decadal variability. *Journal of Climate*, *32*(5), 1419–1441. https://doi.org/10.1175/JCLI-D-18-0307.1

Cattiaux, J., Vautard, R., Cassou, C., Yiou, P., Masson-Delmotte, V., & Codron, F. (2010). Winter 2010 in Europe: A cold extreme in a warming climate. *Geophysical Research Letters*, *37*, L20704. https://doi.org/10.1029/2010GL044613

Cayan, D. R. (1992). Latent and sensible heat flux anomalies over the northern oceans: Driving the sea surface temperature. *Journal of Physical Oceanography*, *22*(8), 859–881. https://doi.org/10.1175/1520-0485(1992)022<0859:LASHFA>2.0.CO;2

Chafik, L., Häkkinen, S., England, M. H., Carton, J. A., Nigam, S., Ruiz-Barradas, A., et al. (2016). Global linkages originating from decadal oceanic variability in the subpolar North Atlantic. *Geophysical Research Letters*, *43*, 10,909–10,919. https://doi.org/10.1002/2016GL071134

Chang, P., Ji, L., & Li, H. (1997). A decadal climate variation in the tropical Atlantic Ocean from thermodynamic air-sea interactions. *Nature*, *385*(6616), 516–518. https://doi.org/10.1038/385516a0

Charlton-Perez, A. J., Baldwin, M. P., Birner, T., Black, R. X., Butler, A. H., Calvo, N., et al. (2013). On the lack of stratospheric dynamical variability in low-top versions of the CMIP5 models. *Journal of Geophysical Research: Atmospheres*, *118*, 2494–2505. https://doi.org/10.1002/jgrd.50125

Chen, X., & Tung, K. K. (2014). Varying planetary heat sink led to global-warming slowdown and acceleration. *Science*, *345*(6199), 897–903. https://doi.org/10.1126/science.1254937

Chen, X., & Tung, K. K. (2017). Global-mean surface temperature variability: Space–time perspective from rotated EOFs. *Climate Dynamics*, *51*(5-6), 1719–1732.

Chen, X., & Tung, K. K. (2018). Global surface warming enhanced by weak Atlantic overturning circulation. *Nature*, *559*(7714), 387–391. https://doi.org/10.1038/s41586-018-0320-y

Chen, X., Wallace, J. M., & Tung, K. K. (2017). Pairwise-rotated EOFs of global SST. *Journal of Climate*, *30*(14), 5473–5489. https://doi.org/10.1175/JCLI-D-16-0786.1

Cheng, H., Edwards, R. L., Broecker, W. S., Denton, G. H., Kong, X., Wang, Y., et al. (2009). Ice age terminations. *Science*, *326*(5950), 248–252. https://doi.org/10.1126/science.1177840

Cheung, A. H., Mann, M. E., Steinman, B. A., Frankcombe, L. M., England, M. H., & Miller, S. K. (2017). Comparison of low-frequency internal climate variability in CMIP5 models and observations. *Journal of Climate*, *30*(12), 4763–4776. https://doi.org/10.1175/JCLI-D-16-0712.1

Chiang, J. C., Cheng, W., & Bitz, C. M. (2008). Fast teleconnections to the tropical Atlantic sector from Atlantic thermohaline adjustment. *Geophysical Research Letters*, *35*, L07704. https://doi.org/10.1029/2008GL033292

Chikamoto, Y., Kimoto, M., Watanabe, M., Ishii, M., & Mochizuki, T. (2012). Relationship between the Pacific and Atlantic stepwise climate change during the 1990s. *Geophysical Research Letters*, *39*, L21710. https://doi.org/10.1029/2012GL053901

Chylek, P., Dubey, M. K., & Lesins, G. (2006). Greenland warming of 1920–1930 and 1995–2005. *Geophysical Research Letters*, *33*, L11707. https://doi.org/10.1029/2006GL026510

Chylek, P., Dubey, M. K., Lesins, G., Li, J., & Hengartner, N. (2014). Imprint of the Atlantic multi-decadal oscillation and Pacific decadal oscillation on southwestern US climate: Past, present, and future. *Climate dynamics*, *43*(1-2), 119–129. https://doi.org/10.1007/s00382-013-1933-3

Chylek, P., Folland, C. K., Dijkstra, H. A., Lesins, G., & Dubey, M. K. (2011). Ice-core data evidence for a prominent near 20 year time-scale of the Atlantic Multidecadal Oscillation. *Geophysical Research Letters*, *38*, L13704. https://doi.org/10.1029/2011GL047501

Chylek, P., Folland, C. K., Lesins, G., & Dubey, M. K. (2010). Twentieth century bipolar seesaw of the Arctic and Antarctic surface air temperatures. *Geophysical Research Letters*, *37*, L08703. https://doi.org/10.1029/2010GL042793

Chylek, P., Folland, C. K., Lesins, G., Dubey, M. K., & Wang, M. (2009). Arctic air temperature change amplification and the Atlantic Multidecadal Oscillation. *Geophysical Research Letters*, *36*, L14801. https://doi.org/10.1029/2009GL038777

Chylek, P., Klett, J. D., Dubey, M. K., & Hengartner, N. (2016). The role of Atlantic Multi-decadal Oscillation in the global mean temperature variability. *Climate Dynamics*, *47*(9-10), 3271–3279. https://doi.org/10.1007/s00382-016-3025-7

Chylek, P., Klett, J. D., Lesins, G., Dubey, M. K., & Hengartner, N. (2014). The Atlantic Multidecadal Oscillation as a dominant factor of oceanic influence on climate. *Geophysical Research Letters*, *41*, 1689–1697. https://doi.org/10.1002/2014GL059274

Clark, P. U., Pisias, N. G., Stocker, T. F., & Weaver, A. J. (2002). The role of the thermohaline circulation in abrupt climate change. *Nature*, *415*(6874), 863–869. https://doi.org/10.1038/415863a

Clement, A., Bellomo, K., Murphy, L. N., Cane, M. A., Mauritsen, T., Rädel, G., & Stevens, B. (2015). The Atlantic Multidecadal Oscillation without a role for ocean circulation. *Science*, *350*(6258), 320–324. https://doi.org/10.1126/science.aab3980

Clement, A., Cane, M. A., Murphy, L. N., Bellomo, K., Mauritsen, T., & Stevens, B. (2016). Response to comment on "the Atlantic Multidecadal Oscillation without a role for ocean circulation". *Science*, *352*(6293), 1527–1527. https://doi.org/10.1126/science.aaf2575

Collins, M., Botzet, M., Carril, A. F., Drange, H., Jouzeau, A., Latif, M., et al. (2006). Interannual to decadal climate predictability in the North Atlantic: A multimodel-ensemble study. *Journal of Climate*, *19*(7), 1195–1203. https://doi.org/10.1175/JCLI3654.1

Cook, E. R., D'Arrigo, R. D., & Mann, M. E. (2002). A well-verified, multiproxy reconstruction of the winter North Atlantic Oscillation index since AD 1400. *Journal of Climate*, *15*(13), 1754–1764. https://doi.org/10.1175/1520-0442(2002)015<1754:AWVMRO>2.0.CO;2

Cunningham, S. A., Kanzow, T., Rayner, D., Baringer, M. O., Johns, W. E., Marotzke, J., et al. (2007). Temporal variability of the Atlantic meridional overturning circulation at 26.5 N. *Science*, *317*(5840), 935–938. https://doi.org/10.1126/science.1141304

Dahl, K. A., Broccoli, A. J., & Stouffer, R. J. (2005). Assessing the role of North Atlantic freshwater forcing in millennial scale climate variability: A tropical Atlantic perspective. *Climate Dynamics*, *24*(4), 325–346. https://doi.org/10.1007/s00382-004-0499-5

Danabasoglu, G. (2008). On multidecadal variability of the Atlantic meridional overturning circulation in the Community Climate System Model version 3. *Journal of Climate*, *21*(21), 5524–5544. https://doi.org/10.1175/2008JCLI2019.1

Danabasoglu, G., Large, W. G., & Briegleb, B. P. (2010). Climate impacts of parameterized Nordic Sea overflows. *Journal of Geophysical Research*, *115*, C11005. https://doi.org/10.1029/2010JC006243

Danabasoglu, G., Yeager, S. G., Bailey, D., Behrens, E., Bentsen, M., Bi, D., et al. (2014). North Atlantic in coordinated ocean-ice reference experiments phase II (CORE-II). Part I: mean states. *Ocean Modelling*, *73*, 76–107. https://doi.org/10.1016/j.ocemod.2013.10.005

Danabasoglu, G., Yeager, S. G., Kim, W. M., Behrens, E., Bentsen, M., Bi, D., et al. (2016). North Atlantic simulations in Coordinated Ocean-ice Reference Experiments phase II (CORE-II). Part II: Inter-annual to decadal variability. *Ocean Modelling*, *97*, 65–90. https://doi.org/10.1016/j.ocemod.2015.11.007

Danabasoglu, G., Yeager, S. G., Kwon, Y. O., Tribbia, J. J., Phillips, A. S., & Hurrell, J. W. (2012). Variability of the Atlantic meridional overturning circulation in CCSM4. *Journal of Climate*, *25*(15), 5153–5172. https://doi.org/10.1175/JCLI-D-11-00463.1

Davini, P., Cagnazzo, C., Neale, R., & Tribbia, J. (2012). Coupling between Greenland blocking and the North Atlantic Oscillation pattern. *Geophysical Research Letters*, *39*, L14701. https://doi.org/10.1029/2012GL052315

Davini, P., von Hardenberg, J., & Corti, S. (2015). Tropical origin for the impacts of the Atlantic Multidecadal Variability on the Euro-Atlantic climate. *Environmental Research Letters*, *10*(9), 094010). https://doi.org/10.1088/1748-9326/10/9/094010

Day, J. J., Hargreaves, J. C., Annan, J. D., & Abe-Ouchi, A. (2012). Sources of multi-decadal variability in Arctic sea ice extent. *Environmental Research Letters*, *7*(3), 034011. https://doi.org/10.1088/1748-9326/7/3/034011

Defant, A. (1941). Die absolute Topographie des physikalischen Meeresniveaus und der Drückflachen sowie die Wasserbewegungen im Raum des Atlantischen Ozeans. In *Wissenschaftliche Ergebnisse der Deutschen Atlantischen Expedition auf dem Forschungs—und Vermessungsschiff "Meteor" 1925–27*, (Vol. 6, second part, 1, pp. 191–260). Berlin: De Gruyter.

DelSole, T., Tippett, M. K., & Shukla, J. (2011). A significant component of unforced multidecadal variability in the recent acceleration of global warming. *Journal of Climate*, *24*(3), 909–926. https://doi.org/10.1175/2010JCLI3659.1

Delworth, T., Manabe, S., & Stouffer, R. J. (1993). Interdecadal variations of the thermohaline circulation in a coupled ocean-atmosphere model. *Journal of Climate*, *6*(11), 1993–2011. https://doi.org/10.1175/1520-0442(1993)006<1993:IVOTTC>2.0.CO;2

Delworth, T. L., & Greatbatch, R. J. (2000). Multidecadal thermohaline circulation variability driven by atmospheric surface flux forcing. *Journal of Climate*, *13*(9), 1481–1495. https://doi.org/10.1175/1520-0442(2000)013<1481:MTCVDB>2.0.CO;2

Delworth, T. L., Manabe, S., & Stouffer, R. J. (1997). Multidecadal climate variability in the Greenland Sea and surrounding regions: A coupled model simulation. *Geophysical Research Letters*, *24*(3), 257–260. https://doi.org/10.1029/96GL03927

Delworth, T. L., & Mann, M. E. (2000). Observed and simulated multidecadal variability in the Northern Hemisphere. *Climate Dynamics*, *16*(9), 661–676. https://doi.org/10.1007/s003820000075

Delworth, T. L., & Zeng, F. (2016). The impact of the North Atlantic Oscillation on climate through its influence on the Atlantic meridional overturning circulation. *Journal of Climate*, *29*(3), 941–962. https://doi.org/10.1175/JCLI-D-15-0396.1

Delworth, T. L., Zeng, F., Vecchi, G. A., Yang, X., Zhang, L., & Zhang, R. (2016). The North Atlantic Oscillation as a driver of rapid climate change in the Northern Hemisphere. *Nature Geoscience*, *9*(7), 509–512. https://doi.org/10.1038/ngeo2738

Delworth, T. L., Zeng, F., Zhang, L., Zhang, R., Vecchi, G. A., & Yang, X. (2017). The central role of ocean dynamics in connecting the North Atlantic Oscillation to the extratropical component of the Atlantic Multidecadal Oscillation. *Journal of Climate*, *30*(10), 3789–3805. https://doi.org/10.1175/JCLI-D-16-0358.1

Deser, C., Alexander, M. A., & Timlin, M. S. (2003). Understanding the persistence of sea surface temperature anomalies in midlatitudes. *Journal of Climate*, *16*(1), 57–72. https://doi.org/10.1175/1520-0442(2003)016<0057:UTPOSS>2.0.CO;2

Deser, C., Alexander, M. A., Xie, S. P., & Phillips, A. S. (2010). Sea surface temperature variability: Patterns and mechanisms. *Annual Review of Marine Science*, *2*(1), 115–143. https://doi.org/10.1146/annurev-marine-120408-151453

Deser, C., & Blackmon, M. L. (1993). Surface climate variations over the North Atlantic Ocean during winter: 1900–1989. *Journal of Climate*, *6*(9), 1743–1753. https://doi.org/10.1175/1520-0442(1993)006<1743:SCVOTN>2.0.CO;2

Deser, C., Phillips, A. S., Tomas, R. A., Okumura, Y. M., Alexander, M. A., Capotondi, A., et al. (2012). ENSO and Pacific decadal variability in the Community Climate System Model version 4. *Journal of Climate*, *25*(8), 2622–2651. https://doi.org/10.1175/JCLI-D-11-00301.1

Dickson, R., Lazier, J., Meincke, J., Rhines, P., & Swift, J. (1996). Long-term coordinated changes in the convective activity of the North Atlantic. *Progress in Oceanography*, *38*(3), 241–295. https://doi.org/10.1016/S0079-6611(97)00002-5

Dickson, R. R., Meincke, J., Malmberg, S. A., & Lee, A. J. (1988). The "great salinity anomaly" in the northern North Atlantic 1968–1982. *Progress in Oceanography*, *20*(2), 103–151. https://doi.org/10.1016/0079-6611(88)90049-3

Dima, M., & Lohmann, G. (2007). A hemispheric mechanism for the Atlantic Multidecadal Oscillation. *Journal of Climate*, *20*(11), 2706–2719. https://doi.org/10.1175/JCLI4174.1

Dong, B., & Sutton, R. T. (2005). Mechanism of interdecadal thermohaline circulation variability in a coupled ocean–atmosphere GCM. *Journal of Climate*, *18*(8), 1117–1135. https://doi.org/10.1175/JCLI3328.1

Dong, B., & Sutton, R. T. (2007). Enhancement of ENSO variability by a weakened Atlantic thermohaline circulation in a coupled GCM. *Journal of Climate*, *20*(19), 4920–4939. https://doi.org/10.1175/JCLI4284.1

Dong, B., Sutton, R. T., & Scaife, A. A. (2006). Multidecadal modulation of El Nino–Southern Oscillation (ENSO) variance by Atlantic Ocean sea surface temperatures. *Geophysical Research Letters*, *33*, L08705. https://doi.org/10.1029/2006GL025766

Dong, B. W., & Sutton, R. T. (2002). Adjustment of the coupled ocean–atmosphere system to a sudden change in the thermohaline circulation. *Geophysical Research Letters*, *29*(15), 1728. https://doi.org/10.1029/2002GL015229

d'Orgeville, M., & Peltier, W. R. (2007). On the Pacific decadal oscillation and the Atlantic multidecadal oscillation: might they be related? *Geophysical Research Letters*, *34*, L23705. https://doi.org/10.1029/2007GL031584

Drews, A., & Greatbatch, R. J. (2016). Atlantic multidecadal variability in a model with an improved North Atlantic Current. *Geophysical Research Letters*, *43*, 8199–8206. https://doi.org/10.1002/2016GL069815

Drews, A., & Greatbatch, R. J. (2017). Evolution of the Atlantic Multidecadal Variability in a model with an improved North Atlantic Current. *Journal of Climate*, *30*(14), 5491–5512. https://doi.org/10.1175/JCLI-D-16-0790.1

Drews, A., Greatbatch, R. J., Ding, H., Latif, M., & Park, W. (2015). The use of a flow field correction technique for alleviating the North Atlantic cold bias with application to the Kiel Climate Model. *Ocean Dynamics*, *65*(8), 1079–1093. https://doi.org/10.1007/s10236-015-0853-7

Drijfhout, S. (2015). Competition between global warming and an abrupt collapse of the AMOC in Earth's energy imbalance. *Scientific reports*, *5*(1), 14877. https://doi.org/10.1038/srep14877

Drinkwater, K. F., Miles, M., Medhaug, I., Otterå, O. H., Kristiansen, T., Sundby, S., & Gao, Y. (2014). The Atlantic Multidecadal Oscillation: Its manifestations and impacts with special emphasis on the Atlantic region north of 60 N. *Journal of Marine Systems*, *133*, 117–130. https://doi.org/10.1016/j.jmarsys.2013.11.001

Dunstone, N. J., Smith, D. M., Booth, B. B. B., Hermanson, L., & Eade, R. (2013). Anthropogenic aerosol forcing of Atlantic tropical storms. *Nature Geoscience*, *6*(7), 534–539. https://doi.org/10.1038/ngeo1854

Dunstone, N. J., Smith, D. M., & Eade, R. (2011). Multi-year predictability of the tropical Atlantic atmosphere driven by the high latitude North Atlantic Ocean. *Geophysical Research Letters*, *38*, L14701. https://doi.org/10.1029/2011GL047949

Eden, C., & Jung, T. (2001). North Atlantic interdecadal variability: oceanic response to the North Atlantic Oscillation (1865–1997). *Journal of Climate*, *14*(5), 676–691. https://doi.org/10.1175/1520-0442(2001)014<0676:NAIVOR>2.0.CO;2

Enfield, D. B., & Mestas-Nuñez, A. M. (1999). Multiscale variabilities in global sea surface temperatures and their relationships with tropospheric climate patterns. *Journal of Climate*, *12*(9), 2719–2733. https://doi.org/10.1175/1520-0442(1999)012<2719:MVIGSS>2.0.CO;2

Enfield, D. B., Mestas-Nuñez, A. M., & Trimble, P. J. (2001). The Atlantic multidecadal oscillation and its relation to rainfall and river flows in the continental US. *Geophysical Research Letters*, *28*(10), 2077–2080. https://doi.org/10.1029/2000GL012745

Farneti, R. (2017). Modelling interdecadal climate variability and the role of the ocean. *Wiley Interdisciplinary Reviews: Climate Change*, *8*(1), e441.

Farneti, R., & Vallis, G. K. (2011). Mechanisms of interdecadal climate variability and the role of ocean–atmosphere coupling. *Climate Dynamics*, *36*(1-2), 289–308. https://doi.org/10.1007/s00382-009-0674-9

Farneti, R., & Vallis, G. K. (2013). Meridional energy transport in the coupled atmosphere–ocean system: Compensation and partitioning. *Journal of Climate*, *26*(18), 7151–7166. https://doi.org/10.1175/JCLI-D-12-00133.1

Fauria, M. M., Grinsted, A., Helama, S., Moore, J., Timonen, M., Martma, T., et al. (2010). Unprecedented low twentieth century winter sea ice extent in the Western Nordic Seas since AD 1200. *Climate Dynamics*, *34*(6), 781–795. https://doi.org/10.1007/s00382-009-0610-z

Feng, S., & Hu, Q. (2008). How the North Atlantic Multidecadal Oscillation may have influenced the Indian summer monsoon during the past two millennia. *Geophysical Research Letters*, *35*, L01707. https://doi.org/10.1029/2007GL032484

Feng, S., Hu, Q., & Oglesby, R. J. (2011). Influence of Atlantic sea surface temperatures on persistent drought in North America. *Climate Dynamics*, *37*(3-4), 569–586. https://doi.org/10.1007/s00382-010-0835-x

Folland, C. K., Colman, A. W., Rowell, D. P., & Davey, M. K. (2001). Predictability of northeast Brazil rainfall and real-time forecast skill, 1987–98. *Journal of Climate*, *14*(9), 1937–1958. https://doi.org/10.1175/1520-0442(2001)014<1937:PONBRA>2.0.CO;2

Folland, C. K., Palmer, T. N., & Parker, D. E. (1986). Sahel rainfall and worldwide sea temperatures, 1901–85. *Nature*, *320*(6063), 602–607. https://doi.org/10.1038/320602a0

Frajka-Williams, E., Beaulieu, C., & Duchez, A. (2017). Emerging negative Atlantic Multidecadal Oscillation index in spite of warm subtropics. *Scientific Reports*, *7*(1), 11224. https://doi.org/10.1038/s41598-017-11046-x

Frajka-Williams, E., Meinen, C. S., Johns, W. E., Smeed, D. A., Duchez, A., Lawrence, A. J., et al. (2016). Compensation between meridional flow components of the Atlantic MOC at 26 N. *Ocean Science*, *12*(2), 481–493. https://doi.org/10.5194/os-12-481-2016

Frankcombe, L. M., & Dijkstra, H. A. (2011). The role of Atlantic-Arctic exchange in North Atlantic multidecadal climate variability. *Geophysical Research Letters*, *38*, L16603. https://doi.org/10.1029/2011GL048158

Frankcombe, L. M., Von Der Heydt, A., & Dijkstra, H. A. (2010). North Atlantic multidecadal climate variability: An investigation of dominant time scales and processes. *Journal of Climate*, *23*(13), 3626–3638. https://doi.org/10.1175/2010JCLI3471.1

Frankignoul, C. (1985). Sea surface temperature anomalies, planetary waves, and air-sea feedback in the middle latitudes. *Reviews of Geophysics*, *23*(4), 357–390. https://doi.org/10.1029/RG023i004p00357

Frankignoul, C., Gastineau, G., & Kwon, Y. O. (2015). Wintertime atmospheric response to North Atlantic ocean circulation variability in a climate model. *Journal of Climate*, *28*(19), 7659–7677. https://doi.org/10.1175/JCLI-D-15-0007.1

Frankignoul, C., Gastineau, G., & Kwon, Y. O. (2017). Estimation of the SST response to anthropogenic and external forcing and its impact on the Atlantic Multidecadal Oscillation and the Pacific Decadal Oscillation. *Journal of Climate*, *30*(24), 9871–9895. https://doi.org/10.1175/JCLI-D-17-0009.1

Frankignoul, C., & Hasselmann, K. (1977). Stochastic climate models, Part II Application to sea-surface temperature anomalies and thermocline variability. *Tellus*, *29*(4), 289–305.

Friedman, A. R., Reverdin, G., Khodri, M., & Gastineau, G. (2017). A new record of Atlantic sea surface salinity from 1896 to 2013 reveals the signatures of climate variability and long-term trends. *Geophysical Research Letters*, *44*, 1866–1876. https://doi.org/10.1002/2017GL072582

Frierson, D. M., Hwang, Y. T., Fučkar, N. S., Seager, R., Kang, S. M., Donohoe, A., et al. (2013). Contribution of ocean overturning circulation to tropical rainfall peak in the Northern Hemisphere. *Nature Geoscience*, *6*(11), 940–944. https://doi.org/10.1038/ngeo1987

Gaetani, M., & Mohino, E. (2013). Decadal prediction of the Sahelian precipitation in CMIP5 simulations. *Journal of Climate*, *26*(19), 7708–7719. https://doi.org/10.1175/JCLI-D-12-00635.1

Ganachaud, A., & Wunsch, C. (2000). Improved estimates of global ocean circulation, heat transport and mixing from hydrographic data. *Nature*, *408*(6811), 453–457. https://doi.org/10.1038/35044048

García-Serrano, J., Guemas, V., & Doblas-Reyes, F. J. (2015). Added-value from initialization in predictions of Atlantic multi-decadal variability. *Climate Dynamics*, *44*(9-10), 2539–2555. https://doi.org/10.1007/s00382-014-2370-7

Garuba, O. A., Lu, J., Singh, H. A., Liu, F., & Rasch, P. (2018). On the relative roles of the atmosphere and ocean in the Atlantic multidecadal variability. *Geophysical Research Letters*, *45*, 9186–9196. https://doi.org/10.1029/2018GL078882

Gastineau, G., D'Andrea, F., & Frankignoul, C. (2013). Atmospheric response to the North Atlantic Ocean variability on seasonal to decadal time scales. *Climate Dynamics*, *40*(9-10), 2311–2330. https://doi.org/10.1007/s00382-012-1333-0

Gastineau, G., & Frankignoul, C. (2012). Cold-season atmospheric response to the natural variability of the Atlantic meridional overturning circulation. *Climate Dynamics*, *39*(1-2), 37–57. https://doi.org/10.1007/s00382-011-1109-y

Gastineau, G., & Frankignoul, C. (2015). Influence of the North Atlantic SST variability on the atmospheric circulation during the twentieth century. *Journal of Climate*, *28*(4), 1396–1416. https://doi.org/10.1175/JCLI-D-14-00424.1

Gastineau, G., L'hévéder, B., Codron, F., & Frankignoul, C. (2016). Mechanisms determining the winter atmospheric response to the Atlantic overturning circulation. *Journal of Climate*, *29*(10), 3767–3785. https://doi.org/10.1175/JCLI-D-15-0326.1

Ghosh, R., Müller, W. A., Baehr, J., & Bader, J. (2017). Impact of observed North Atlantic multidecadal variations to European summer climate: A linear baroclinic response to surface heating. *Climate Dynamics*, *48*(11-12), 3547–3563. https://doi.org/10.1007/s00382-016-3283-4

Glueck, M. F., & Stockton, C. W. (2001). Reconstruction of the North Atlantic oscillation, 1429–1983. *International Journal of Climatology: A Journal of the Royal Meteorological Society*, *21*(12), 1453–1465. https://doi.org/10.1002/joc.684

Goldenberg, S. B., Landsea, C. W., Mestas-Nuñez, A. M., & Gray, W. M. (2001). The recent increase in Atlantic hurricane activity: Causes and implications. *Science*, *293*(5529), 474–479. https://doi.org/10.1126/science.1060040

Gordon, A. L. (1986). Interocean exchange of thermocline water. *Journal of Geophysical Research*, *91*(C4), 5037–5046. https://doi.org/10.1029/JC091iC04p05037

Goswami, B. N., Madhusoodanan, M. S., Neema, C. P., & Sengupta, D. (2006). A physical mechanism for North Atlantic SST influence on the Indian summer monsoon. *Geophysical Research Letters*, *33*, L02706. https://doi.org/10.1029/2005GL024803

Gray, S. T., Graumlich, L. J., Betancourt, J. L., & Pederson, G. T. (2004). A tree-ring based reconstruction of the Atlantic Multidecadal Oscillation since 1567 AD. *Geophysical Research Letters*, *31*, L12205. https://doi.org/10.1029/2004GL019932

Gray, W. M. (1968). Global View of the origin of tropical disturbances and storms. *Monthly Weather Review*, *96*(10), 669–700. https://doi.org/10.1175/1520-0493(1968)096<0669:GVOTOO>2.0.CO;2

Gray, W. M. (1990). Strong association between West African rainfall and US landfall of intense hurricanes. *Science*, *249*(4974), 1251–1256. https://doi.org/10.1126/science.249.4974.1251

Green, B., Marshall, J., & Donohoe, A. (2017). Twentieth century correlations between extratropical SST variability and ITCZ shifts. *Geophysical Research Letters*, *44*, 9039–9047. https://doi.org/10.1002/2017GL075044

Griffies, S. M., & Bryan, K. (1997a). Predictability of North Atlantic multidecadal climate variability. *Science*, *275*(5297), 181–184. https://doi.org/10.1126/science.275.5297.181

Griffies, S. M., & Bryan, K. (1997b). A predictability study of simulated North Atlantic multidecadal variability. *Climate Dynamics*, *13*(7-8), 459–487. https://doi.org/10.1007/s003820050177

Griffies, S. M., & Tziperman, E. (1995). A linear thermohaline oscillator driven by stochastic atmospheric forcing. *Journal of Climate*, *8*(10), 2440–2453. https://doi.org/10.1175/1520-0442(1995)008<2440:ALTODB>2.0.CO;2

Grist, J. P., Josey, S. A., Marsh, R., Good, S. A., Coward, A. C., De Cuevas, B. A., et al. (2010). The roles of surface heat flux and ocean heat transport convergence in determining Atlantic Ocean temperature variability. *Ocean Dynamics*, *60*(4), 771–790. https://doi.org/10.1007/s10236-010-0292-4

Grossmann, I., & Klotzbach, P. J. (2009). A review of North Atlantic modes of natural variability and their driving mechanisms. *Journal of Geophysical Research*, *114*, D24107. https://doi.org/10.1029/2009JD012728

Gulev, S. K., Latif, M., Keenlyside, N., Park, W., & Koltermann, K. P. (2013). North Atlantic Ocean control on surface heat flux on multidecadal timescales. *Nature*, *499*(7459), 464–467. https://doi.org/10.1038/nature12268

Hakim, G. J., Emile-Geay, J., Steig, E. J., Noone, D., Anderson, D. M., Tardif, R., et al. (2016). The last millennium climate reanalysis project: Framework and first results. *Journal of Geophysical Research: Atmospheres*, *121*, 6745–6764. https://doi.org/10.1002/2016JD024751

Häkkinen, S., Rhines, P. B., & Worthen, D. L. (2011). Atmospheric blocking and Atlantic multidecadal ocean variability. *Science*, *334*(6056), 655–659. https://doi.org/10.1126/science.1205683

Häkkinen, S., Rhines, P. B., & Worthen, D. L. (2013). Northern North Atlantic sea surface height and ocean heat content variability. *Journal of Geophysical Research: Oceans*, *118*, 3670–3678. https://doi.org/10.1002/jgrc.20268

Han, Z., Luo, F., Li, S., Gao, Y., Furevik, T., & Svendsen, L. (2016). Simulation by CMIP5 models of the Atlantic Multidecadal Oscillation and its climate impacts. *Advances in Atmospheric Sciences*, *33*(12), 1329–1342. https://doi.org/10.1007/s00376-016-5270-4

Harlaß, J., Latif, M., & Park, W. (2018). Alleviating tropical Atlantic sector biases in the Kiel climate model by enhancing horizontal and vertical atmosphere model resolution: Climatology and interannual variability. *Climate Dynamics*, *50*(7-8), 2605–2635. https://doi.org/10.1007/s00382-017-3760-4

Hasselmann, K. (1976). Stochastic climate models. Part I. Theory. *Tellus*, *28*(6), 473–485.

Hastenrath, S. (1980). Heat budget of tropical ocean and atmosphere. *Journal of Physical Oceanography*, *10*(2), 159–170. https://doi.org/10.1175/1520-0485(1980)010<0159:HBOTOA>2.0.CO;2

Hastenrath, S. (1982). On meridional heat transports in the world ocean. *Journal of Physical Oceanography*, *12*(8), 922–927. https://doi.org/10.1175/1520-0485(1982)012<0922:OMHTIT>2.0.CO;2

Hátún, H., Payne, M. R., Beaugrand, G., Reid, P. C., Sandø, A. B., Drange, H., et al. (2009). Large bio-geographical shifts in the north-eastern Atlantic Ocean: From the subpolar gyre, via plankton, to blue whiting and pilot whales. *Progress in Oceanography*, *80*(3-4), 149–162. https://doi.org/10.1016/j.pocean.2009.03.001

Hawkins, E., & Sutton, R. (2007). Variability of the Atlantic thermohaline circulation described by three-dimensional empirical orthogonal functions. *Climate Dynamics*, *29*(7-8), 745–762. https://doi.org/10.1007/s00382-007-0263-8

Hawkins, E., & Sutton, R. (2008). Potential predictability of rapid changes in the Atlantic meridional overturning circulation. *Geophysical Research Letters*, *35*, L11603. https://doi.org/10.1029/2008GL034059

Hermanson, L., Eade, R., Robinson, N. H., Dunstone, N. J., Andrews, M. B., Knight, J. R., et al. (2014). Forecast cooling of the Atlantic subpolar gyre and associated impacts. *Geophysical Research Letters*, *41*, 5167–5174. https://doi.org/10.1002/2014GL060420

Hermanson, L., & Sutton, R. T. (2010). Case studies in interannual to decadal climate predictability. *Climate Dynamics*, *35*(7-8), 1169–1189. https://doi.org/10.1007/s00382-009-0672-y

Hetzinger, S., Halfar, J., Mecking, J. V., Keenlyside, N. S., Kronz, A., Steneck, R. S., et al. (2012). Marine proxy evidence linking decadal North Pacific and Atlantic climate. *Climate Dynamics*, *39*(6), 1447–1455. https://doi.org/10.1007/s00382-011-1229-4

Hirt, A. M., Lanci, L., & Koinig, K. (2003). Mineral magnetic record of Holocene environmental changes in Sägistalsee, Switzerland. *Journal of Paleolimnology*, *30*(3), 321–331. https://doi.org/10.1023/A:1026028728241

Hodson, D. L., Robson, J. I., & Sutton, R. T. (2014). An anatomy of the cooling of the North Atlantic Ocean in the 1960s and 1970s. *Journal of Climate*, *27*(21), 8229–8243. https://doi.org/10.1175/JCLI-D-14-00301.1

Hodson, D. L., Sutton, R. T., Cassou, C., Keenlyside, N., Okumura, Y., & Zhou, T. (2010). Climate impacts of recent multidecadal changes in Atlantic Ocean sea surface temperature: A multimodel comparison. *Climate Dynamics*, *34*(7-8), 1041–1058. https://doi.org/10.1007/s00382-009-0571-2

Holland, D. M., Thomas, R. H., De Young, B., Ribergaard, M. H., & Lyberth, B. (2008). Acceleration of Jakobshavn Isbrae triggered by warm subsurface ocean waters. *Nature Geoscience*, *1*(10), 659–664. https://doi.org/10.1038/ngeo316

Holland, M. M., Bitz, C. M., Eby, M., & Weaver, A. J. (2001). The role of ice–ocean interactions in the variability of the North Atlantic thermohaline circulation. *Journal of Climate*, *14*(5), 656–675. https://doi.org/10.1175/1520-0442(2001)014<0656:TROIOI>2.0.CO;2

Holland, W. R., & Hirschman, A. D. (1972). A numerical calculation of the circulation in the North Atlantic Ocean. *Journal of Physical Oceanography*, *2*(4), 336–354. https://doi.org/10.1175/1520-0485(1972)002<0336:ANCOTC>2.0.CO;2

Holzhauser, H., & Zumbühl, H. J. (1999). Glacier fluctuations in the western Swiss and French Alps in the 16th century. *Climate Change*, *43*(1), 223–237. https://doi.org/10.1023/A:1005546300948

Howat, I. M., Joughin, I., Fahnestock, M., Smith, B. E., & Scambos, T. A. (2008). Synchronous retreat and acceleration of southeast Greenland outlet glaciers 2000–06: Ice dynamics and coupling to climate. *Journal of Glaciology*, *54*(187), 646–660. https://doi.org/10.3189/002214308786570908

Hu, Q., & Feng, S. (2008). Variation of the North American summer monsoon regimes and the Atlantic multidecadal oscillation. *Journal of Climate*, *21*(11), 2371–2383. https://doi.org/10.1175/2007JCLI2005.1

Hu, Q., Feng, S., & Oglesby, R. J. (2011). Variations in North American summer precipitation driven by the Atlantic Multidecadal Oscillation. *Journal of Climate*, *24*(21), 5555–5570. https://doi.org/10.1175/2011JCLI4060.1

Hurrell, J. W. (1995). Decadal trends in the North Atlantic Oscillation: Regional temperatures and precipitation. *Science*, *269*(5224), 676–679. https://doi.org/10.1126/science.269.5224.676

Huss, M., Hock, R., Bauder, A., & Funk, M. (2010). 100-year mass changes in the Swiss Alps linked to the Atlantic Multidecadal Oscillation. *Geophysical Research Letters*, *37*, L10501. https://doi.org/10.1029/2010GL042616

Ionita, M., Scholz, P., Lohmann, G., Dima, M., & Prange, M. (2016). Linkages between atmospheric blocking, sea ice export through Fram Strait and the Atlantic Meridional Overturning Circulation. *Scientific Reports*, *6*(1), 32881. https://doi.org/10.1038/srep32881

Jackson, L. C., Peterson, K. A., Roberts, C. D., & Wood, R. A. (2016). Recent slowing of Atlantic overturning circulation as a recovery from earlier strengthening. *Nature Geoscience*, *9*(7), 518–522. https://doi.org/10.1038/ngeo2715

Johannessen, O. M., Bengtsson, L., Miles, M. W., Kuzmina, S. I., Semenov, V. A., Alekseev, G. V., et al. (2004). Arctic climate change: Observed and modelled temperature and sea-ice variability. *Tellus A: Dynamic Meteorology and Oceanography*, *56*(4), 328–341. https://doi.org/10.1111/j.1600-0870.2004.00060.x

Joyce, T. M., & Zhang, R. (2010). On the path of the Gulf Stream and the Atlantic meridional overturning circulation. *Journal of Climate*, *23*(11), 3146–3154. https://doi.org/10.1175/2010JCLI3310.1

Jungclaus, J. H., Haak, H., Latif, M., & Mikolajewicz, U. (2005). Arctic–North Atlantic interactions and multidecadal variability of the meridional overturning circulation. *Journal of Climate*, *18*(19), 4013–4031. https://doi.org/10.1175/JCLI3462.1

Jungclaus, J. H., & Koenigk, T. (2010). Low-frequency variability of the arctic climate: The role of oceanic and atmospheric heat transport variations. *Climate Dynamics*, *34*(2-3), 265–279. https://doi.org/10.1007/s00382-009-0569-9

Kang, I. S., No, H. H., & Kucharski, F. (2014). ENSO amplitude modulation associated with the mean SST changes in the tropical central Pacific induced by Atlantic multidecadal oscillation. *Journal of Climate*, *27*(20), 7911–7920. https://doi.org/10.1175/JCLI-D-14-00018.1

Kang, S. M., Held, I. M., Frierson, D. M., & Zhao, M. (2008). The response of the ITCZ to extratropical thermal forcing: Idealized slab-ocean experiments with a GCM. *Journal of Climate*, *21*(14), 3521–3532. https://doi.org/10.1175/2007JCLI2146.1

Kanzow, T., Cunningham, S. A., Rayner, D., Hirschi, J. J. M., Johns, W. E., Baringer, M. O., et al. (2007). Observed flow compensation associated with the MOC at 26.5 N in the Atlantic. *Science*, *317*(5840), 938–941. https://doi.org/10.1126/science.1141293

Kavvada, A., Ruiz-Barradas, A., & Nigam, S. (2013). AMO's structure and climate footprint in observations and IPCC AR5 climate simulations. *Climate Dynamics*, *41*(5-6), 1345–1364. https://doi.org/10.1007/s00382-013-1712-1

Keenlyside, N., & Omrani, N. E. (2014). Has a warm North Atlantic contributed to recent European cold winters? *Environmental Research Letters*, *9*(6), 061001. https://doi.org/10.1088/1748-9326/9/6/061001

Keenlyside, N. S., Ba, J., Mecking, J., Omrani, N. E., Latif, M., Zhang, R., & Msadek, R. (2016). North Atlantic multi-decadal variability—Mechanisms and predictability. In *Climate change: Multidecadal and beyond*, (pp. 141–157). Singapore: World Scientific Publishing.

Keigwin, L. D., Sachs, J. P., & Rosenthal, Y. (2003). A 1600-year history of the Labrador Current off Nova Scotia. *Climate Dynamics*, *21*(1), 53–62. https://doi.org/10.1007/s00382-003-0316-6

Kerr, R. A. (2000). A North Atlantic climate pacemaker for the centuries. *Science*, *288*(5473), 1984–1985. https://doi.org/10.1126/science.288.5473.1984

Kilbourne, K. H., Alexander, M. A., & Nye, J. A. (2014). A low latitude paleoclimate perspective on Atlantic multidecadal variability. *Journal of Marine Systems*, *133*, 4–13. https://doi.org/10.1016/j.jmarsys.2013.09.004

Kilbourne, K. H., Quinn, T. M., Webb, R., Guilderson, T., Nyberg, J., & Winter, A. (2008). Paleoclimate proxy perspective on Caribbean climate since the year 1751: Evidence of cooler temperatures and multidecadal variability. *Paleoceanography and Paleoclimatology*, *23*, PA3220. https://doi.org/10.1029/2008PA001598

Killworth, P. D. (1983). Deep convection in the world ocean. *Reviews of Geophysics*, *21*(1), 1–26. https://doi.org/10.1029/RG021i001p00001

Kim, W. M., Yeager, S., Chang, P., & Danabasoglu, G. (2018). Low-frequency North Atlantic Climate Variability in the Community Earth System Model large ensemble. *Journal of Climate*, *31*(2), 787–813. https://doi.org/10.1175/JCLI-D-17-0193.1

Kim, W. M., Yeager, S. G., & Danabasoglu, G. (2018). Key role of internal ocean dynamics in Atlantic Multidecadal Variability during the last half century. *Geophysical Research Letters*, *45*, 13,449–13,457. https://doi.org/10.1029/2018GL080474

Kitzberger, T., Brown, P. M., Heyerdahl, E. K., Swetnam, T. W., & Veblen, T. T. (2007). Contingent Pacific–Atlantic Ocean influence on multicentury wildfire synchrony over western North America. *Proceedings of the National Academy of Sciences*, *104*(2), 543–548. https://doi.org/10.1073/pnas.0606078104

Klotzbach, P., Gray, W., & Fogarty, C. (2015). Active Atlantic hurricane era at its end? *Nature Geoscience*, *8*(10), 737–738. https://doi.org/10.1038/ngeo2529

Klotzbach, P. J., & Gray, W. M. (2008). Multidecadal variability in North Atlantic tropical cyclone activity. *Journal of Climate*, *21*(15), 3929–3935. https://doi.org/10.1175/2008JCLI2162.1

Knight, J. R. (2009). The Atlantic multidecadal oscillation inferred from the forced climate response in coupled general circulation models. *Journal of Climate*, *22*(7), 1610–1625. https://doi.org/10.1175/2008JCLI2628.1

Knight, J. R., Allan, R. J., Folland, C. K., Vellinga, M., & Mann, M. E. (2005). A signature of persistent natural thermohaline circulation cycles in observed climate. *Geophysical Research Letters*, *32*, L20708. https://doi.org/10.1029/2005GL024233

Knight, J. R., Folland, C. K., & Scaife, A. A. (2006). Climate impacts of the Atlantic multidecadal oscillation. *Geophysical Research Letters*, *33*, L17706. https://doi.org/10.1029/2006GL026242

Knudsen, M. F., Jacobsen, B. H., Seidenkrantz, M. S., & Olsen, J. (2014). Evidence for external forcing of the Atlantic Multidecadal Oscillation since termination of the Little Ice Age. *Nature Communications*, *5*(1), 3323. https://doi.org/10.1038/ncomms4323

Knudsen, M. F., Seidenkrantz, M. S., Jacobsen, B. H., & Kuijpers, A. (2011). Tracking the Atlantic Multidecadal Oscillation through the last 8,000 years. *Nature Communications*, *2*(1), 178. https://doi.org/10.1038/ncomms1186

Koenigk, T., Beatty, C. K., Caian, M., Döscher, R., & Wyser, K. (2012). Potential decadal predictability and its sensitivity to sea ice albedo parameterization in a global coupled model. *Climate Dynamics*, *38*(11-12), 2389–2408. https://doi.org/10.1007/s00382-011-1132-z

Koenigk, T., & Brodeau, L. (2014). Ocean heat transport into the Arctic in the twentieth and twenty-first century in EC-Earth. *Climate Dynamics*, *42*(11-12), 3101–3120. https://doi.org/10.1007/s00382-013-1821-x

Koseki, S., Keenlyside, N., Demissie, T., Toniazzo, T., Counillon, F., Bethke, I., et al. (2018). Causes of the large warm bias in the Angola–Benguela frontal zone in the Norwegian earth system model. *Climate Dynamics*, *50*(11-12), 4651–4670. https://doi.org/10.1007/s00382-017-3896-2

Kravtsov, S. (2017). Pronounced differences between observed and CMIP5-simulated multidecadal climate variability in the twentieth century. *Geophysical Research Letters*, *44*, 5749–5757. https://doi.org/10.1002/2017GL074016

Kravtsov, S., & Spannagle, C. (2008). Multidecadal climate variability in observed and modeled surface temperatures. *Journal of Climate*, *21*(5), 1104–1121. https://doi.org/10.1175/2007JCLI1874.1

Kravtsov, S., Wyatt, M. G., Curry, J. A., & Tsonis, A. A. (2014). Two contrasting views of multidecadal climate variability in the twentieth century. *Geophysical Research Letters*, *41*, 6881–6888. https://doi.org/10.1002/2014GL061416

Kucharski, F., Ikram, F., Molteni, F., Farneti, R., Kang, I. S., No, H. H., et al. (2016). Atlantic forcing of Pacific decadal variability. *Climate Dynamics*, *46*(7-8), 2337–2351. https://doi.org/10.1007/s00382-015-2705-z

Kuhlbrodt, T., Griesel, A., Montoya, M., Levermann, A., Hofmann, M., & Rahmstorf, S. (2007). On the driving processes of the Atlantic meridional overturning circulation. *Reviews of Geophysics*, *45*, RG2001. https://doi.org/10.1029/2004RG000166

Kushnir, Y. (1994). Interdecadal variations in North Atlantic sea surface temperature and associated atmospheric conditions. *Journal of Climate*, *7*(1), 141–157. https://doi.org/10.1175/1520-0442(1994)007<0141:IVINAS>2.0.CO;2

Kwon, Y. O., & Frankignoul, C. (2012). Stochastically-driven multidecadal variability of the Atlantic meridional overturning circulation in CCSM3. *Climate Dynamics*, *38*(5-6), 859–876. https://doi.org/10.1007/s00382-011-1040-2

Kwon, Y. O., & Frankignoul, C. (2014). Mechanisms of multidecadal Atlantic meridional overturning circulation variability diagnosed in depth versus density space. *Journal of Climate*, *27*(24), 9359–9376. https://doi.org/10.1175/JCLI-D-14-00228.1

Lanci, L., & Hirt, A. M. (2015). Evidence of Atlantic Multidecadal Oscillation in the magnetic properties of Alpine lakes during the last 2500 years. *Palaeogeography, Palaeoclimatology, Palaeoecology*, *440*, 47–52. https://doi.org/10.1016/j.palaeo.2015.08.040

Lanci, L., Hirt, A. M., Lotter, A. F., & Sturm, M. (2001). A record of Holocene climate in the mineral magnetic record of Alpine lakes: Sägistalsee and Hinterburgsee. *Earth and Planetary Science Letters*, *188*(1-2), 29–44. https://doi.org/10.1016/S0012-821X(01)00301-6

Lanci, L., Hirt, A. M., Lowrie, W., Lotter, A. F., Lemcke, G., & Sturm, M. (1999). Mineral-magnetic record of Late Quaternary climatic changes in a high Alpine lake. *Earth and Planetary Science Letters*, *170*(1-2), 49–59. https://doi.org/10.1016/S0012-821X(99)00098-9

Landsea, C. W. (2005). Meteorology: Hurricanes and global warming. *Nature*, *438*(7071), E11–E12. https://doi.org/10.1038/nature04477

Landsea, C. W., Pielke, R. A., Mestas-Nunez, A. M., & Knaff, J. A. (1999). Atlantic basin hurricanes: Indices of climatic changes. *Climatic Change*, *42*(1), 89–129. https://doi.org/10.1023/A:1005416332322

Langehaug, H. R., Mjell, T. L., Otterå, O. H., Eldevik, T., Ninnemann, U. S., & Kleiven, H. F. (2016). On the reconstruction of ocean circulation and climate based on the "Gardar Drift". *Paleoceanography*, *31*, 399–415. https://doi.org/10.1002/2015PA002920

Latif, M., Böning, C., Willebrand, J., Biastoch, A., Dengg, J., Keenlyside, N., et al. (2006). Is the thermohaline circulation changing? *Journal of Climate*, *19*(18), 4631–4637. https://doi.org/10.1175/JCLI3876.1

Latif, M., Keenlyside, N., & Bader, J. (2007). Tropical sea surface temperature, vertical wind shear, and hurricane development. *Geophysical Research Letters*, *34*, L01710. https://doi.org/10.1029/2006GL027969

Latif, M., & Keenlyside, N. S. (2011). A perspective on decadal climate variability and predictability. *Deep Sea Research Part II: Topical Studies in Oceanography*, *58*(17-18), 1880–1894. https://doi.org/10.1016/j.dsr2.2010.10.066

Latif, M., Roeckner, E., Botzet, M., Esch, M., Haak, H., Hagemann, S., et al. (2004). Reconstructing, monitoring, and predicting multidecadal-scale changes in the North Atlantic thermohaline circulation with sea surface temperature. *Journal of Climate*, *17*(7), 1605–1614. https://doi.org/10.1175/1520-0442(2004)017<1605:RMAPMC>2.0.CO;2

Lee, D. E., Ting, M., Vigaud, N., Kushnir, Y., & Barnston, A. G. (2018). Atlantic Multidecadal Variability as a modulator of precipitation variability in the southwest United States. *Journal of Climate*, *31*(14), 5525–5542. https://doi.org/10.1175/JCLI-D-17-0372.1

LeGrande, A. N., Schmidt, G. A., Shindell, D. T., Field, C. V., Miller, R. L., Koch, D. M., et al. (2006). Consistent simulations of multiple proxy responses to an abrupt climate change event. *Proceedings of the National Academy of Sciences*, *103*(4), 837–842. https://doi.org/10.1073/pnas.0510095103

Levine, A. F., Frierson, D. M., & McPhaden, M. J. (2018). AMO forcing of multidecadal Pacific ITCZ variability. *Journal of Climate*, *31*(14), 5749–5764. https://doi.org/10.1175/JCLI-D-17-0810.1

Levine, A. F., McPhaden, M. J., & Frierson, D. M. (2017). The impact of the AMO on multidecadal ENSO variability. *Geophysical Research Letters*, *44*, 3877–3886. https://doi.org/10.1002/2017GL072524

Levitus, S., Antonov, J. I., Boyer, T. P., Baranova, O. K., Garcia, H. E., Locarnini, R. A., et al. (2012). World ocean heat content and thermosteric sea level change (0–2000 m), 1955–2010. *Geophysical Research Letters*, *39*, L10603. https://doi.org/10.1029/2012GL051106

Levitus, S., Matishov, G., Seidov, D., & Smolyar, I. (2009). Barents Sea multidecadal variability. *Geophysical Research Letters*, *36*, L19604. https://doi.org/10.1029/2009GL039847

Li, D., Zhang, R., & Knutson, T. (2018). Comparison of Mechanisms for low-frequency variability of summer Arctic sea ice in three coupled models. *Journal of Climate*, *31*(3), 1205–1226. https://doi.org/10.1175/JCLI-D-16-0617.1

Li, D., Zhang, R., & Knutson, T. R. (2017). On the discrepancy between observed and CMIP5 multi-model simulated Barents Sea winter sea ice decline. *Nature Communications*, *8*, 14991. https://doi.org/10.1038/ncomms14991

Li, F., Orsolini, Y. J., Wang, H., Gao, Y., & He, S. (2018). Atlantic multidecadal oscillation modulates the impacts of Arctic sea ice decline. *Geophysical Research Letters*, *45*, 2497–2506. https://doi.org/10.1002/2017GL076210

Li, J., Sun, C., & Jin, F. F. (2017, April). A decadal-scale air-sea interaction theory for North Atlantic multidecadal variability: The NAT-NAO-AMOC-AMO coupled mode and its remote influences. In *EGU General Assembly Conference Abstracts* (Vol. 19, p. 5987). EGU2017, Proceedings from the conference held 23-28 April, 2017 in Vienna, Austria.

Li, S., & Bates, G. T. (2007). Influence of the Atlantic multidecadal oscillation on the winter climate of East China. *Advances in Atmospheric Sciences*, *24*(1), 126–135. https://doi.org/10.1007/s00376-007-0126-6

Li, S., Perlwitz, J., Quan, X., & Hoerling, M. P. (2008). Modelling the influence of North Atlantic multidecadal warmth on the Indian summer rainfall. *Geophysical Research Letters*, *35*, L05804. https://doi.org/10.1029/2007GL032901

Li, X., Xie, S. P., Gille, S. T., & Yoo, C. (2016). Atlantic-induced pan-tropical climate change over the past three decades. *Nature Climate Change*, *6*(3), 275–279. https://doi.org/10.1038/nclimate2840

Liu, H., Wang, C., Lee, S. K., & Enfield, D. (2015). Inhomogeneous influence of the Atlantic warm pool on United States precipitation. *Atmospheric Science Letters*, *16*(1), 63–69. https://doi.org/10.1002/asl2.521

Lohmann, K., Drange, H., & Bentsen, M. (2009). A possible mechanism for the strong weakening of the North Atlantic subpolar gyre in the mid-1990s. *Geophysical Research Letters*, *36*, L15602. https://doi.org/10.1029/2009GL039166

Lohmann, K., Jungclaus, J. H., Matei, D., Mignot, J., Menary, M., Langehaug, H. R., et al. (2014). The role of subpolar deep water formation and Nordic Seas overflows in simulated multidecadal variability of the Atlantic meridional overturning circulation. *Ocean Science*, *10*(2), 227–241. https://doi.org/10.5194/os-10-227-2014

Lozier, M. S. (2010). Deconstructing the conveyor belt. *Science*, *328*(5985), 1507–1511. https://doi.org/10.1126/science.1189250

Lozier, M. S. (2012). Overturning in the North Atlantic. *Annual Review of Marine Science*, *4*(1), 291–315. https://doi.org/10.1146/annurev-marine-120710-100740

Lozier, M. S., Li, F., Bacon, S., Bahr, F., Bower, A. S., Cunningham, S. A., et al. (2019). A sea change in our view of overturning in the subpolar North Atlantic. *Science*, *363*(6426), 516–521. https://doi.org/10.1126/science.aau6592

Lozier, M. S., Roussenov, V., Reed, M. S., & Williams, R. G. (2010). Opposing decadal changes for the North Atlantic meridional overturning circulation. *Nature Geoscience*, *3*(10), 728–734. https://doi.org/10.1038/ngeo947

Lu, R., Chen, W., & Dong, B. (2008). How does a weakened Atlantic thermohaline circulation lead to an intensification of the ENSO-south Asian summer monsoon interaction? *Geophysical Research Letters*, *35*, L08706. https://doi.org/10.1029/2008GL033394

Lu, R., Dong, B., & Ding, H. (2006). Impact of the Atlantic Multidecadal Oscillation on the Asian summer monsoon. *Geophysical Research Letters*, *33*, L24701. https://doi.org/10.1029/2006GL027655

Luo, F., Li, S., & Furevik, T. (2011). The connection between the Atlantic multidecadal oscillation and the Indian summer monsoon in Bergen climate model version 2.0. *Journal of Geophysical Research*, *116*, D19117. https://doi.org/10.1029/2011JD015848

Luterbacher, J., Xoplaki, E., Dietrich, D., Rickli, R., Jacobeit, J., Beck, C., et al. (2002). Reconstruction of sea level pressure fields over the Eastern North Atlantic and Europe back to 1500. *Climate Dynamics*, *18*(7), 545–561. https://doi.org/10.1007/s00382-001-0196-6

Lyu, K., Yu, J. Y., & Paek, H. (2017). The influences of the Atlantic multidecadal oscillation on the mean strength of the North Pacific subtropical high during boreal winter. *Journal of Climate*, *30*(1), 411–426. https://doi.org/10.1175/JCLI-D-16-0525.1

Mahajan, S., Zhang, R., & Delworth, T. L. (2011). Impact of the Atlantic meridional overturning circulation (AMOC) on Arctic surface air temperature and sea ice variability. *Journal of Climate*, *24*(24), 6573–6581. https://doi.org/10.1175/2011JCLI4002.1

Mahajan, S., Zhang, R., Delworth, T. L., Zhang, S., Rosati, A. J., & Chang, Y. S. (2011). Predicting Atlantic meridional overturning circulation (AMOC) variations using subsurface and surface fingerprints. *Deep Sea Research Part II: Topical Studies in Oceanography*, *58*(17-18), 1895–1903. https://doi.org/10.1016/j.dsr2.2010.10.067

Mann, M. E., & Emanuel, K. A. (2006). Atlantic hurricane trends linked to climate change. *Eos, Transactions American Geophysical Union*, *87*(24), 233–241. https://doi.org/10.1029/2006EO240001

Mann, M. E., Zhang, Z., Rutherford, S., Bradley, R. S., Hughes, M. K., Shindell, D., et al. (2009). Global signatures and dynamical origins of the Little Ice Age and Medieval Climate Anomaly. *Science*, *326*(5957), 1256–1260. https://doi.org/10.1126/science.1177303

Mantua, N. J., Hare, S. R., Zhang, Y., Wallace, J. M., & Francis, R. C. (1997). A Pacific interdecadal climate oscillation with impacts on salmon production. *Bulletin of the American Meteorological Society*, *78*(6), 1069–1079. https://doi.org/10.1175/1520-0477(1997)078<1069:APICOW>2.0.CO;2

Marini, C., & Frankignoul, C. (2014). An attempt to deconstruct the Atlantic multidecadal oscillation. *Climate Dynamics*, *43*(3-4), 607–625. https://doi.org/10.1007/s00382-013-1852-3

Marsh, R. (2000). Recent variability of the North Atlantic thermohaline circulation inferred from surface heat and freshwater fluxes. *Journal of Climate*, *13*(18), 3239–3260. https://doi.org/10.1175/1520-0442(2000)013<3239:RVOTNA>2.0.CO;2

Marshall, J., Donohoe, A., Ferreira, D., & McGee, D. (2014). The ocean's role in setting the mean position of the Inter-Tropical Convergence Zone. *Climate Dynamics*, *42*(7-8), 1967–1979. https://doi.org/10.1007/s00382-013-1767-z

Marshall, J., Johnson, H., & Goodman, J. (2001). A study of the interaction of the North Atlantic Oscillation with ocean circulation. *Journal of Climate*, *14*(7), 1399–1421. https://doi.org/10.1175/1520-0442(2001)014<1399:ASOTIO>2.0.CO;2

Marshall, J., & Schott, F. (1999). Open-ocean convection: Observations, theory, and models. *Reviews of Geophysics*, *37*(1), 1–64. https://doi.org/10.1029/98RG02739

Martin, E. R., & Thorncroft, C. (2014b). Sahel rainfall in multimodel CMIP5 decadal hindcasts. *Geophysical Research Letters*, *41*, 2169–2175. https://doi.org/10.1002/2014GL059338

Martin, E. R., Thorncroft, C., & Booth, B. B. (2014). The multidecadal Atlantic SST—Sahel rainfall teleconnection in CMIP5 simulations. *Journal of Climate*, *27*(2), 784–806. https://doi.org/10.1175/JCLI-D-13-00242.1

Martin, E. R., & Thorncroft, C. D. (2014a). The impact of the AMO on the West African monsoon annual cycle. *Quarterly Journal of the Royal Meteorological Society*, *140*(678), 31–46. https://doi.org/10.1002/qj.2107

Matei, D., Pohlmann, H., Jungclaus, J., Müller, W., Haak, H., & Marotzke, J. (2012). Two tales of initializing decadal climate prediction experiments with the ECHAM5/MPI-OM model. *Journal of Climate*, *25*(24), 8502–8523. https://doi.org/10.1175/JCLI-D-11-00633.1

McCabe, G. J., Palecki, M. A., & Betancourt, J. L. (2004). Pacific and Atlantic Ocean influences on multidecadal drought frequency in the United States. *Proceedings of the National Academy of Sciences*, *101*(12), 4136–4141. https://doi.org/10.1073/pnas.0306738101

McCarthy, G., Frajka-Williams, E., Johns, W. E., Baringer, M. O., Meinen, C. S., Bryden, H. L., et al. (2012). Observed interannual variability of the Atlantic meridional overturning circulation at 26. 5 N. *Geophysical Research Letters*, *39*, L19609. https://doi.org/10.1029/2012GL052933

McCarthy, G. D., Haigh, I. D., Hirschi, J. J. M., Grist, J. P., & Smeed, D. A. (2015). Ocean impact on decadal Atlantic climate variability revealed by sea-level observations. *Nature*, *521*(7553), 508–510. https://doi.org/10.1038/nature14491

McGregor, S., Stuecker, M. F., Kajtar, J. B., England, M. H., & Collins, M. (2018). Model tropical Atlantic biases underpin diminished Pacific decadal variability. *Nature Climate Change*, *8*(6), 493–498. https://doi.org/10.1038/s41558-018-0163-4

McGregor, S., Timmermann, A., Stuecker, M. F., England, M. H., Merrifield, M., Jin, F. F., & Chikamoto, Y. (2014). Recent Walker circulation strengthening and Pacific cooling amplified by Atlantic warming. *Nature Climate Change*, *4*(10), 888–892. https://doi.org/10.1038/nclimate2330

McManus, J. F., Francois, R., Gherardi, J. M., Keigwin, L. D., & Brown-Leger, S. (2004). Collapse and rapid resumption of Atlantic meridional circulation linked to deglacial climate changes. *Nature*, *428*(6985), 834–837. https://doi.org/10.1038/nature02494

Mecking, J. V., Keenlyside, N. S., & Greatbatch, R. J. (2014). Stochastically-forced multidecadal variability in the North Atlantic: A model study. *Climate Dynamics*, *43*(1-2), 271–288. https://doi.org/10.1007/s00382-013-1930-6

Medhaug, I., & Furevik, T. (2011). North Atlantic 20th century multidecadal variability in coupled climate models: Sea surface temperature and ocean overturning circulation.

Medhaug, I., Langehaug, H. R., Eldevik, T., Furevik, T., & Bentsen, M. (2012). Mechanisms for decadal scale variability in a simulated Atlantic meridional overturning circulation. *Climate Dynamics*, *39*(1-2), 77–93. https://doi.org/10.1007/s00382-011-1124-z

Menary, M. B., Hodson, D. L., Robson, J. I., Sutton, R. T., Wood, R. A., & Hunt, J. A. (2015). Exploring the impact of CMIP5 model biases on the simulation of North Atlantic decadal variability. *Geophysical Research Letters*, *42*, 5926–5934. https://doi.org/10.1002/2015GL064360

Mignot, J., & Frankignoul, C. (2003). On the interannual variability of surface salinity in the Atlantic. *Climate Dynamics*, *20*(6), 555–565. https://doi.org/10.1007/s00382-002-0294-0

Mignot, J., Khodri, M., Frankignoul, C., & Servonnat, J. (2011). Volcanic impact on the Atlantic Ocean over the last millennium. *Climate of the Past Discussions*, *7*(4), 2511–2554. https://doi.org/10.5194/cpd-7-2511-2011

Miles, M. W., Divine, D. V., Furevik, T., Jansen, E., Moros, M., & Ogilvie, A. E. (2014). A signal of persistent Atlantic multidecadal variability in Arctic sea ice. *Geophysical Research Letters*, *41*, 463–469. https://doi.org/10.1002/2013GL058084

Mjell, T. L., Ninnemann, U. S., Kleiven, H. F., & Hall, I. R. (2016). Multidecadal changes in Iceland Scotland Overflow Water vigor over the last 600 years and its relationship to climate. *Geophysical Research Letters*, *43*, 2111–2117. https://doi.org/10.1002/2016GL068227

Mohino, E., Janicot, S., & Bader, J. (2011). Sahel rainfall and decadal to multi-decadal sea surface temperature variability. *Climate Dynamics*, *37*(3-4), 419–440. https://doi.org/10.1007/s00382-010-0867-2

Mohino, E., Keenlyside, N., & Pohlmann, H. (2016). Decadal prediction of Sahel rainfall: where does the skill (or lack thereof) come from? *Climate Dynamics*, *47*(11), 3593–3612. https://doi.org/10.1007/s00382-016-3416-9

Monerie, P. A., Robson, J., Dong, B., & Dunstone, N. (2018). A role of the Atlantic Ocean in predicting summer surface air temperature over North East Asia? *Climate Dynamics*, *51*(1-2), 473–491. https://doi.org/10.1007/s00382-017-3935-z

Moore, G. W. K., Halfar, J., Majeed, H., Adey, W., & Kronz, A. (2017). Amplification of the Atlantic Multidecadal Oscillation associated with the onset of the industrial-era warming. *Scientific Reports*, *7*(1), 40861. https://doi.org/10.1038/srep40861

Moros, M., Andrews, J. T., Eberl, D. D., & Jansen, E. (2006). Holocene history of drift ice in the northern North Atlantic: Evidence for different spatial and temporal modes. *Paleoceanography*, *21*, PA2017. https://doi.org/10.1029/2005PA001214

Msadek, R., Delworth, T. L., Rosati, A., Anderson, W., Vecchi, G., Chang, Y. S., et al. (2014). Predicting a decadal shift in North Atlantic climate variability using the GFDL forecast system. *Journal of Climate*, *27*(17), 6472–6496. https://doi.org/10.1175/JCLI-D-13-00476.1

Msadek, R., Dixon, K. W., Delworth, T. L., & Hurlin, W. (2010). Assessing the predictability of the Atlantic meridional overturning circulation and associated fingerprints. *Geophysical Research Letters*, *37*, L19608. https://doi.org/10.1029/2010GL044517

Msadek, R., Frankignoul, C., & Li, L. Z. (2011). Mechanisms of the atmospheric response to North Atlantic multidecadal variability: A model study. *Climate Dynamics*, *36*(7-8), 1255–1276. https://doi.org/10.1007/s00382-010-0958-0

Msadek, R., Johns, W. E., Yeager, S. G., Danabasoglu, G., Delworth, T. L., & Rosati, A. (2013). The Atlantic meridional heat transport at 26.5 N and its relationship with the MOC in the RAPID array and the GFDL and NCAR coupled models. *Journal of Climate*, *26*(12), 4335–4356. https://doi.org/10.1175/JCLI-D-12-00081.1

Mueller, W. A., Pohlmann, H., Sienz, F., & Smith, D. (2014). Decadal climate predictions for the period 1901–2010 with a coupled climate model. *Geophysical Research Letters*, *41*, 2100–2107. https://doi.org/10.1002/2014GL059259

Murphy, L. N., Bellomo, K., Cane, M., & Clement, A. (2017). The role of historical forcings in simulating the observed Atlantic multidecadal oscillation. *Geophysical Research Letters*, *44*, 2472–2480. https://doi.org/10.1002/2016GL071337

Myers, P. G., Fanning, A. F., & Weaver, A. J. (1996). JEBAR, bottom pressure torque, and Gulf Stream separation. *Journal of Physical Oceanography*, *26*(5), 671–683. https://doi.org/10.1175/1520-0485(1996)026<0671:JBPTAG>2.0.CO;2

Newman, M., Alexander, M. A., Ault, T. R., Cobb, K. M., Deser, C., Di Lorenzo, E., et al. (2016). The Pacific decadal oscillation, revisited. *Journal of Climate*, *29*(12), 4399–4427. https://doi.org/10.1175/JCLI-D-15-0508.1

Nigam, S., & Guan, B. (2011). Atlantic tropical cyclones in the twentieth century: Natural variability and secular change in cyclone count. *Climate Dynamics*, *36*(11-12), 2279–2293. https://doi.org/10.1007/s00382-010-0908-x

Nigam, S., Guan, B., & Ruiz-Barradas, A. (2011). Key role of the Atlantic multidecadal oscillation in 20th century drought and wet periods over the Great Plains. *Geophysical Research Letters*, *38*, L16713. https://doi.org/10.1029/2011GL048650

Nigam, S., Ruiz-Barradas, A., & Chafik, L. (2018). Gulf Stream excursions and sectional detachment generate the decadal pulses in the Atlantic Multidecadal Oscillation. *Journal of Climate*, *31*(7), 2853–2870. https://doi.org/10.1175/JCLI-D-17-0010.1

Nye, J. A., Joyce, T. M., Kwon, Y. O., & Link, J. S. (2011). Silver hake tracks changes in Northwest Atlantic circulation. *Nature Communications*, *2*(1), 412. https://doi.org/10.1038/ncomms1420

Oka, A., Hasumi, H., Okada, N., Sakamoto, T. T., & Suzuki, T. (2006). Deep convection seesaw controlled by freshwater transport through the Denmark Strait. *Ocean Modelling*, *15*(3-4), 157–176. https://doi.org/10.1016/j.ocemod.2006.08.004

Okumura, Y. M., Deser, C., Hu, A., Timmermann, A., & Xie, S. P. (2009). North Pacific climate response to freshwater forcing in the subarctic North Atlantic: Oceanic and atmospheric pathways. *Journal of Climate*, *22*(6), 1424–1445. https://doi.org/10.1175/2008JCLI2511.1

Omrani, N. E., Bader, J., Keenlyside, N. S., & Manzini, E. (2016). Troposphere–stratosphere response to large-scale North Atlantic Ocean variability in an atmosphere/ocean coupled model. *Climate Dynamics*, *46*(5-6), 1397–1415. https://doi.org/10.1007/s00382-015-2654-6

Omrani, N. E., Keenlyside, N. S., Bader, J., & Manzini, E. (2014). Stratosphere key for wintertime atmospheric response to warm Atlantic decadal conditions. *Climate Dynamics*, *42*(3-4), 649–663. https://doi.org/10.1007/s00382-013-1860-3

O'Reilly, C. H., Huber, M., Woollings, T., & Zanna, L. (2016). The signature of low-frequency oceanic forcing in the Atlantic Multidecadal Oscillation. *Geophysical Research Letters*, *43*, 2810–2818. https://doi.org/10.1002/2016GL067925

Ortega, P., Lehner, F., Swingedouw, D., Masson-Delmotte, V., Raible, C. C., Casado, M., & Yiou, P. (2015). A model-tested North Atlantic Oscillation reconstruction for the past millennium. *Nature*, *523*(7558), 71–74. https://doi.org/10.1038/nature14518

Ortega, P., Robson, J., Sutton, R. T., & Andrews, M. B. (2017). Mechanisms of decadal variability in the Labrador Sea and the wider North Atlantic in a high-resolution climate model. *Climate Dynamics*, *49*(7-8), 2625–2647. https://doi.org/10.1007/s00382-016-3467-y

Otterå, O. H., Bentsen, M., Drange, H., & Suo, L. (2010). External forcing as a metronome for Atlantic multidecadal variability. *Nature Geoscience*, *3*(10), 688–694. https://doi.org/10.1038/ngeo955

Otto-Bliesner, B. L., Brady, E. C., Fasullo, J., Jahn, A., Landrum, L., Stevenson, S., et al. (2016). Climate variability and change since 850 CE: An ensemble approach with the Community Earth System Model. *Bulletin of the American Meteorological Society*, *97*(5), 735–754. https://doi.org/10.1175/BAMS-D-14-00233.1

Outten, S., & Esau, I. (2017). Bjerknes compensation in the Bergen Climate Model. *Climate Dynamics*, *49*(7-8), 2249–2260. https://doi.org/10.1007/s00382-016-3447-2

Pant, G. B., Rupa Kumar, K., & Borgaonkar, H. P. (1988). Statistical models of climate reconstruction using Tree-ring data. *Proceedings of the Indian National Academy of Sciences*, *50*, 354–364.

Park, T., Park, W., & Latif, M. (2016). Correcting North Atlantic sea surface salinity biases in the Kiel Climate Model: Influences on ocean circulation and Atlantic Multidecadal Variability. *Climate Dynamics*, *47*(7-8), 2543–2560. https://doi.org/10.1007/s00382-016-2982-1

Park, W., & Latif, M. (2008). Multidecadal and multicentennial variability of the meridional overturning circulation. *Geophysical Research Letters*, *35*, L22703. https://doi.org/10.1029/2008GL035779

Parker, A. O., Schmidt, M. W., & Chang, P. (2015). Tropical North Atlantic subsurface warming events as a fingerprint for AMOC variability during Marine Isotope Stage 3. *Paleoceanography*, *30*, 1425–1436. https://doi.org/10.1002/2015PA002832

Pedlosky, J. (2013). *Ocean circulation theory*. Berlin: Springer Science & Business Media.

Peings, Y., & Magnusdottir, G. (2014). Forcing of the wintertime atmospheric circulation by the multidecadal fluctuations of the North Atlantic Ocean. *Environmental Research Letters*, *9*(3), 034018. https://doi.org/10.1088/1748-9326/9/3/034018

Peings, Y., & Magnusdottir, G. (2016). Wintertime atmospheric response to Atlantic multidecadal variability: Effect of stratospheric representation and ocean–atmosphere coupling. *Climate Dynamics*, *47*(3-4), 1029–1047. https://doi.org/10.1007/s00382-015-2887-4

Peings, Y., Simpkins, G., & Magnusdottir, G. (2016). Multidecadal fluctuations of the North Atlantic Ocean and feedback on the winter climate in CMIP5 control simulations. *Journal of Geophysical Research: Atmospheres*, *121*, 2571–2592. https://doi.org/10.1002/2015JD024107

Persechino, A., Mignot, J., Swingedouw, D., Labetoulle, S., & Guilyardi, É. (2013). Decadal predictability of the Atlantic meridional overturning circulation and climate in the IPSL-CM5A-LR model. *Climate Dynamics*, *40*(9-10), 2359–2380. https://doi.org/10.1007/s00382-012-1466-1

Peterson, I. K., Pettipas, R., & Rosing-Asvid, A. (2015). Trends and variability in sea ice and icebergs off the Canadian east coast. *Atmosphere-Ocean*, *53*(5), 582–594. https://doi.org/10.1080/07055900.2015.1057684

Pickart, R. S., & Spall, M. A. (2007). Impact of Labrador Sea convection on the North Atlantic meridional overturning circulation. *Journal of Physical Oceanography*, *37*(9), 2207–2227. https://doi.org/10.1175/JPO3178.1

Piecuch, C. G., Ponte, R. M., Little, C. M., Buckley, M. W., & Fukumori, I. (2017). Mechanisms underlying recent decadal changes in subpolar North Atlantic Ocean heat content. *Journal of Geophysical Research: Oceans*, *122*, 7181–7197. https://doi.org/10.1002/2017JC012845

Pohlmann, H., Botzet, M., Latif, M., Roesch, A., Wild, M., & Tschuck, P. (2004). Estimating the decadal predictability of a coupled AOGCM. *Journal of Climate*, *17*(22), 4463–4472. https://doi.org/10.1175/3209.1

Polyakov, I. V., Alekseev, G. V., Bekryaev, R. V., Bhatt, U. S., Colony, R., Johnson, M. A., et al. (2003). Long-term ice variability in Arctic marginal seas. *Journal of Climate*, *16*(12), 2078–2085. https://doi.org/10.1175/1520-0442(2003)016<2078:LIVIAM>2.0.CO;2

Polyakov, I. V., Alexeev, V. A., Bhatt, U. S., Polyakova, E. I., & Zhang, X. (2010). North Atlantic warming: Patterns of long-term trend and multidecadal variability. *Climate Dynamics*, *34*(2-3), 439–457. https://doi.org/10.1007/s00382-008-0522-3

Polyakov, I. V., Bekryaev, R. V., Alekseev, G. V., Bhatt, U. S., Colony, R. L., Johnson, M. A., et al. (2003). Variability and trends of air temperature and pressure in the maritime Arctic, 1875–2000. *Journal of Climate*, *16*(12), 2067–2077. https://doi.org/10.1175/1520-0442(2003)016<2067:VATOAT>2.0.CO;2

Qasmi, S., Cassou, C., & Boé, J. (2017). Teleconnection between Atlantic multidecadal variability and European temperature: Diversity and evaluation of the Coupled Model Intercomparison Project Phase 5 Models. *Geophysical Research Letters*, *44*, 11–140. https://doi.org/10.1002/2017GL074886

Rahmstorf, S. (2002). Ocean circulation and climate during the past 120,000 years. *Nature*, *419*(6903), 207–214. https://doi.org/10.1038/nature01090

Rayner, N. A., Parker, D. E., Horton, E. B., Folland, C. K., Alexander, L. V., Rowell, D. P., et al. (2003). Global analyses of sea surface temperature, sea ice, and night marine air temperature since the late nineteenth century. *Journal of Geophysical Research*, *108*(D14), 4407. https://doi.org/10.1029/2002JD002670

Reynolds, D. J., Hall, I. R., Slater, S. M., Scourse, J. D., Halloran, P. R., & Sayer, M. D. J. (2017). Reconstructing past seasonal to multicentennial-scale variability in the NE Atlantic Ocean using the long-lived marine bivalve mollusk Glycymeris glycymeris. *Paleoceanography*, *32*, 1153–1173. https://doi.org/10.1002/2017PA003154

Reynolds, D. J., Scourse, J. D., Halloran, P. R., Nederbragt, A. J., Wanamaker, A. D., Butler, P. G., et al. (2016). Annually resolved North Atlantic marine climate over the last millennium. *Nature Communications*, *7*(1), 13502. https://doi.org/10.1038/ncomms13502

Reynolds, R. W. (1978). Sea surface temperature anomalies in the North Pacific Ocean. *Tellus*, *30*(2), 97–103.

Richter, I., Xie, S. P., Behera, S. K., Doi, T., & Masumoto, Y. (2014). Equatorial Atlantic variability and its relation to mean state biases in CMIP5. *Climate Dynamics*, *42*(1-2), 171–188. https://doi.org/10.1007/s00382-012-1624-5

Rimbu, N., Lohmann, G., & Ionita, M. (2014). Interannual to multidecadal Euro-Atlantic blocking variability during winter and its relationship with extreme low temperatures in Europe. *Journal of Geophysical Research: Atmospheres*, *119*, 13–621. https://doi.org/10.1002/2014JD021983

Roberts, C. D., Garry, F. K., & Jackson, L. C. (2013). A multimodel study of sea surface temperature and subsurface density fingerprints of the Atlantic meridional overturning circulation. *Journal of Climate*, *26*(22), 9155–9174. https://doi.org/10.1175/JCLI-D-12-00762.1

Robson, J., Hodson, D., Hawkins, E., & Sutton, R. (2014). Atlantic overturning in decline? *Nature Geoscience*, *7*(1), 2–3. https://doi.org/10.1038/ngeo2050

Robson, J., Ortega, P., & Sutton, R. (2016). A reversal of climatic trends in the North Atlantic since 2005. *Nature Geoscience*, *9*(7), 513–517. https://doi.org/10.1038/ngeo2727

Robson, J., Sutton, R., Lohmann, K., Smith, D., & Palmer, M. D. (2012). Causes of the rapid warming of the North Atlantic Ocean in the mid-1990s. *Journal of Climate*, *25*(12), 4116–4134. https://doi.org/10.1175/JCLI-D-11-00443.1

Robson, J., Sutton, R., & Smith, D. (2013). Predictable climate impacts of the decadal changes in the ocean in the 1990s. *Journal of Climate*, *26*(17), 6329–6339. https://doi.org/10.1175/JCLI-D-12-00827.1

Robson, J., Sutton, R., & Smith, D. (2014). Decadal predictions of the cooling and freshening of the North Atlantic in the 1960s and the role of ocean circulation. *Climate Dynamics*, *42*(9-10), 2353–2365. https://doi.org/10.1007/s00382-014-2115-7

Robson, J. I., Sutton, R. T., & Smith, D. M. (2012). Initialized decadal predictions of the rapid warming of the North Atlantic Ocean in the mid 1990s. *Geophysical Research Letters*, *39*, L19713. https://doi.org/10.1029/2012GL053370

Ruiz-Barradas, A., Nigam, S., & Kavvada, A. (2013). The Atlantic Multidecadal Oscillation in twentieth century climate simulations: Uneven progress from CMIP3 to CMIP5. *Climate Dynamics*, *41*(11-12), 3301–3315. https://doi.org/10.1007/s00382-013-1810-0

Ruprich-Robert, Y., Delworth, T., Msadek, R., Castruccio, F., Yeager, S., & Danabasoglu, G. (2018). Impacts of the Atlantic multidecadal variability on North American summer climate and heat waves. *Journal of Climate*, *31*(9), 3679–3700. https://doi.org/10.1175/JCLI-D-17-0270.1

Ruprich-Robert, Y., Msadek, R., Castruccio, F., Yeager, S., Delworth, T., & Danabasoglu, G. (2017). Assessing the climate impacts of the observed Atlantic multidecadal variability using the GFDL CM2. 1 and NCAR CESM1 global coupled models. *Journal of Climate*, *30*(8), 2785–2810. https://doi.org/10.1175/JCLI-D-16-0127.1

Saenger, C., Cohen, A. L., Oppo, D. W., Halley, R. B., & Carilli, J. E. (2009). Surface-temperature trends and variability in the low-latitude North Atlantic since 1552. *Nature Geoscience*, *2*(7), 492–495. https://doi.org/10.1038/ngeo552

Sanchez-Franks, A., & Zhang, R. (2015). Impact of the Atlantic meridional overturning circulation on the decadal variability of the Gulf Stream path and regional chlorophyll and nutrient concentrations. *Geophysical Research Letters*, *42*, 9889–9887. https://doi.org/10.1002/2015GL066262

Sankar, S., Svendsen, L., Gokulapalan, B., Joseph, P. V., & Johannessen, O. M. (2016). The relationship between Indian summer monsoon rainfall and Atlantic multidecadal variability over the last 500 years. *Tellus A: Dynamic Meteorology and Oceanography*, *68*(1), 31717. https://doi.org/10.3402/tellusa.v68.31717

Sarkisyan, A. S., & Ivanov, V. F. (1971). Joint effect of baroclinicity and bottom relief as an important factor in the dynamics of the sea current. *Investiya Academy of Sciences, USSR, Atmospheric and Ocean Sciences*, *1*, 173–188.

Schlesinger, M. E., & Ramankutty, N. (1994). An oscillation in the global climate system of period 65–70 years. *Nature*, *367*(6465), 723–726. https://doi.org/10.1038/367723a0

Schmidt, M. W., Chang, P., Hertzberg, J. E., Them, T. R., Ji, L., & Otto-Bliesner, B. L. (2012). Impact of abrupt deglacial climate change on tropical Atlantic subsurface temperatures. *Proceedings of the National Academy of Sciences*, *109*(36), 14,348–14,352. https://doi.org/10.1073/pnas.1207806109

Schmitz, W. J. Jr. (1995). On the interbasin-scale thermohaline circulation. *Reviews of Geophysics*, *33*(2), 151–173. https://doi.org/10.1029/95RG00879

Schubert, S., Gutzler, D., Wang, H., Dai, A., Delworth, T., Deser, C., et al. (2009). A US CLIVAR project to assess and compare the responses of global climate models to drought-related SST forcing patterns: overview and results. *Journal of Climate*, *22*(19), 5251–5272. https://doi.org/10.1175/2009JCLI3060.1

Screen, J. A., & Simmonds, I. (2010). The central role of diminishing sea ice in recent Arctic temperature amplification. *Nature*, *464*(7293), 1334–1337. https://doi.org/10.1038/nature09051

Seale, A., Christoffersen, P., Mugford, R. I., & O'Leary, M. (2011). Ocean forcing of the Greenland Ice Sheet: Calving fronts and patterns of retreat identified by automatic satellite monitoring of eastern outlet glaciers. *Journal of Geophysical Research*, *116*(F3). https://doi.org/10.1029/2010JF001847

Seidov, D., Mishonov, A., Reagan, J., & Parsons, R. (2017). Multidecadal variability and climate shift in the North Atlantic Ocean. *Geophysical Research Letters*, *44*, 4985–4993. https://doi.org/10.1002/2017GL073644

Semenov, V. A., & Bengtsson, L. (2003). Modes of the wintertime Arctic temperature variability. *Geophysical Research Letters*, *30*(15), 1781. https://doi.org/10.1029/2003GL017112

Semenov, V. A., & Latif, M. (2012). The early twentieth century warming and winter Arctic sea ice. *The Cryosphere*, *6*(6), 1231–1237. https://doi.org/10.5194/tc-6-1231-2012

Semenov, V. A., Latif, M., Dommenget, D., Keenlyside, N. S., Strehz, A., Martin, T., & Park, W. (2010). The impact of North Atlantic–Arctic multidecadal variability on Northern Hemisphere surface air temperature. *Journal of Climate*, *23*(21), 5668–5677. https://doi.org/10.1175/2010JCLI3347.1

Serreze, M. C., Barrett, A. P., Stroeve, J. C., Kindig, D. N., & Holland, M. M. (2009). The emergence of surface-based Arctic amplification. *The Cryosphere*, *3*(1), 11–19. https://doi.org/10.5194/tc-3-11-2009

Shaffrey, L., & Sutton, R. (2006). Bjerknes compensation and the decadal variability of the energy transports in a coupled climate model. *Journal of Climate*, *19*(7), 1167–1181. https://doi.org/10.1175/JCLI3652.1

Shanahan, T. M., Overpeck, J. T., Anchukaitis, K. J., Beck, J. W., Cole, J. E., Dettman, D. L., et al. (2009). Atlantic forcing of persistent drought in West Africa. *Science*, *324*(5925), 377–380. https://doi.org/10.1126/science.1166352

Sheen, K. L., Smith, D. M., Dunstone, N. J., Eade, R., Rowell, D. P., & Vellinga, M. (2017). Skilful prediction of Sahel summer rainfall on inter-annual and multi-year timescales. *Nature Communications*, *8*, 14966. https://doi.org/10.1038/ncomms14966

Sheffield, J., Camargo, S. J., Fu, R., Hu, Q., Jiang, X., Johnson, N., et al. (2013). North American climate in CMIP5 experiments. Part II: Evaluation of historical simulations of intraseasonal to decadal variability. *Journal of Climate*, *26*(23), 9247–9290. https://doi.org/10.1175/JCLI-D-12-00593.1

Shi, F., Li, J., & Wilson, R. J. (2014). A tree-ring reconstruction of the South Asian summer monsoon index over the past millennium. *Scientific Reports*, *4*, 6739.

Simpson, I. R., Deser, C., McKinnon, K. A., & Barnes, E. A. (2018). Modeled and observed multidecadal variability in the North Atlantic Jet Stream and its connection to sea surface temperatures. *Journal of Climate*, *31*(20), 8313–8338. https://doi.org/10.1175/JCLI-D-18-0168.1

Singh, H. K., Hakim, G. J., Tardif, R., Emile-Geay, J., & Noone, D. C. (2018). Insights into Atlantic multidecadal variability using the Last Millennium Reanalysis framework. *Climate of the Past*, *14*(2), 157–174. https://doi.org/10.5194/cp-14-157-2018

Smedsrud, L. H., Esau, I., Ingvaldsen, R. B., Eldevik, T., Haugan, P. M., Li, C., et al. (2013). The role of the Barents Sea in the Arctic climate system. *Reviews of Geophysics*, *51*, 415–449. https://doi.org/10.1002/rog.20017

Smeed, D. A., Josey, S. A., Beaulieu, C., Johns, W. E., Moat, B. I., Frajka-Williams, E., et al. (2018). The North Atlantic Ocean is in a state of reduced overturning. *Geophysical Research Letters*, *45*, 1527–1533. https://doi.org/10.1002/2017GL076350

Smeed, D. A., McCarthy, G., Cunningham, S. A., Frajka-Williams, E., Rayner, D., Johns, W. E., et al. (2014). Observed decline of the Atlantic meridional overturning circulation 2004–2012. *Ocean Science*, *10*(1), 29–38. https://doi.org/10.5194/os-10-29-2014

Smirnov, D., & Vimont, D. J. (2012). Extratropical forcing of tropical Atlantic variability during boreal summer and fall. *Journal of Climate*, *25*(6), 2056–2076. https://doi.org/10.1175/JCLI-D-11-00104.1

Smith, D. M., Eade, R., Dunstone, N. J., Fereday, D., Murphy, J. M., Pohlmann, H., & Scaife, A. A. (2010). Skilful multi-year predictions of Atlantic hurricane frequency. *Nature Geoscience*, *3*(12), 846–849. https://doi.org/10.1038/ngeo1004

Srokosz, M. A., & Bryden, H. L. (2015). Observing the Atlantic Meridional Overturning Circulation yields a decade of inevitable surprises. *Science*, *348*(6241), 1255575. https://doi.org/10.1126/science.1255575

Steiger, N. J., Hakim, G. J., Steig, E. J., Battisti, D. S., & Roe, G. H. (2014). Assimilation of time-averaged pseudoproxies for climate reconstruction. *Journal of Climate*, *27*(1), 426–441. https://doi.org/10.1175/JCLI-D-12-00693.1

Steinman, B. A., Mann, M. E., & Miller, S. K. (2015). Atlantic and Pacific multidecadal oscillations and Northern Hemisphere temperatures. *Science*, *347*(6225), 988–991. https://doi.org/10.1126/science.1257856

Stolpe, M. B., Medhaug, I., & Knutti, R. (2017). Contribution of Atlantic and Pacific multidecadal variability to twentieth-century temperature changes. *Journal of Climate*, *30*(16), 6279–6295. https://doi.org/10.1175/JCLI-D-16-0803.1

Stolpe, M. B., Medhaug, I., Sedláček, J., & Knutti, R. (2018). Multidecadal variability in global surface temperatures related to the Atlantic Meridional Overturning Circulation. *Journal of Climate*, *31*(7), 2889–2906. https://doi.org/10.1175/JCLI-D-17-0444.1

Stommel, H. (1957). A survey of ocean current theory. *Deep Sea Research (1953)*, *4*, 149–184. https://doi.org/10.1016/0146-6313(56)90048-X

Stommel, H. (1958). The abyssal circulation. *Deep-Sea Research*, *5*(1), 80–82. https://doi.org/10.1016/S0146-6291(58)80014-4

Stouffer, R. J., Yin, J., Gregory, J. M., Dixon, K. W., Spelman, M. J., Hurlin, W., et al. (2006). Investigating the causes of the response of the thermohaline circulation to past and future climate changes. *Journal of Climate*, *19*(8), 1365–1387. https://doi.org/10.1175/JCLI3689.1

Straneo, F., Hamilton, G. S., Sutherland, D. A., Stearns, L. A., Davidson, F., Hammill, M. O., et al. (2010). Rapid circulation of warm subtropical waters in a major glacial fjord in East Greenland. *Nature Geoscience*, *3*(3), 182–186. https://doi.org/10.1038/ngeo764

Straneo, F., & Heimbach, P. (2013). North Atlantic warming and the retreat of Greenland's outlet glaciers. *Nature*, *504*(7478), 36–43. https://doi.org/10.1038/nature12854

Sun, C., Kucharski, F., Li, J., Jin, F. F., Kang, I. S., & Ding, R. (2017). Western tropical Pacific multidecadal variability forced by the Atlantic multidecadal oscillation. *Nature Communications*, *8*, 15998. https://doi.org/10.1038/ncomms15998

Sun, C., Li, J., Kucharski, F., Xue, J., & Li, X. (2018). Contrasting spatial structures of Atlantic Multidecadal Oscillation between observations and slab ocean model simulations. *Climate Dynamics*, *52*(3-4), 1395–1411.

Sutton, R., & Mathieu, P. P. (2002). Response of the atmosphere-ocean mixed-layer system to anomalous ocean heat-flux convergence. *Quarterly Journal of the Royal Meteorological Society*, *128*(582), 1259–1275. https://doi.org/10.1256/003590002320373283

Sutton, R. T., & Dong, B. (2012). Atlantic Ocean influence on a shift in European climate in the 1990s. *Nature Geoscience*, *5*(11), 788–792. https://doi.org/10.1038/ngeo1595

Sutton, R. T., & Hodson, D. L. (2005). Atlantic Ocean forcing of North American and European summer climate. *Science*, *309*(5731), 115–118. https://doi.org/10.1126/science.1109496

Sutton, R. T., & Hodson, D. L. (2007). Climate response to basin-scale warming and cooling of the North Atlantic Ocean. *Journal of Climate*, *20*(5), 891–907. https://doi.org/10.1175/JCLI4038.1

Sutton, R. T., & Hodson, D. L. R. (2003). Influence of the ocean on North Atlantic climate variability 1871–1999. *Journal of Climate*, *16*(20), 3296–3313. https://doi.org/10.1175/1520-0442(2003)016<3296:IOTOON>2.0.CO;2

Sutton, R. T., McCarthy, G. D., Robson, J., Sinha, B., Archibald, A. T., & Gray, L. J. (2018). Atlantic multidecadal variability and the UK ACSIS program. *Bulletin of the American Meteorological Society*, *99*(2), 415–425. https://doi.org/10.1175/BAMS-D-16-0266.1

Svendsen, L., Hetzinger, S., Keenlyside, N., & Gao, Y. (2014). Marine-based multiproxy reconstruction of Atlantic multidecadal variability. *Geophysical Research Letters*, *41*, 1295–1300. https://doi.org/10.1002/2013GL059076

Svendsen, L., Keenlyside, N., Bethke, I., Gao, Y., & Omrani, N. E. (2018). Pacific contribution to the early twentieth-century warming in the Arctic. *Nature Climate Change*, *8*(9), 793–797. https://doi.org/10.1038/s41558-018-0247-1

Sverdrup, H. U. (1947). Wind-driven currents in a baroclinic ocean; with application to the equatorial currents of the eastern Pacific. *Proceedings of the National Academy of Sciences*, *33*(11), 318–326. https://doi.org/10.1073/pnas.33.11.318

Sverdrup, H. U. (1957). Oceanography. *Handbuch der Physik*, *48*, 608–670.

Swingedouw, D., Ortega, P., Mignot, J., Guilyardi, E., Masson-Delmotte, V., Butler, P. G., et al. (2015). Bidecadal North Atlantic ocean circulation variability controlled by timing of volcanic eruptions. *Nature Communications*, *6*(1), 6545. https://doi.org/10.1038/ncomms7545

Talandier, C., Deshayes, J., Treguier, A. M., Capet, X., Benshila, R., Debreu, L., et al. (2014). Improvements of simulated Western North Atlantic current system and impacts on the AMOC. *Ocean Modelling*, *76*, 1–19. https://doi.org/10.1016/j.ocemod.2013.12.007

Talley, L. D. (2003). Shallow, intermediate, and deep overturning components of the global heat budget. *Journal of Physical Oceanography*, *33*(3), 530–560. https://doi.org/10.1175/1520-0485(2003)033<0530:SIADOC>2.0.CO;2

Talley, L. D., Reid, J. L., & Robbins, P. E. (2003). Data-based meridional overturning streamfunctions for the global ocean. *Journal of Climate*, *16*(19), 3213–3226. https://doi.org/10.1175/1520-0442(2003)016<3213:DMOSFT>2.0.CO;2

Tandon, N. F., & Kushner, P. J. (2015). Does external forcing interfere with the AMOC's influence on North Atlantic sea surface temperature? *Journal of Climate*, *28*(16), 6309–6323. https://doi.org/10.1175/JCLI-D-14-00664.1
Teng, H., Branstator, G., & Meehl, G. A. (2011). Predictability of the Atlantic overturning circulation and associated surface patterns in two CCSM3 climate change ensemble experiments. *Journal of Climate*, *24*(23), 6054–6076. https://doi.org/10.1175/2011JCLI4207.1
Terray, L. (2012). Evidence for multiple drivers of North Atlantic multi-decadal climate variability. *Geophysical Research Letters*, *39*, L19712. https://doi.org/10.1029/2012GL053046
Thompson, D. W., Wallace, J. M., Kennedy, J. J., & Jones, P. D. (2010). An abrupt drop in Northern Hemisphere sea surface temperature around 1970. *Nature*, *467*(7314), 444–447. https://doi.org/10.1038/nature09394
Timmermann, A., Latif, M., Voss, R., & Grötzner, A. (1998). Northern Hemispheric interdecadal variability: A coupled air–sea mode. *Journal of Climate*, *11*(8), 1906–1931. https://doi.org/10.1175/1520-0442-11.8.1906
Timmermann, A., Okumura, Y., An, S. I., Clement, A., Dong, B., Guilyardi, E., et al. (2007). The influence of a weakening of the Atlantic meridional overturning circulation on ENSO. *Journal of Climate*, *20*(19), 4899–4919. https://doi.org/10.1175/JCLI4283.1
Ting, M., Kushnir, Y., & Li, C. (2014). North Atlantic multidecadal SST oscillation: External forcing versus internal variability. *Journal of Marine Systems*, *133*, 27–38. https://doi.org/10.1016/j.jmarsys.2013.07.006
Ting, M., Kushnir, Y., Seager, R., & Li, C. (2009). Forced and internal twentieth-century SST trends in the North Atlantic. *Journal of Climate*, *22*(6), 1469–1481. https://doi.org/10.1175/2008JCLI2561.1
Ting, M., Kushnir, Y., Seager, R., & Li, C. (2011). Robust features of Atlantic multi-decadal variability and its climate impacts. *Geophysical Research Letters*, *38*, L17705. https://doi.org/10.1029/2011GL048712
Tokinaga, H., Xie, S. P., & Mukougawa, H. (2017). Early 20th-century Arctic warming intensified by Pacific and Atlantic multidecadal variability. *Proceedings of the National Academy of Sciences*, *114*(24), 6227–6232. https://doi.org/10.1073/pnas.1615880114
Trenary, L., & DelSole, T. (2016). Does the Atlantic Multidecadal Oscillation get its predictability from the Atlantic Meridional Overturning circulation? *Journal of Climate*, *29*(14), 5267–5280. https://doi.org/10.1175/JCLI-D-16-0030.1
Trenberth, K. E., & Caron, J. M. (2001). Estimates of meridional atmosphere and ocean heat transports. *Journal of Climate*, *14*(16), 3433–3443. https://doi.org/10.1175/1520-0442(2001)014<3433:EOMAAO>2.0.CO;2
Trenberth, K. E., & Fasullo, J. T. (2008). An observational estimate of inferred ocean energy divergence. *Journal of Physical Oceanography*, *38*(5), 984–999. https://doi.org/10.1175/2007JPO3833.1
Trenberth, K. E., & Shea, D. J. (2006). Atlantic hurricanes and natural variability in 2005. *Geophysical Research Letters*, *33*, L12704. https://doi.org/10.1029/2006GL026894
Trenberth, K. E., & Solomon, A. (1994). The global heat balance: Heat transports in the atmosphere and ocean. *Climate Dynamics*, *10*(3), 107–134. https://doi.org/10.1007/BF00210625
Trouet, V., Esper, J., Graham, N. E., Baker, A., Scourse, J. D., & Frank, D. C. (2009). Persistent positive North Atlantic Oscillation mode dominated the medieval climate anomaly. *Science*, *324*(5923), 78–80. https://doi.org/10.1126/science.1166349
Tung, K. K., & Zhou, J. (2013). Using data to attribute episodes of warming and cooling in instrumental records. *Proceedings of the National Academy of Sciences*, *110*(6), 2058–2063. https://doi.org/10.1073/pnas.1212471110
Van der Swaluw, E., Drijfhout, S. S., & Hazeleger, W. (2007). Bjerknes compensation at high northern latitudes: The ocean forcing the atmosphere. *Journal of climate*, *20*(24), 6023–6032. https://doi.org/10.1175/2007JCLI1562.1
Vásquez-Bedoya, L. F., Cohen, A. L., Oppo, D. W., & Blanchon, P. (2012). Corals record persistent multidecadal SST variability in the Atlantic Warm Pool since 1775 AD. *Paleoceanography and Paleoclimatology*, *27*, PA3231. https://doi.org/10.1029/2012PA002313
Vellinga, M., & Wood, R. A. (2002). Global climatic impacts of a collapse of the Atlantic thermohaline circulation. *Climatic Change*, *54*(3), 251–267. https://doi.org/10.1023/A:1016168827653
Vellinga, M., & Wu, P. (2004). Low-latitude freshwater influence on centennial variability of the Atlantic thermohaline circulation. *Journal of Climate*, *17*(23), 4498–4511. https://doi.org/10.1175/3219.1
Veres, M. C., & Hu, Q. (2013). AMO-forced regional processes affecting summertime precipitation variations in the central United States. *Journal of Climate*, *26*(1), 276–290. https://doi.org/10.1175/JCLI-D-11-00670.1
Visbeck, M., Chassignet, E. P., Curry, R. G., Delworth, T. L., Dickson, R. R., & Krahmann, G. (2003). The ocean's response to North Atlantic Oscillation variability. *The North Atlantic Oscillation: Climatic significance and environmental impact*, *134*, 113–145.
Wang, C., Dong, S., Evan, A. T., Foltz, G. R., & Lee, S. K. (2012). Multidecadal covariability of North Atlantic sea surface temperature, African dust, Sahel rainfall, and Atlantic hurricanes. *Journal of Climate*, *25*(15), 5404–5415. https://doi.org/10.1175/JCLI-D-11-00413.1
Wang, C., Dong, S., & Munoz, E. (2010). Seawater density variations in the North Atlantic and the Atlantic meridional overturning circulation. *Climate Dynamics*, *34*(7-8), 953–968. https://doi.org/10.1007/s00382-009-0560-5
Wang, C., Enfield, D. B., Lee, S. K., & Landsea, C. W. (2006). Influences of the Atlantic warm pool on Western Hemisphere summer rainfall and Atlantic hurricanes. *Journal of Climate*, *19*(12), 3011–3028. https://doi.org/10.1175/JCLI3770.1
Wang, C., Lee, S. K., & Enfield, D. B. (2008a). Atlantic warm pool acting as a link between Atlantic multidecadal oscillation and Atlantic tropical cyclone activity. *Geochemistry, Geophysics, Geosystems*, *9*, Q05V03. https://doi.org/10.1029/2007GC001809
Wang, C., Lee, S. K., & Enfield, D. B. (2008b). Climate response to anomalously large and small Atlantic warm pools during the summer. *Journal of Climate*, *21*(11), 2437–2450. https://doi.org/10.1175/2007JCLI2029.1
Wang, C., & Zhang, L. (2013). Multidecadal ocean temperature and salinity variability in the tropical North Atlantic: Linking with the AMO, AMOC, and subtropical cell. *Journal of Climate*, *26*(16), 6137–6162. https://doi.org/10.1175/JCLI-D-12-00721.1
Wang, C., Zhang, L., Lee, S. K., Wu, L., & Mechoso, C. R. (2014). A global perspective on CMIP5 climate model biases. *Nature Climate Change*, *4*(3), 201–205. https://doi.org/10.1038/nclimate2118
Wang, H., Legg, S. A., & Hallberg, R. W. (2015). Representations of the Nordic Seas overflows and their large scale climate impact in coupled models. *Ocean Modelling*, *86*, 76–92. https://doi.org/10.1016/j.ocemod.2014.12.005
Wang, J., Yang, B., & Ljungqvist, F. C. (2015). A millennial summer temperature reconstruction for the eastern Tibetan Plateau from tree-ring width. *Journal of Climate*, *28*(13), 5289–5304. https://doi.org/10.1175/JCLI-D-14-00738.1
Wang, J., Yang, B., Ljungqvist, F. C., Luterbacher, J., Osborn, T. J., Briffa, K. R., & Zorita, E. (2017). Internal and external forcing of multidecadal Atlantic climate variability over the past 1,200 years. *Nature Geoscience*, *10*(7), 512–517. https://doi.org/10.1038/ngeo2962
Wang, X., Brown, P. M., Zhang, Y., & Song, L. (2011). Imprint of the Atlantic multidecadal oscillation on tree-ring widths in Northeastern Asia since 1568. *PloS one*, *6*(7), e22740. https://doi.org/10.1371/journal.pone.0022740
Wang, X., Li, J., Sun, C., & Liu, T. (2017). NAO and its relationship with the Northern Hemisphere mean surface temperature in CMIP5 simulations. *Journal of Geophysical Research: Atmospheres*, *122*, 4202–4227. https://doi.org/10.1002/2016JD025979
Wang, Y., Li, S., & Luo, D. (2009). Seasonal response of Asian monsoonal climate to the Atlantic Multidecadal Oscillation. *Journal of Geophysical Research*, *114*, D02112. https://doi.org/10.1029/2008JD010929

Ward, M. N. (1998). Diagnosis and short-lead time prediction of summer rainfall in tropical North Africa at interannual and multidecadal timescales. *Journal of Climate*, *11*(12), 3167–3191. https://doi.org/10.1175/1520-0442(1998)011<3167:DASLTP>2.0.CO;2
Warren, B. A. (1981). Deep circulation of the world ocean. Evolution of physical oceanography, 6-41.
Weaver, A. J., & Valcke, S. (1998). On the variability of the thermohaline circulation in the GFDL coupled model. *Journal of Climate*, *11*(4), 759–767. https://doi.org/10.1175/1520-0442(1998)011<0759:OTVOTT>2.0.CO;2
Wills, R. C., Armour, K. C., Battisti, D. S., & Hartmann, D. L. (2019). Ocean–atmosphere dynamical coupling fundamental to the Atlantic Multidecadal Oscillation. *Journal of Climate*, *32*(1), 251–272. https://doi.org/10.1175/JCLI-D-18-0269.1
Wood, K. R., Overland, J. E., Jónsson, T., & Smoliak, B. V. (2010). Air temperature variations on the Atlantic-Arctic boundary since 1802. *Geophysical Research Letters*, *37*, L17708. https://doi.org/10.1029/2010GL044176
Woollings, T., Hannachi, A., Hoskins, B., & Turner, A. (2010). A regime view of the North Atlantic Oscillation and its response to anthropogenic forcing. *Journal of Climate*, *23*(6), 1291–1307. https://doi.org/10.1175/2009JCLI3087.1
Woollings, T., Hoskins, B., Blackburn, M., & Berrisford, P. (2008). A new Rossby wave–breaking interpretation of the North Atlantic Oscillation. *Journal of the Atmospheric Sciences*, *65*(2), 609–626. https://doi.org/10.1175/2007JAS2347.1
Wu, L., Li, C., Yang, C., & Xie, S. P. (2008). Global teleconnections in response to a shutdown of the Atlantic meridional overturning circulation. *Journal of Climate*, *21*(12), 3002–3019. https://doi.org/10.1175/2007JCLI1858.1
Wu, S., Liu, Z., Zhang, R., & Delworth, T. L. (2011). On the observed relationship between the Pacific Decadal Oscillation and the Atlantic Multi-decadal Oscillation. *Journal of Oceanography*, *67*(1), 27–35. https://doi.org/10.1007/s10872-011-0003-x
Wu, Y., Park, T., Park, W., & Latif, M. (2018). North Atlantic climate model bias influence on multiyear predictability. *Earth and Planetary Science Letters*, *481*, 171–176. https://doi.org/10.1016/j.epsl.2017.10.012
Wu, Z., Huang, N. E., Wallace, J. M., Smoliak, B. V., & Chen, X. (2011). On the time-varying trend in global-mean surface temperature. *Climate Dynamics*, *37*(3-4), 759–773. https://doi.org/10.1007/s00382-011-1128-8
Wunsch, C., & Heimbach, P. (2013). Two decades of the Atlantic meridional overturning circulation: Anatomy, variations, extremes, prediction, and overcoming its limitations. *Journal of Climate*, *26*(18), 7167–7186. https://doi.org/10.1175/JCLI-D-12-00478.1
Wunsch, C., & Roemmich, D. (1985). Is the North Atlantic in Sverdrup balance? *Journal of Physical Oceanography*, *15*(12), 1876–1880. https://doi.org/10.1175/1520-0485(1985)015<1876:ITNAIS>2.0.CO;2
Wurtzel, J. B., Black, D. E., Thunell, R. C., Peterson, L. C., Tappa, E. J., & Rahman, S. (2013). Mechanisms of southern Caribbean SST variability over the last two millennia. *Geophysical Research Letters*, *40*, 5954–5958. https://doi.org/10.1002/2013GL058458
Wüst, G. (1935). Schichtung und Zirkulation des Atlantischen Ozeans. Die Stratosphare. Wiss. Ergebn. Dtsch. Atl. Exped, 6, 180.
Wyatt, M. G., Kravtsov, S., & Tsonis, A. A. (2012). Atlantic multidecadal oscillation and Northern Hemisphere's climate variability. *Climate Dynamics*, *38*(5-6), 929–949. https://doi.org/10.1007/s00382-011-1071-8
Xie, S. P., & Philander, S. G. H. (1994). A coupled ocean-atmosphere model of relevance to the ITCZ in the eastern Pacific. *Tellus A*, *46*(4), 340–350. https://doi.org/10.3402/tellusa.v46i4.15484
Xu, X., Chassignet, E. P., & Wang, F. (2018). On the variability of the Atlantic meridional overturning circulation transports in coupled CMIP5 simulations. In *Climate Dynamics*, (pp. 1–21). Germany: Springer. https://doi.org/10.1007/s00382-018-4529-0
Xu, Z., Chang, P., Richter, I., & Tang, G. (2014). Diagnosing southeast tropical Atlantic SST and ocean circulation biases in the CMIP5 ensemble. *Climate Dynamics*, *43*(11), 3123–3145. https://doi.org/10.1007/s00382-014-2247-9
Yamamoto, A., & Palter, J. B. (2016). The absence of an Atlantic imprint on the multidecadal variability of wintertime European temperature. *Nature Communications*, *7*(1), 10930. https://doi.org/10.1038/ncomms10930
Yan, X., Zhang, R., & Knutson, T. R. (2017). The role of Atlantic overturning circulation in the recent decline of Atlantic major hurricane frequency. *Nature Communications*, *8*(1), 1695. https://doi.org/10.1038/s41467-017-01377-8
Yan, X., Zhang, R., & Knutson, T. R. (2018). Underestimated AMOC variability and implications for AMV and predictability in CMIP models. *Geophysical Research Letters*, *45*, 4319–4328. https://doi.org/10.1029/2018GL077378
Yan, X., Zhang, R., & Knutson, T. R. (2019). A multivariate AMV index and associated discrepancies between observed and CMIP5 externally forced AMV. *Geophysical Research Letters*, *46*, 4421–4431. https://doi.org/10.1029/2019GL082787
Yang, J. (2015). Local and remote wind stress forcing of the seasonal variability of the Atlantic Meridional Overturning Circulation (AMOC) transport at 26.5°N. *Journal of Geophysical Research: Oceans*, *120*, 2488–2503. https://doi.org/10.1002/2014JC010317
Yang, J., & Neelin, J. D. (1993). Sea-ice interaction with the thermohaline circulation. *Geophysical Research Letters*, *20*(3), 217–220. https://doi.org/10.1029/92GL02920
Yang, J., & Neelin, J. D. (1997). Decadal variability in coupled sea-ice–thermohaline circulation systems. *Journal of Climate*, *10*(12), 3059–3076. https://doi.org/10.1175/1520-0442(1997)010<3059:DVICSI>2.0.CO;2
Yang, X., Rosati, A., Zhang, S., Delworth, T. L., Gudgel, R. G., Zhang, R., et al. (2013). A predictable AMO-like pattern in the GFDL fully coupled ensemble initialization and decadal forecasting system. *Journal of Climate*, *26*(2), 650–661. https://doi.org/10.1175/JCLI-D-12-00231.1
Yeager, S. (2015). Topographic coupling of the Atlantic overturning and gyre circulations. *Journal of Physical Oceanography*, *45*(5), 1258–1284. https://doi.org/10.1175/JPO-D-14-0100.1
Yeager, S., & Danabasoglu, G. (2014). The origins of late-twentieth-century variations in the large-scale North Atlantic circulation. *Journal of Climate*, *27*(9), 3222–3247. https://doi.org/10.1175/JCLI-D-13-00125.1
Yeager, S., Karspeck, A., Danabasoglu, G., Tribbia, J., & Teng, H. (2012). A decadal prediction case study: Late twentieth-century North Atlantic Ocean heat content. *Journal of Climate*, *25*(15), 5173–5189. https://doi.org/10.1175/JCLI-D-11-00595.1
Yeager, S. G., Danabasoglu, G., Rosenbloom, N., Strand, W., Bates, S., Meehl, G., et al. (2018). Predicting near-term changes in the Earth System: A large ensemble of initialized decadal prediction simulations using the Community Earth System Model. *Bulletin of the American Meteorological Society*, *99*(9), 1867–1886. https://doi.org/10.1175/BAMS-D-17-0098.1
Yeager, S. G., Karspeck, A. R., & Danabasoglu, G. (2015). Predicted slowdown in the rate of Atlantic sea ice loss. *Geophysical Research Letters*, *42*, 10–704. https://doi.org/10.1002/2015GL065364
Yeager, S. G., & Robson, J. I. (2017). Recent progress in understanding and predicting Atlantic decadal climate variability. *Current Climate Change Reports*, *3*(2), 112–127. https://doi.org/10.1007/s40641-017-0064-z
Yu, J. Y., Kao, P. K., Paek, H., Hsu, H. H., Hung, C. W., Lu, M. M., & An, S. I. (2015). Linking emergence of the central Pacific El Niño to the Atlantic multidecadal oscillation. *Journal of Climate*, *28*(2), 651–662. https://doi.org/10.1175/JCLI-D-14-00347.1
Yuan, T., Oreopoulos, L., Zelinka, M., Yu, H., Norris, J. R., Chin, M., et al. (2016). Positive low cloud and dust feedbacks amplify tropical North Atlantic Multidecadal Oscillation. *Geophysical Research Letters*, *43*, 1349–1356. https://doi.org/10.1002/2016GL067679
Zampieri, M., Scoccimarro, E., & Gualdi, S. (2013). Atlantic influence on spring snowfall over the Alps in the past 150 years. *Environmental Research Letters*, *8*(3), 034026. https://doi.org/10.1088/1748-9326/8/3/034026

Zanchettin, D., Bothe, O., Graf, H. F., Omrani, N. E., Rubino, A., & Jungclaus, J. H. (2016). A decadally delayed response of the tropical Pacific to Atlantic multidecadal variability. *Geophysical Research Letters*, *43*, 784–792. https://doi.org/10.1002/2015GL067284
Zanchettin, D., Bothe, O., Müller, W., Bader, J., & Jungclaus, J. H. (2014). Different flavors of the Atlantic multidecadal variability. *Climate Dynamics*, *42*(1-2), 381–399. https://doi.org/10.1007/s00382-013-1669-0
Zhang, D., Msadek, R., McPhaden, M. J., & Delworth, T. (2011). Multidecadal variability of the North Brazil Current and its connection to the Atlantic meridional overturning circulation. *Journal of Geophysical Research*, *116*, C04012. https://doi.org/10.1029/2010JC006812
Zhang, J., & Zhang, R. (2015). On the evolution of Atlantic meridional overturning circulation fingerprint and implications for decadal predictability in the North Atlantic. *Geophysical Research Letters*, *42*, 5419–5426. https://doi.org/10.1002/2015GL064596
Zhang, L., Delworth, T. L., & Zeng, F. (2017). The impact of multidecadal Atlantic meridional overturning circulation variations on the Southern Ocean. *Climate Dynamics*, *48*(5-6), 2065–2085. https://doi.org/10.1007/s00382-016-3190-8
Zhang, L., & Wang, C. (2013). Multidecadal North Atlantic sea surface temperature and Atlantic meridional overturning circulation variability in CMIP5 historical simulations. *Journal of Geophysical Research: Oceans*, *118*, 5772–5791. https://doi.org/10.1002/jgrc.20390
Zhang, L., & Zhao, C. (2015). Processes and mechanisms for the model SST biases in the North Atlantic and North Pacific: A link with the Atlantic meridional overturning circulation. *Journal of Advances in Modeling Earth Systems*, *7*, 739–758. https://doi.org/10.1002/2014MS000415
Zhang, R. (2007). Anticorrelated multidecadal variations between surface and subsurface tropical North Atlantic. *Geophysical Research Letters*, *34*, L12713. https://doi.org/10.1029/2007GL030225
Zhang, R. (2008). Coherent surface-subsurface fingerprint of the Atlantic meridional overturning circulation. *Geophysical Research Letters*, *35*, L20705. https://doi.org/10.1029/2008GL035463
Zhang, R. (2010). Latitudinal dependence of Atlantic meridional overturning circulation (AMOC) variations. *Geophysical Research Letters*, *37*, L16703. https://doi.org/10.1029/2010GL044474
Zhang, R. (2015). Mechanisms for low-frequency variability of summer Arctic sea ice extent. *Proceedings of the National Academy of Sciences*, *112*(15), 4570–4575.201422296. https://doi.org/10.1073/pnas.1422296112
Zhang, R. (2017). On the persistence and coherence of subpolar sea surface temperature and salinity anomalies associated with the Atlantic multidecadal variability. *Geophysical Research Letters*, *44*, 7865–7875. https://doi.org/10.1002/2017GL074342
Zhang, R., & Delworth, T. L. (2005). Simulated tropical response to a substantial weakening of the Atlantic thermohaline circulation. *Journal of Climate*, *18*(12), 1853–1860. https://doi.org/10.1175/JCLI3460.1
Zhang, R., & Delworth, T. L. (2006). Impact of Atlantic multidecadal oscillations on India/Sahel rainfall and Atlantic hurricanes. *Geophysical Research Letters*, *33*, L17712. https://doi.org/10.1029/2006GL026267
Zhang, R., & Delworth, T. L. (2007). Impact of the Atlantic multidecadal oscillation on North Pacific climate variability. *Geophysical Research Letters*, *34*, L23708. https://doi.org/10.1029/2007GL031601
Zhang, R., & Delworth, T. L. (2009). A new method for attributing climate variations over the Atlantic Hurricane Basin's main development region. *Geophysical Research Letters*, *36*, L06701. https://doi.org/10.1029/2009GL037260
Zhang, R., Delworth, T. L., & Held, I. M. (2007). Can the Atlantic Ocean drive the observed multidecadal variability in Northern Hemisphere mean temperature? *Geophysical Research Letters*, *34*, L02709. https://doi.org/10.1029/2006GL028683
Zhang, R., Delworth, T. L., Rosati, A., Anderson, W. G., Dixon, K. W., Lee, H. C., & Zeng, F. (2011). Sensitivity of the North Atlantic Ocean circulation to an abrupt change in the Nordic Sea overflow in a high resolution global coupled climate model. *Journal of Geophysical Research*, *116*, C12024. https://doi.org/10.1029/2011JC007240
Zhang, R., Delworth, T. L., Sutton, R., Hodson, D. L., Dixon, K. W., Held, I. M., et al. (2013). Have aerosols caused the observed Atlantic multidecadal variability? *Journal of the Atmospheric Sciences*, *70*(4), 1135–1144. https://doi.org/10.1175/JAS-D-12-0331.1
Zhang, R., Sutton, R., Danabasoglu, G., Delworth, T. L., Kim, W. M., Robson, J., & Yeager, S. G. (2016). Comment on "The Atlantic Multidecadal Oscillation without a role for ocean circulation". *Science*, *352*(6293), 1527–1527. https://doi.org/10.1126/science.aaf1660
Zhang, R., & Vallis, G. K. (2006). Impact of great salinity anomalies on the low-frequency variability of the North Atlantic climate. *Journal of Climate*, *19*(3), 470–482. https://doi.org/10.1175/JCLI3623.1
Zhang, R., & Vallis, G. K. (2007). The role of bottom vortex stretching on the path of the North Atlantic western boundary current and on the northern recirculation gyre. *Journal of Physical Oceanography*, *37*(8), 2053–2080. https://doi.org/10.1175/JPO3102.1
Zhang, W., Vecchi, G. A., Murakami, H., Villarini, G., Delworth, T. L., Yang, X., & Jia, L. (2018). Dominant role of Atlantic Multidecadal Oscillation in the recent decadal changes in western North Pacific tropical cyclone activity. *Geophysical Research Letters*, *45*, 354–362. https://doi.org/10.1002/2017GL076397
Zhao, Y., Bigg, G. R., Billings, S. A., Hanna, E., Sole, A. J., Wei, H. L., et al. (2016). Inferring the variation of climatic and glaciological contributions to West Greenland iceberg discharge in the twentieth century. *Cold Regions Science and Technology*, *121*, 167–178. https://doi.org/10.1016/j.coldregions.2015.08.006
Zhou, J., & Tung, K. K. (2013). Deducing multidecadal anthropogenic global warming trends using multiple regression analysis. *Journal of the Atmospheric Sciences*, *70*(1), 3–8. https://doi.org/10.1175/JAS-D-12-0208.1
Zhou, J., Tung, K. K., & Li, K. F. (2016). Multi-decadal variability in the Greenland ice core records obtained using intrinsic timescale decomposition. *Climate Dynamics*, *47*(3-4), 739–752. https://doi.org/10.1007/s00382-015-2866-9
Zhou, X., Li, S., Luo, F., Gao, Y., & Furevik, T. (2015). Air–sea coupling enhances the East Asian winter climate response to the Atlantic Multidecadal Oscillation. *Advances in Atmospheric Sciences*, *32*(12), 1647–1659. https://doi.org/10.1007/s00376-015-5030-x

Erratum

In the originally published version of this article, the seventh author's name was erroneously listed as "Danial E. Amrhein" instead of "Daniel E. Amrhein." The author byline has since been corrected, and this version may be considered the authoritative version of record.